REGENERATIVE CAPACITY OF REACTIVE ASTROCYTES *IN VITRO* AND *IN VIVO*

Luísa Lange Canhos

Graduate School of
Systemic Neurosciences
LMU Munich

Dissertation der
Graduate School of Systemic Neurosciences der
Ludwig-Maximilians-Universität München

June, 2018

Supervisor
Prof. Dr. Magdalena Götz

Head of Department of Physiological Genomics
BioMedical Center – BMC
Ludwig-Maximilians-Universität München

Institute of Stem Cell Research
Helmholtz Zentrum München

Co-Supervisor
PD, Dr. Swetlana Sirko

Department of Physiological Genomics
BioMedical Center – BMC
Ludwig-Maximilians-Universität München

Institute of Stem Cell Research
Helmholtz Zentrum München

First Reviewer:	Prof. Dr. Magdalena Götz
Second Reviewer:	Dr. Florence Bareyre
External Reviewer:	Prof. Dr. Elly Hol
Date of Submission:	28.06.2018
Date of Defense:	24.09.2018

TABLE OF CONTENTS

ABSTRACT

Reactive astrogliosis is a reaction of the central nervous system (CNS) common to diverse types of injury, but only upon invasive injury a subset of reactive astrocytes acquires proliferative capacity *in vivo* and exhibits stem cell potential through self-renewal and multipotency *in vitro*. Given that in the adult mammalian brain only adult neural stem cells (aNSCs) located in specific niches are able to self-renew and give rise to neurons, it is important to test to which extent reactive astrocytes can enact their NSC potential also *in vivo* when exposed to different environmental conditions. For this purpose, experimental mouse models were used to investigate (i) whether and to which extent astrocytes in the injured cerebral cortex grey matter exhibit self-renewal *in vivo* when exposed to sequential pathological stimuli; (ii) whether reactive astrocytes can give rise to different cell types *in vivo* when placed in neurogenesis-supportive environments.

In order to analyze the proliferative behavior of reactive astrocytes in the adult murine cerebral cortex in response to repetitive pathological stimuli, I established a double labeling paradigm based on sequential delivery of two thymidine analogues, BrdU and EdU. Furthermore, in order to verify the results obtained with this paradigm I performed clonal analysis of reactive astrocytes using $Glast^{CreERT2}$-mediated recombination in the R26-Confetti reporter line. Results from both experimental paradigms demonstrate that a distinct subset of reactive astrocytes within the cortical parenchyma is able to re-enter the cell cycle and give rise to 3-cell clones upon repetitive injuries, which had so far not been observed. Furthermore, astrocyte cell-cycle reentry is modulated by monocyte infiltration, as it was increased in their absence in transgenic $CCR2^{-/-}$ mice.

Moreover, we used BrdU and EdU double labeling to investigate whether proliferation was a property confined to a specific subset of astrocytes, or if different sets of reactive astrocytes could be activated to enter cell cycle. Our analysis showed that the astrocyte proliferative pool is not fixed, and new astrocytes can be recruited into proliferation upon a second pathological event. Intriguingly, our results suggest a strong drive towards astroglial population homeostasis, which has so far not been described in these cells.

To analyze the differentiation capacity of RAs *in vivo*, cortical reactive astrocytes and aNSCs from the subependymal zone (SEZ) of adult actin-GFP mice cultured as neurospheres were transplanted heterotypically into the adult dentate gyrus (DG) and the E13 embryonic brain. Our analysis showed that the progeny of reactive astrocytes remained restricted within the glial lineage in both environments, whereas aNSCs gave rise to immature neurons in the DG and to mature neurons in a few regions of the embryonic brain. Taken together although reactive astrocytes show multipotency and can give rise to neurons *in vitro*, they are largely unable to generate neurons *in vivo*.

Furthermore, in light of a recently reopened debate that questions reactive astrocyte stem cell potential, our results from transplantation experiments provoked further investigation on this matter. There is new evidence supporting that all neurospheres obtained from injured cortical tissue are actually originated from SEZ aNSCs. As our transplantation results showed a distinct differentiation profile of reactive astrocytes when compared to aNSCs in both host environments, we performed experiments to add evidence to this debate.

For this purpose, we developed two independent experimental paradigms in which cortical cells (but not SEZ cells) were labeled prior to injury through double transgenic Emx1-GFP mice and through delivery of AAV-iCre into the cortex of floxed GFP-Reporter mice. Our results obtained with both experimental paradigms show that cells of cortical origin can give rise to neurospheres *in vitro* following stab wound lesion.

Altogether, through this study we have achieved many novel insights into astrocyte reaction to injury, regulation of astrocytic population through different proliferation strategies, and into the stem cell potential of reactive astrocytes *in vivo*. Our findings advance the general understanding of astrocyte biology in the context of CNS pathology and open the way to many new questions in this field.

1 Introduction

The adult mammalian central nervous system (CNS) has a very limited capacity for self-repair, as upon damage neurons get irreversibly lost, leading to functional disruptions in the neural circuitry. This can cause life-long lasting deficits and highly debilitating pathologies in affected patients. The repair of the damaged CNS continues to represent one of the biggest current challenges in regenerative medicine, as there are still no therapies available to replace neuronal loss and achieve full functional damage restoration in the CNS.

Contrary to the long held idea that the adult mammalian brain was completely devoid of the capacity of generating new neurons, the notion that there is actually robust ongoing neurogenesis and neuronal integration in this system has been widely accepted since a few decades (Altman, 1962, 1963, Altman and Das, 1965, 1966; Goldman and Nottebohm, 1983; Kaplan and Hinds, 1977). The fall of this long sustained dogma triggered a paradigm shift in many areas of neuroscience, and changed our general understanding of CNS function (Gross, 2000).

The realization that the CNS is a more plastic and dynamic system than previously thought led to a change in mindset that has caused a revolution in the field of CNS repair, as different approaches are being explored in order to replace damaged neurons and restore impaired neuronal function. Some approaches in particular have showed promising achievements (for reviews, see Barker et al., 2018; Grade and Götz, 2017), for example by instructing local cells within the damage area to produce neurons (Gascón et al., 2016, 2017; Heinrich et al., 2014), as well as by introducing external cells into the damaged CNS to replace lost neurons (Barker et al., 2013; Falkner et al., 2016; Grealish et al., 2015; Michelsen et al., 2015).

Yet another dogma that has also recently met its end is the idea that neuronal and glial cells were generated from different progenitors during development. The discovery that the stem cells that give rise to neurons during development and adulthood are in fact, astroglial cells (Doetsch et al., 1999; Malatesta et al., 2000; Seri et al., 2001) that share many common features with parenchymal astrocytes (Robel et al., 2011), has opened the road to many new questions for a better understanding of astrocytes in

different parts of the CNS, as they may be particularly valuable for endogenous repair in the injured CNS.

Astrocytes are ubiquitously distributed throughout the CNS and exhibit a range of diverse roles that are essential for normal brain development and function, such as synaptic pruning, regulation of neural network activity, maintenance of tissue homeostasis and regulation of blood flow (Clarke and Barres, 2013; Kimelberg and Nedergaard, 2010). Specialized astrocytes that act as neural stem cells (NSCs) in the adult mammalian brain are confined to specific brain regions, the so-called neurogenic niches, which are, in most mammals, the lateral ventricle subependymal zone (SEZ) and the hippocampal dentate gyrus (DG) (Riquelme et al., 2008). Although astrocytes in the healthy adult brain do not proliferate outside these niches, acute invasive injury triggers proliferation and activation of stem cell potential in a subset of parenchymal astrocytes in the cerebral cortex gray matter, together with the upregulation of many genes that are commonly expressed in adult neural stem cells (aNSCs) (Bardehle et al., 2013; Buffo et al., 2008; Dimou and Götz, 2014; Götz et al., 2015; Sirko et al., 2013, 2015).

In order to be able to explore the potential of parenchymal astrocytes in neural repair it is utterly necessary to acquire a better comprehension of the plasticity and limitations of these cells, and how they can be modulated *in vivo*. The aim of this project was to functionally investigate the stem cell potential of cerebral cortex gray matter reactive astrocytes following acute invasive injury through methodological approaches applied both *in vitro* and *in vivo*.

On the following sections I will discuss some important concepts and technical implications that are relevant for understanding the specific questions we addressed in the scope of this project and the methodological approaches we decided to employ to answer our questions.

1.1 Stem cells: definition and methodological approaches

First and foremost, as the core question in this project involves evaluating reactive astrocyte stem cell potential, it is very important to first define the concept of a stem cell.

Stem cells are generally defined by their behavior, and this definition is based on two basic hallmarks: (1) self-renewal, which is the ability of a cell to divide and generate

progeny identical to itself and (2) multilineage differentiation, that is the ability to give rise to progeny of distinct cell lineages (Figure 1A) (Weissman, 2000). Although the classical definition of a stem cell involves indefinite self-renewal (or at least throughout the lifetime of the individual) and the ability to give rise to all cell types within a tissue, it is hard to find cells that completely fulfill these criteria, especially in the adult organism.

One class of adult stem cells that can fit this definition very well are the hematopoietic stem cells, as they can self-renew for a time that goes beyond the life span of an individual, and can give rise to all types of cells of the blood and immune system (Weissman, 2000). However, other stem cell populations have a much more limited capacity, such as the neural stem cells, which are at the central focus of this project.

In summary, the definition of a stem cell is very broad and there are no agreed quantitative criteria for their objective classification, for example a fixed number of divisions the cell has to undergo to classify it as self-renewing, or of the amount of different cell lineages it has to produce to be defined as a stem cell. As a result, there are different types of stem cells with strikingly distinct capacities, as well as much debate on whether a given cell type classifies as a stem cell or not.

Since stem cells are defined by their behavior and there is no specific marker to ultimately identify a stem cell (for example, by the expression of a certain gene), there are different methodological approaches to investigate cell behavior and assess whether a given cell type exhibits stem cell hallmarks. Importantly, this investigation can take place within the endogenous niche of a given cell (*in situ*), or the cell can be extracted from its original location and one can investigate how it behaves in a new environment (*ex situ*) (Figure 1B,C). Both approaches are valuable, but it is important to be aware that they provide different types of information about the cell's behavior. *In situ* methodological approaches provide information on what a cell does, and the lineage it gives rise to; whereas through *ex situ* approaches one gathers information on what a cell can do, in other words, on its potential (Figure 1B,C) (Götz et al., 2015).

Taking the adult neural tissue as an example, it is possible to analyze a putative aNSC *in situ* through a variety of methods to obtain information about what it does in its intrinsic environment, and the progeny it generates, which is referred to as its lineage (Figure 1B). One can analyze the incorporation of proliferation markers or ablate dividing cells in the niche and analyze the repopulation dynamics (Doetsch et al., 1999; Seri et al., 2001). Alternatively, one can actively follow the cell and its progeny over time

through clonal analysis (Bonaguidi et al., 2011; Calzolari et al., 2015; Encinas et al., 2011) or live-imaging (Barbosa et al., 2015; Pilz et al., 2018).

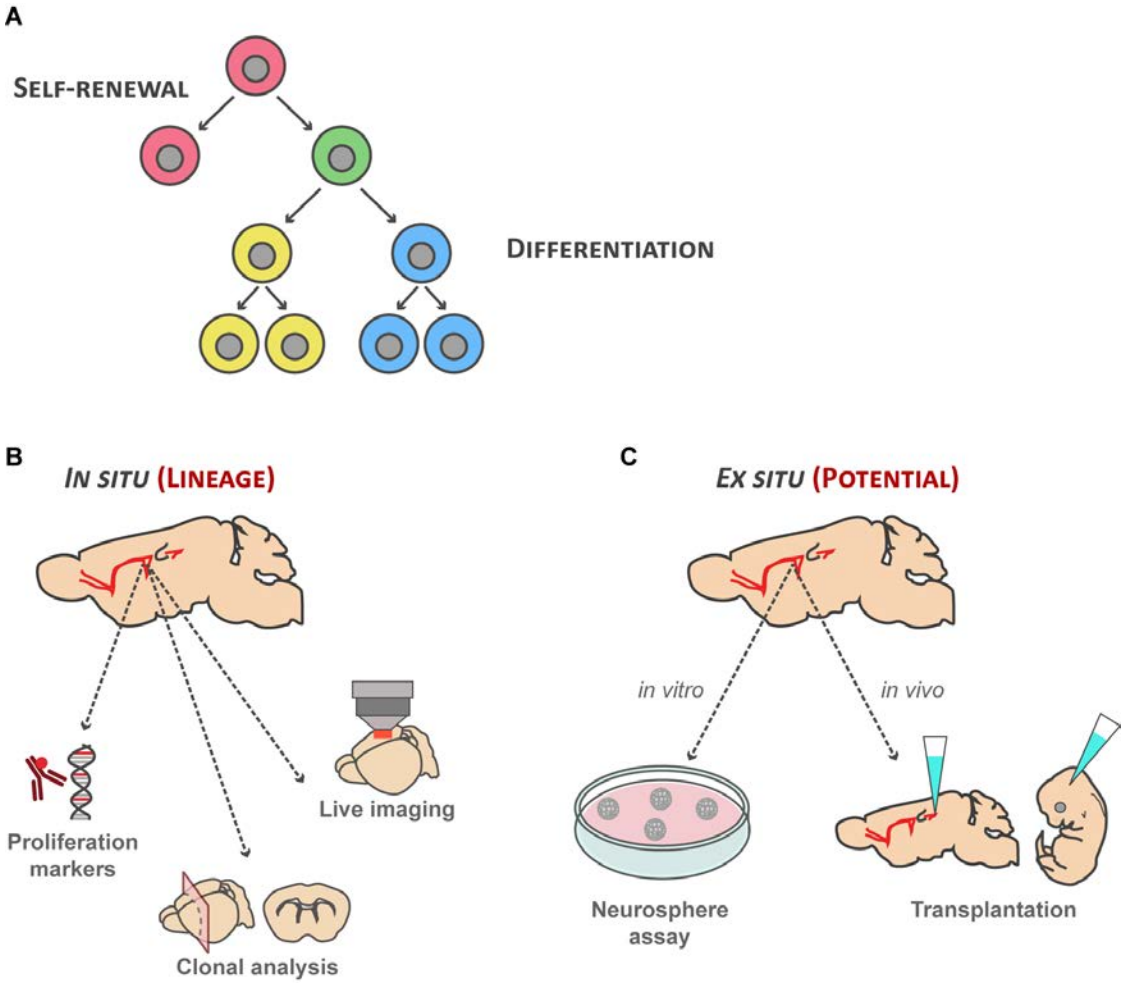

Figure 1. Stem cell definition and methodological approaches to investigate stem cell properties. (**A**) The two defining hallmarks of stem cells are self-renewal, or the capacity to give rise to progeny identical to itself through cell division, and multilineage differentiation, which is the capacity to generate progeny of different lineages. (**B**) One can evaluate what a cell does in its endogenous environment by analyzing a cell's lineage. (**C**) Alternatively, one can investigate what a cell can do when relocated to a new environment, which provides information on the cell's potential. A few examples for (b) and (c) are illustrated based on previous studies performed with aNSCs.

Alternatively, one can investigate what a cell can do when relocated to a different environment, and this gives us information of a cell's potential (Figure 1C) (Götz et al., 2015). A seminal work that uncovered the existence of NSCs in the adult mammalian brain consisted on examining the behavior of neural cells *in vitro* through the neurosphere assay (Reynolds and Weiss, 1992). The neurosphere assay remains until today the gold standard method for testing for NSC potential, as it consists of evaluating the two stem cell hallmarks. Neural cells are plated *in vitro* in a low density, or even as single cells, and if they proliferate and give rise to clonal spheres that can be passaged

over time, they show the property of self-renewal. Furthermore, if cells contained in these neurospheres can differentiate into the three neural lineages (astroglial, oligodendroglial and neuronal), one can conclude that the cell that gave rise to this neurosphere is multipotent (Reynolds and Rietze, 2005). Another approach to evaluate a cell's potential is to transplant it into a different environment and evaluate if it can self-renew or give rise to different cell types under new environmental cues (Lim et al., 1997; Neumeister et al., 2009; Richardson et al., 2005; Suhonen et al., 1996).

In conclusion, these different methodological approaches provide valuable information about how a given cell population behaves in its environment and what it can potentially do when exposed to different cues in a new environment. By employing both approaches one can gain more comprehensive information about the biology of a cell and how its behavior can be modulated.

In this project we decided to employ both types of methodological approaches to investigate the plasticity of cerebral cortex reactive astrocytes both *in situ* in the cortical environment through cell proliferation labeling and clonal analysis; and *ex situ* by relocating these cells to different environments, *in vitro* through the neurosphere assay, and *in vivo* through transplantations, as I will describe in more detail in the following sections.

1.2 Neural stem cells

In the CNS the neural stem cells that are responsible for generating most of the neurons in the cortex during development are the radial glial cells (RGC) (Taverna et al., 2014). These cells share several hallmarks with astrocytes, such as the expression of many proteins important for the regulation of neurotransmitters in the extracellular space (e.g. GLAST and GLT1), an important function of astrocytic cells, or ultrastructural hallmarks, such as glycogen granules (Götz and Huttner, 2005; Robel et al., 2011).

Interestingly, the neural stem cells present in the adult brain (aNSCs) are derived from RGCs that are spared during development through slow division rates (Furutachi et al., 2015; Merkle et al., 2004), and also share the same common hallmarks with astrocytes (Beckervordersandforth et al., 2010; Llorens-bobadilla et al., 2015; Robel et al., 2011).

Of note, although both RGCs and aNSCs are classified as stem cells, they only exhibit their stem cell hallmarks *in vitro*, and fail to do so *in vivo*. In the neurosphere assay *in vitro*, both cell types show long-term self-renewal and multipotency, however *in vivo* their self-renewal is rather limited and they generate mostly unilineage progeny (Götz et al., 2015). RGCs exhibit up to 9 cell divisions *in vivo* and most of them generate either only neurons or astrocytes (Gao et al., 2014), whereas aNSCS exhibit up to 4 cell divisions *in vivo* and give rise mostly to neurons (Calzolari et al., 2015; Encinas et al., 2011).

1.3 Astrocytes and their importance in CNS function

Although astrocytes have a widespread distribution and are among the most abundant cells in the CNS, being even more numerous than neurons in the human cortex (Nedergaard et al., 2003), their functional importance has only started to be elucidated in the past few decades. Astrocytes are a very heterogeneous cell type that exhibit a plethora of different functions (Oberheim et al., 2012; Zhang and Barres, 2010), amongst which are the regulation of ion and neurotransmitter concentrations in the extracellular space (Rothstein et al., 1996; Verkhratsky et al., 2014), metabolic support of neurons (Allaman et al., 2011), regulation of blood flow (Attwell et al., 2010; MacVicar and Newman, 2015), active participation in neuronal information processing (Araque et al., 2014; Haydon, 2001), synaptic pruning (Clarke and Barres, 2013), clearance of waste from the brain through the glymphatic system (Jessen et al., 2015) and the aforementioned specialized function of neurogenesis in NSCs.

Altogether, astrocytes exert crucial roles for CNS function and, not surprisingly, impairments in astrocytic function lead to CNS malfunction and diseases. An increase of understanding of astrocyte function has led to a paradigm shift over the last two decades, in which astrocytes are now starting to be seen as active players in CNS physiology and pathology. Growing evidence supports the idea that impairment of astrocyte function is the primary cause or the main factor in many different neurological diseases, a concept coined astropathy (Pekny et al., 2015). Therefore, a better understanding of astrocyte properties in different CNS pathologies can provide invaluable insights for further comprehension of neurological dysfunction and development of treatments for CNS damage or disease.

1.4 Reactive astrogliosis

Most CNS pathologies are accompanied by a response or activation of astrocytes, a process termed reactive astrogliosis. Even though astrogliosis is present in nearly all neurological pathologies, reactive astrocytes can exhibit different types of states and properties depending on the pathology (Liddelow and Barres, 2017; Liddelow et al., 2017; Pekny et al., 2015; Sirko et al., 2013). Furthermore, as astrocytes show distinct responses to different pathologies, and as each pathology is very complex in itself, there is still a debate on whether astrogliosis is beneficial or detrimental for CNS repair (Pekny et al., 2014; Sofroniew, 2005). There is evidence supporting a dual role of reactive astrocytes depending on the time window of CNS damage (Pekny et al., 2014), however growing evidence supports clear beneficial effects of reactive astrocytes in CNS neuroprotection and repair, even in supporting axonal growth (Anderson et al., 2016; Bush et al., 1999; Sofroniew, 2005).

Reactive astrogliosis is generally defined as morphological, transcriptional and functional changes that astrocytes undergo in response to injury, such as trauma and ischemic events, or CNS diseases, such as neurodegenerative or neuroinflammatory diseases (Pekny and Pekna, 2014). There are many common hallmarks of astrogliosis present across different types of CNS pathology, such as cellular hypertrophy and upregulation of glial acydic fibrillary protein (GFAP). GFAP is the main component of astrocyte intermediate filaments, and its role has been implicated mainly with structural functions, as its deletion leads to a reduction in the resistance of CNS tissue to mechanical stress (Pekny and Pekna, 2004). However, GFAP function is not limited to a structural role, and the complexity of this protein and its functions are still being uncovered. Several other GFAP functions have been described, such as cellular motility or migration, modulation of cell proliferation, vesicle mobility, astrocyte-neuron interaction, blood-brain barrier (BBB) permeability and myelination (Middeldorp and Hol, 2011). Furthermore, many different GFAP isoforms have been discovered in recent years and the functions of each isoform are still not well understood (Hol and Pekny, 2015).

Interestingly, reactive astrocytes in the brain parenchyma share many hallmarks with NSCs, not only at the gene expression level, such as upregulation of GFAP and many other genes that are characteristic to NSCs (Götz et al., 2015; Robel et al., 2011; Sirko et al., 2015), but also functionally, as upon invasive brain injury they enter cell cycle *in vivo* and a subset of them shows stem cell potential *in vitro* (Buffo et al., 2008; Sirko et al., 2013). Altogether, when exposed to certain types of CNS damage astrocytes are able to

resume cell proliferation and re-express proteins present in RGCs at earlier developmental stages or in aNSCs. Nevertheless, it is important to note that although they RAs and NSCs share many similarities, they exhibit as well fundamental differences. In the neurosphere assay, aNSCs show a greater stem cell capacity both on self-renewal and differentiation parameters (Sirko et al., 2009, 2013), and ultimately, aNSCs give rise to neurons *in vivo*, whereas reactive astrocytes do not.

1.5 Mechanisms involved in the regulation of astrocyte reactivity

Astrocytes are located in close contact to blood vessels and, therefore, are in an advantageous position to sense signals coming from the blood stream into the CNS. Molecules of different types and origins can play a role in triggering astrocyte activation. These molecules can activate astrocytes through 3 different ways: they could be present in the blood stream, be secreted within the CNS by endogenous cells, or be present in the cerebrospinal fluid (CSF) and enter the CNS through BBB disruption.

Cytokines and growth factors get into contact with astrocytes either through the blood stream or through local paracrine secretion, and play a major role in astrocyte activation in CNS pathology. Among these types of molecules, epidermal growth factor (EGF), vascular endothelial growth factor (VEGF) and fibroblast growth factor 2 (FGF2) and transforming growth factor alpha and beta (TGFα, TGFβ), play major roles in astrocyte activation and regulation of functional properties of reactive astrocytes (Nieto-Sampedro, 1988; Rabchevsky et al., 1998; Robel et al., 2011; You et al., 2017). EGF, VEGF and FGF2 are released by various cell types within the CNS upon damage, and they promote upregulation of their receptors. Activation of these growth-factor signaling pathways induces astrocyte proliferation through convergence on the mammalian target of rapamycin (mTOR) and mitogen-activated protein kinase (MAPK) pathways (Codeluppi et al., 2009). VEGF also has an important role on BBB permeability (Chapouly et al., 2015), which can affect the interaction of astrocytes with other signaling molecules. These signaling pathways are also present in the adult neurogenic niches and regulate aNSC proliferation and survival (Robel et al., 2011).

A key factor that has been shown to be of major importance for regulation of astroglial cell proliferation, both in the neurogenic niches, as well as in the damaged CNS is Sonic Hedgehog (SHH) (Amankulor et al., 2009; Pitter et al., 2014; Reinchisi et al.,

2013). Astrocyte proliferation in the CNS parenchyma is only observed upon invasive injury with BBB disruption (Sirko et al., 2013), and it has been shown that SHH is upregulated and present in high levels in the CSF after injury. This suggests a possible molecular mechanism for activation of astrocyte proliferation in this type of injury, but the lack thereof in other types of CNS pathology in which the BBB is not disturbed (Sirko et al., 2013).

Other factors that can trigger and modulate reactive astrogliosis are molecules or neurotransmitters that are locally released upon injury, such as reactive oxygen species (ROS), glutamate or ATP. These molecules are among the first and with strongest activation following injury, as they are released by damaged neurons or other cells (Sofroniew, 2009)

In summary, reactive astrogliosis is a complex process that arises from the interaction of astrocytes with signals originated from different cell types within the CNS, but also from signals that are originated externally. This cross-talk leads to the activation of different signaling pathways, and ultimately, to changes in astrocyte transcriptional regulation, morphology and function.

Now that the basic conceptual background and investigation approaches that are key to this study have been laid out, we can proceed to the specific questions addressed in this project.

1.6 Astrogliosis and proliferation: can cortical reactive astrocytes self-renew *in vivo*?

Although cortical reactive astrocytes can self-renew for many passages *in vitro*, *in vivo* they can divide only once. It remains however unknown whether astrocytes can be instructed to self-renew *in vivo* under different conditions. We therefore evaluated whether we could stimulate astrocytes to undergo more rounds of cell division and therefore enact their self-renewal potential *in vivo* if exposed to multiple pathological stimuli (*see Section 1.9*).

1.7 Environment-dependent plasticity of reactive astrocytes: can they give rise to neurons in a neurogenic environment?

As we know that cortical reactive astrocytes exhibit stem cell potential and can give rise to neurons *in vitro* in the neurosphere assay, however remain within their lineage within their endogenous environment (Bardehle et al., 2013; Buffo et al., 2008), we questioned if this is a restriction that is intrinsic to these cells, or if it is rather a condition imposed by the environment in which they are located.

It is known that the cortex, as well as all other regions of the brain excluding the neurogenic niches, is essentially gliogenic, and aNSCs heterotypically transplanted outside of the neurogenic niches give rise to glial cells only (Seidenfaden et al., 2006). Therefore, as for aNSCs, the lineage restriction observed in cortical reactive astrocytes may be limited by the local environment, and astrocytes might be able to give rise to other cell types when placed in more permissive environments, for example the adult neurogenic niches, or the developing embryonic brain. We therefore performed transplantation experiments where we relocated cortical reactive astrocytes to neurogenesis-permissive environment to evaluate if they could give rise to neurons *in vivo* under supportive conditions (*see Section 1.9*).

1.8 Origin of neurosphere-forming cells isolated from lesioned cerebral cortex: local dedifferentiation or migration from SEZ aNSCs?

As mentioned in previous sections, astrocytes from the cerebral cortex gray matter parenchyma become reactive following an invasive injury, de-differentiate, enter cell cycle and start to proliferate, and a subset of them shows stem cell potential *in vitro* (Buffo et al., 2008). The fact that parenchymal astrocytes go through cell division and generate progeny is undisputed, as this has even been even demonstrated through live *in vivo* imaging (Bardehle et al., 2013).

However, in contrast to previous work from our group showing that astrocytes in the cortical gray matter acquire stem cell properties *in vitro* in response to an acute invasive injury (Buffo et al., 2008), recent evidence supports the idea that the neurosphere-forming astrocytes present in the cerebral cortex following ischemic stroke

are actually derived from aNSCs that migrate from the SEZ to the injury site (Faiz et al., 2015).

Since data gathered from different studies on *in vitro* and *in vivo* self-renewal and differentiation properties of SEZ aNSCs and cortical reactive astrocytes show evident differences between these two cell types (Shimada et al., 2012; Sirko et al., 2009, 2013), we investigated in our injury model whether the neurosphere forming cells in the injured cortex are indeed aNSCs migrating from the SEZ (and changing their properties on this migration) or are locally derived from resident parenchymal astrocytes (*see Section 1.9*).

1.9 Aims

The main goal of this project was to achieve a better comprehension about the stem cell potential that cerebral cortex reactive astrocytes acquire following invasive injury, and to functionally evaluate the extense of this acquired plasticity through several different approaches. The main rationale behind our investigation was that both aNSCs and cortical reactive astrocytes show stem cell potential *in vitro*, but however they do not enact this potential *in vivo*, where their behavior is much more restricted. We therefore evaluated how these cells would behave under different environmental cues.

Firstly, as we know that cortical astrocytes do not divide in the healthy brain, but upon invasive injury proliferate and undergo maximally one cell division *in vivo* (Bardehle et al., 2013), and can self-renew for a long term *in vitro* (Figure 2) (Buffo et al., 2008), we questioned whether these cels would also show self-renewal *in vivo* if they would be instructed to do so. For this end, we applied sequential pathological stimuli and evaluated astrocyte proliferation both through DNA labeling tools and clonal analysis to investigate if astrocytes could undergo more rounds of cell division *in vivo* (Figure 2, question I).

Secondly, since astrocytes remain within their lineage in the cortex, but show the potential to generate neurons *in vitro*, we evaluated whether these cells could give rise to neurons in environments that support neurogenesis, namely the adult hippocampal neurogenic niche, and the embryonic developing brain (Figure 2, question II).

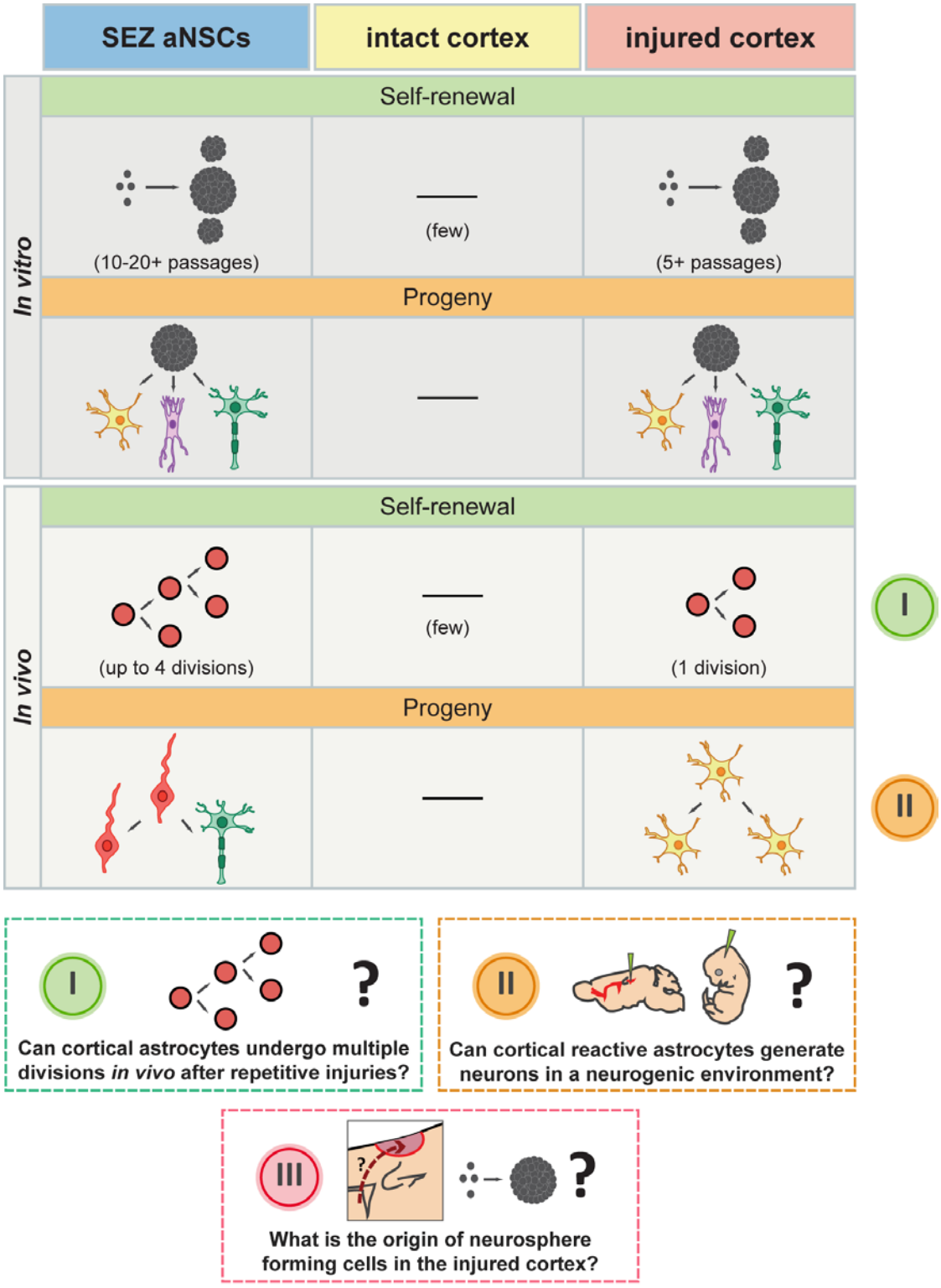

Figure 2. General aims of this PhD project. Parenchymal cortical astrocytes do not proliferate in the healthy brain, but upon invasive injury enter cell division and exhibit stem cell potential *in vitro*. As aNSCs show a big discrepancy between their potential *in vitro* and lineage *in vivo*, we set out to evaluate whether cerebral cortex reactive astrocytes could exhibit different stem cell hallmarks *in vivo* when exposed to different environmental cues. Our main questions in this project are outlined in the three question boxes below

Lastly, as neurospheres derived from injured cortex or SEZ tissue show very distinct potentials not only *in vitro*, but also *in vivo* through results we obtained within this project, we set out to confirm whether the recent claim that all neurospheres from the cortical injured tissue were generated by migrating aNSCs from the SEZ would still hold with further experiments (Figure 2, question III)

2 Material and Methods

2.1 Solutions

The composition of all solutions used in the different experiments within the scope of this work is given on the table below:

Table 1. Composition and application of solutions used throughout experiments.

Solution	*Composition*	*Application*
DNA Lysis Buffer	NaOH (0.5 M), NaCl (1.5 M) in H_20	DNA extraction (genotypings)
TE Buffer	Tris base (10 mM), EDTA (1 mM) in H_2O (pH=8.0)	DNA extraction (genotypings)
PCR Buffer 10x	500 mM KCl, 100 mM Tris base in H_2O (pH=8,7)	PCR reaction (genotypings)
Neurosphere Medium	1% penicillin-streptomycin, 1% supplement B27, L-Glutamine 2 mM, 20 ng/ml EGF and FGF in DMEM/F-12	Neurosphere assay (cell culture)
Protease Inhibitor Solution	Ovomucoid 1 mg/mL, 50 µg/mL bovine serum albumin and 40 µg/mL DNaseI in L-15 medium	Neurosphere assay (cell culture)
Differentiation Medium	1% penicillin-streptomycin, 1% supplement B27, L-Glutamine 2 mM, 1% FBS in DMEM/F-12	Differentiation assay (cell culture)
Phosphate-Buffered Saline (PBS)	Na_2HPO_4 x $2H_20$ (48 mM), KH_2PO_4 (272 mM), NaCl (137 mM), KCl (149 mM) in H_20 (pH=7.4)	Perfusion, immunostainings
4% Paraformaldehyde (PFA)	Na_2HPO_4 x $2H_20$ (133 mM), PFA (133.2 mM), 32% NaOH to dissolve PFA in H_2O (pH=7.4)	Perfusion, immunostainings
Krebs-Ringer-Hepes Buffer	NaCl (125 mM), KCl (4.8 mM), $CaCl_2$*$2H_2O$ (1.3 mM), $MgSO_4$*$7H_2O$ (1.2 mM), KH_2PO_4 (1.2 mM), D-Glucose (5.6 mM) and HEPES (25mM) in H_20	Immunocytochemistry
Sodium Tetraborate Buffer	$Na_2B_4O_7$ (0.1 M) in PBS (pH=8.5)	Immunohistochemistry

Solution	*Composition*	*Application*
Sodium Citrate Buffer	$C_6H_7NaO_7$ (0.01 M), Tween 20 (0.05%) in H_2O (pH=6.0)	Immunohistochemistry
PO_4 Buffer	NaH_2PO_4*$2H_2O$ (0.6 M), NaOH (0.67 M) in H_2O (pH=7.4)	Preparation of storing solution
Storage Solution	Glycerol (30%), ethylenglycol (30%) in PO_4 buffer (pH=7.4)	Long-term storage of brain sections

2.2 Experimental animals

Female and male adult mice (2-3 months old) of the following lines were used: C57Bl6/J, double transgenic mice obtained from crosses between $GLAST^{CreERT2}$ mice (Mori et al., 2006) and R26R-Confetti mice (Snippert et al., 2010) (referred to as GLAST/Confetti), homozygous knock-in $CCR2^{RFP/RFP}$ mice (Saederup et al., 2010) that result in a full knockout of the CCR2 gene (and therefore referred to as $CCR2^{-/-}$), Aldh1l1-eGFP OFC789Gsat (Gong et al., 2003) (referred to as Aldh1L1-eGFP), ACTB-eGFP (Okabe et al., 1997) (referred to as Actin-GFP), CAG-CAT-eGFP mice (Nakamura et al., 2006) (referred to as GFP-Reporter), and double transgenic mice obtained from crosses between $Emx1^{Cre}$ mice (Iwasato et al., 2000) and CAG-CAT-eGFP mice (Nakamura et al., 2006) (referred to as Emx1-GFP). All mice were housed in a 12:12h light-dark cycle and were provided with food and water *ad libitum*. For experiments with Aldh1L1-eGFP mice also 20 months old mice were used.

2.3 Genotypings

All transgenic animals were genotyped before being used in the experiments. For Actin-GFP mice, genotyping could be performed via direct identification of GFP fluorescence in animals or tissue samples by use of a BlueStar Flashlight and VG-1 filter glasses (NIGHTSEA). For all other transgenic lines, genotyping was performed through standard polymerase chain reaction (PCR) and the following DNA purification and amplification protocols were used:

2.3.1 Tissue digestion and DNA extraction

DNA extraction for genotyping was performed with technical support of Detlef Franzen. Firstly, either tail or ear clip samples were digested through incubation in 500 µl lysis buffer (*see Section 2.1*) containing 5 µl of proteinase K (100 µg/ml of buffer, Sigma P2308) overnight at 50 °C in a shaker at 700 rpm. Samples were then centrifuged at 12,000 rpm for 20 min at 4°C and the supernatant was transferred to a new tube. Next, 500 µl of isopropanol were added to each tube and samples were gently mixed by inverting the tubes. Samples were then centrifuged for 20 min at 12,000 rpm at 4°C in order to pellet the DNA. Supernatant was discarded and open tubes were placed upside down to dry for 5 min. Finally, the DNA was dissolved in 100 µl TE buffer (*see Section 2.1*) and incubated at 50°C for 30 min at 700 rpm. Samples were kept at 4°C until further processing.

2.3.2 Polymerase chain reaction

Standard polymerase chain reaction (PCR) was performed under specific conditions for each mouse line. The primers, reagent mix and PCR cycle conditions used for genotyping each mouse line are listed in detail below:

Table 2. Primers used for genotyping.

Mouse line	Gene	Primer ID	Sequence
GLAST/Confetti	*GLAST^{CreERT2}*	Primer F8	GAG GCA CTT GGC TAG GCT CTG AGG A
		Primer R3	GAG GAG ATC CTG ACC GAT CAG TTG G
		Primer CER1	GGT GTA CGG TCA GTA AAT TGG ACA T
	Rosa26 confetti mutant	Rosa26 confetti F	GAA TTA ATT CCG GTA TAA CTT CG
		Rosa26 confetti R	AGA GTA TAA AAC TCG GGT GAG C
	Rosa26 WT	Rosa26 WT F	CTC CTG GCT TCT GAG GAC C
		Rosa26 WT R	CCA GAT GAC TAC CTA TCC TC
CCR2$^{RFP/RFP}$	*CCR2*	CCR2 F	TAA ACC TGG TCA CCA CAT GC
		CCR2 WT R	GGA GTA GAG TGG AGG CAG GA
		CCR2 mut R	CTT GAT GAC GTC CTC GGA G
Emx1-GFP	*Emx1-Cre*	Cre F	GTG AGT GCA TGT GCC AGG CTT
		Cre R	TGG GGT GAG GAT AGT TGA GCG
		Test Cre	GCG GCA TAA CCA GTG AAA CAG
	CAG-CAT-eGFP	AG-2	CTG CTA ACC ATG TTC ATG CC
		CAT-2	GGT ACA TTG AGC AAC TGA CTG

Table 3. PCR solution mix for each gene.

	GLAST^{CreERT2}	***Rosa26 confetti***	***Rosa26 WT***	***CCR2***	***Cre mutant***	***Cre WT***	***eGFP***
H_2O	10 µl	19.8 µl	19.8 µl	10.5 µl	13.3 µl	13.3 µl	12 µl
25 mM MgCl	2.5 µl			2.5 µl			1.5 µl
Buffer (10x)	2.5 µl	2.5 µl (*)	2.5 µl (*)	2.5 µl	2.5 µl (*)	2.5 µl (*)	2.5 µl
Primer 1	F8: 1 µl	F: 0.5 µl	F: 0.5 µl	F: 0.5 µl	Cre F: 1 µl	Cre F: 1 µl	AG-2: 1 µl
Primer 2	R3: 0.5 µl	R: 0.5 µl	R: 0.5 µl	WT R: 0.5 µl	Cre R: 1 µl	Test Cre: 1 µl	CAT-2: 1 µl
Primer 3	CER1: 0.5 µl			mut R: 0.5 µl			
Q-Solution	5 µl			5 µl	5 µl	5 µl	5 µl
dNTPs	0.5 µl	0.5 µl	0.5 µl	0.5 µl	0.5 µl	0.5 µl	0.5 µl
Taq	0.5 µl	0.2 µl (*)	0.2 µl (*)	0.5 µl	0.2 µl (*)	0.2 µl (*)	0.5 µl
DNA	2 µl	1 µl	1 µl	2 µl	1 µl	1 µl	1 µl
End volume	25 µl	25 µl	25 µl	25 µl	25 µl	25 µl	25 µl

(*) Reagents from QIAGEN Taq DNA Polymerase kit (Cat No. 201203).

In every PCR batch we included a positive control (previously verified DNA sample), a negative control (wildtype DNA sample) and a DNA-free control (with water instead of DNA). These controls were used for the analysis of the results and to rule out any contaminations in the reaction.

Table 4. Thermocycler conditions for each PCR reaction.

	GLAST^{CreERT2}	*Rosa26 confetti*	*Rosa26 WT*	*CCR2*	*Cre mutant*	*Cre WT*	*eGFP*
Initialization	94°C, 5'	95°C, 5'	95°C, 5'	94°C, 2'	94°C, 5'	94°C, 5'	95°C, 5'
X cycles	35 X	35 X	35 X	10 X	36 X	36 X	30 X
i) Denaturation	94°C, 30''	95°C, 30''	95°C, 30''	94°C, 30''	94°C, 30''	94°C, 30''	95°C, 30''
ii) Annealing	56°C, 40''	60°C, 30''	60°C, 30''	65°C, 30''	64°C, 1'	64°C, 1'	55°C, 30''
iii) Elongation	72°C, 40''	72°C, 45''	72°C, 45''	72°C, 30''	72°C, 30''	72°C, 30''	72°C, 1'
X cycles				25 X			
i) Denaturation				94°C, 30''			
ii) Annealing				52°C, 30''			
iii) Elongation				72°C, 30''			
Final elongation	72°C, 5'	72°C, 7'	72°C, 7'	72°C, 2'	72°C, 5'	72°C, 5'	72°C, 10'
Final hold	4°C, ∞	4°C, ∞	4°C, ∞	4°C, ∞	16°C, ∞	16°C, ∞	4°C, ∞

2.3.3 Gel electrophoresis

10 µl of each PCR product were ran at 100-120V for approximately one hour in 2% agarose gel containing ethidium bromide or SYBR Safe for visualization of DNA bands. Detection of DNA bands was performed with UV-light.

2.4 Tamoxifen induction

GLAST/Confetti mice received in total 3 intraperitoneal (i.p.) injections of 80 µg tamoxifen per gram of body weight (stock solution: 20 mg/ml tamoxifen in corn oil with 10% ethanol mixed by sonication for 15 min), which were delivered every other day within the period of 5 days. After the last tamoxifen injection there was a waiting period of 7 days before an injury was performed.

2.5 Surgical procedures

All surgical procedures were performed in compliance with animal welfare policies and approved by the Government of Upper Bavaria under the license numbers 55.2-1-54-2532-171-2011 and 55.2-1-54-2532-210-2016.

All mice undergoing surgery were anesthetized with an intraperitoneal injection of midazolam (5 mg/kg of body weight), medetomidine (0.5 mg/kg) and fentanyl (0.05 mg/kg). Bepanthen (Bayer) was administered to the eyes to prevent dryness and damage. Animals undergoing surgical procedures in the brain were shaved on the top of the head and, after fixing the mouse to a stereotactic apparatus, an incision was made on the head and lidocain gel 2% was applied on the skull surface briefly for local anesthesia. Next, the procedure for each type of surgery was performed as described in detail below. At the end of all surgical procedures, anesthesia was antagonized with an i.p. injection of atipamezol (2.5 mg/kg), flumazenil (0.5 mg/kg) and buprenorphine (0.1 mg/kg), and animals were left to recover on a heating pad until they were fully awake. Meloxicam (1 mg/kg) was administered as a postoperative analgesic for 3 days following surgery.

2.5.1 Stab wound lesion

A unilateral craniotomy was performed between bregma and lambda cranial sutures to expose the surface of the brain. Stab wound (SW) was inflicted by inserting a V

lancet-shaped knife (19 gauge, Alcon) into the somatosensory cortex gray matter using the following coordinates from bregma:

Medio-lateral (x): between +1.8 and +2.0 mm
Antero-posterior (y): from -0.8 to-2.0 mm
Dorso-ventral (y) (from the surface of the brain): -0.6 mm

The craniotomy was covered once more with the skull flap and the skin was sutured. For animals in repetitive lesions experiments the second injury was performed either 5 days (for neurosphere culture experiments) or 14 days (for all other experiments) after the first one in the same manner and on the same location. This was achieved with high precision by following the coordinates and by using recorded information of blood vessels as landmarks to assist on recognizing the injury site. For neurosphere assay experiments, animals were sacrificed 5 days after the last injury, which is the time point where astrocyte proliferation *in vivo* reaches its peak and neurosphere culture yields the greatest number of spheres. In all other SW experiments animals were sacrificed 24 days after the first lesion for the analysis of BrdU and EdU cells labeled *in vivo*.

2.5.2 Transplantation in adult mice

For analysis of the differentiation potential of reactive astrocytes and aNSCs in the neurogenic niches of the adult murine brain, we transplanted neurosphere-derived cells from the injured cortex and SEZ of actin-GFP mice into the SEZ and DG of adult C57Bl6/J mice. Firstly, coordinates for transplantation sites were taken with a Hamilton syringe and a superficial and small hole was drilled on the skull above each transplantation site. The dura was perforated with a syringe and cells were transplanted into both neurogenic niches using the following coordinates from bregma:

<u>SEZ:</u>
Medio-lateral (x): ±1.2 mm
Antero-posterior (y): +0.7 mm
Dorso-ventral (z) (from the surface of the brain): -from -1.9 to -1.7 mm

<u>DG:</u>
Medio-lateral (x): ±1.6 mm
Antero-posterior (y): -2.0 mm

Dorso-ventral (z) (from the surface of the brain): -from -2.1 to -1.9 mm

A total of 15,000 donor cells in a 1 µl volume were transplanted into each site. The cell suspension was injected with a Hamilton syringe (33 gauge) and distributed dorso-ventrally over 300 µm in 3 injection points. To have an internal control for our experiments, cells coming from both sources (injured cortex and SEZ) were always transplanted in the same animal, but in different brain hemispheres. Transplanted animals were perfused at 2 or 4 weeks post transplantation (wpt) for immunohistochemical analysis of cell differentiation.

2.5.3 Transplantation in E13 embryos

All embryo transplantations were performed by Dr. Sven Falk. Briefly, timed pregnant females at E13 stage were anaesthetized as described above and fixed to a heating pad covered with a sterile diaper pad. Females were fixed to the pad with tape, the abdominal fur was cleared out with hair removal cream and an incision was made on the abdomen, through which the uterine horns containing embryos were exposed. Embryos were kept hydrated with sterile PBS while exposed out of the body cavity. Cell suspensions were mixed with FastGreen FCF 1% w/v and injected with a glass capillary though the uterine wall into the lateral ventricle of the developing embryo brains. A total of 6 embryos were injected per surgery, and for each pregnant female, cells from only one source (either injured cortex or SEZ) were used for injections. After completion of injections, the uterine horns were carefully returned to the body cavity, and both the muscle layer and the skin were sutured. Anesthesia was antagonized as described above. Transplanted animals were perfused at 2 or 4 wpt (at P7 and P21 developmental stages) for immunohistochemical analysis of cell differentiation.

2.5.4 Virus injections

For analysis of the origin of neurosphere forming cells isolated from cortical tissue, we injected viruses on the somatosensory cortex gray matter to label resident cells and latter performed SW surgery, followed by neurosphere assay with tissue from the injured cortex.

Viral injections were performed unilatery at the following coordinates from bregma:

Medio-lateral (x): +2.0 mm

Antero-posterior (y): -1.4 mm

Dorso-ventral (z) (from the surface of the brain): between -0.7 and -0.5 mm

A small and superficial hole was drilled following the coordinates, and a volume of 0.5 to 1 µl of virus was injected with a glass capillary at a rate of 30 nl/min.

Viral production was performed with technical support of Ines Mühlhahn and Dr. Chulan Lao. The following viruses were used for these experiments:

i. AAV-gfaABC1D-tdTomato (referred to as AAV-tdTomato) (Shigetomi et al., 2013)

ii. (rAAV2/5) pAAV-gfaABC1D-iCre (referred to as AAV-iCre) (Druckmann et al., 2014)

After undergoing viral injection, animals were either perfused 3 weeks later for immunohistochemical analysis of cell labeling in the uninjured brain, or underwent SW surgery 2 weeks after injection. In the latter case, animals were either perfused for immunohistochemical analysis or had live tissue isolated for neurosphere assay experiments at 5 days post injury.

2.6 BrdU and EdU labeling

5-bromo-2'-deoxyuridine or BrdU (Sigma) and 5-ethynyl-2'-deoxyuridine or EdU (Thermo Fisher) are thymidine analogues that get incorporated into the cell's DNA upon replication and therefore were used to label proliferating cells. BrdU and EdU were administered to the animals via drinking water containing 1% sucrose at a concentration of 1 mg/ml and 0.2 mg/ml, respectively. In all animals used for immunostaining analysis, BrdU water was administered for the first 10 days after SW, followed by a 4-day washout period in which animals only received regular water, followed once more by a 10-day labeling period in which animals received EdU water. Exceptions to this protocol were performed in experiments designed as controls for BrdU/EdU labeling and detection. To check for specificity of BrdU and EdU detection and rule out the existence of cross-reactivity of antibodies and chemical reaction detection methods, animals received either BrdU or EdU in drinking water for 5 days, or BrdU and EdU sequentially in drinking water, each for 5 days. To check whether there were differences in the sensitivity of detection or in the incorporation of both thymidine analogues, an animal received both

BrdU and EdU combined in drinking water for 5 days. To analyze whether the order of delivery of the thymidine analogues could have an effect in their incorporation, an animal was given BrdU and EdU water in an inverse order (EdU water in the first, and BrdU water in the second time frame). Finally, to investigate whether the interaction between both thymidine analogues could have toxic effects on the cells, a group of animals received only BrdU water for both time frames.

2.7 Neurosphere culture

2.7.1 Neurosphere assay

Animals were sacrificed by cervical dislocation and brains were collected in ice-cold Hank's Balanced Salt Solution (HBSS, Thermo Fisher) buffered with 10mM HEPES (Thermo Fisher). Tissue from intact and injured somatosensory gray matter was isolated by removing an area of 1.25 mm in radius from the lesion site with a punch and subsequently removing the remaining white matter and meninges with a forceps. Tissue from SEZ was isolated by separating both brain hemispheres with a sagital cut using a scalpel, and accessing the lateral ventricule wall by removing the hippocampus with a fine forceps. A thin layer of anterior SEZ tissue was then dissected with the forceps. All samples were immediately immersed in 0.5 to 1 ml neurosphere medium (*see Section 2.1*) (all components from Thermo Fisher) after collection. Samples were gently mechanically dissociated and subsequently digested with Trypsin (0.025%) (Thermo Fisher) for 20 min at 37 °C and enzymatic digestion was stopped with a protease inhibitor solution (*see Section 2.1*) (all components from Sigma, except for DNaseI from Worthington). Cells were centrifuged at 1500 rpm for 5 min, resuspended in neurosphere medium containing FGF-2 and EGF growth factors and plated at a density of 5 cells/µl in 24-well cell culture plates for neurosphere quantification or in 25cm^2 culture flasks for growing neurospheres for transplantation. Neurospheres were quantified at 14 days *in vitro* (div). To assess self-renewal, neurospheres were subsequently passaged and quantified. Neurosphere suspensions were collected and centrifuged for 5 min at 1500 rpm and resuspended in Trypsin (0.125%) (Thermo Fisher) and incubated for digestion at 37°C for 15 min. Cells were then processed in the same way as described above.

For dissection of cortical tissue of GFP-Reporter mice injected with AAV-iCre, only the tissue with GFP expression was extracted. This was performed via direct

identification of GFP fluorescence in the brain by use of a BlueStar Flashlight and VG-1 filter glasses (NIGHTSEA) during dissection.

2.7.2 Differentiation assay

To assess the differentiation potential of neurospheres, these were picked with a 20 µl pipette and plated on glass coverslips previously coated with 100 µg/ml poly-L-ornithine (Sigma) and 20 µg/ml laminin (Roche). The neurospheres were kept for 7 days in differentiation medium (*see Section 2.1*) containing 1% fetal bovine serum (PAN-Biotech) and in the absence of growth factors, and were analyzed via immunocytochemistry for the determination of neurosphere cell composition.

2.7.3 Dissociation of neurospheres for transplantation

Single cell suspensions for transplantation experiments were prepared from neurosphere cultures from the injured cortex and SEZ cultured 14 div. First, the entire content of the culture flasks (5 mL per flask) was transferred to 15 ml Falcon tubes and centrifuged for 5 min at 1500 rpm. The supernatant was discarded and cells were resuspended in 500 µl Trypsin (0.0625%). Cells from the SEZ were incubated for 8 min at 37°C, and cells from the injured cortex for 15 min. Digestion was stopped by addition of 1 ml of protease inhibitor solution (*see Section 2.1*), for 5 min at room temperature. Cell suspensions were centrifuged for 4 min at 800 rpm, the supernatant was discarded and cells were resuspended and counted on the Neubauer chamber with addition of 1:1 trypan blue. Cell suspensions were transferred to 0.5 ml Eppendorf tubes and centrifuged for 5 min at 1000 rpm. Finally, the supernatant was discarded and each cell pellet was resuspended in a calculated volume of neurosphere medium to achieve an end single cell suspension of 15,000 cells/µl.

2.8 Immunocytochemistry

After 7 days of differentiation, neurospheres were incubated in Krebs-Ringer-Hepes Buffer (*see Section 2.1*), containing 0.1% bovine serum albumin (Sigma) for 5 min, followed by incubation with mouse IgM anti-O4 antibody for 20 min, washing and subsequential fixation with PFA 4% (*see Section 2.1*) for 5 min. Neurospheres were then incubated with mouse IgG2b anti-βIII-tubulin and rabbit anti-GFAP primary antibodies for 20 min, followed by washing and incubation with species- and subclass-specific

fluorophore-coupled secondary antibodies (1:500) for 20 min, and lastly, incubated for 5 min with DAPI (1:10,000, Sigma, D9542) for nuclear labeling and mounted on glass slides with Aqua-Poly/Mount (Polysciences). Detailed information of all primary antibodies used for immunocytochemistry of differentiated neurospheres is listed on the tables below:

Table 5. Primary antibodies used for immunocytochemistry.

Antigen / clone	*Host / isotype*	*Dilution*	*Company*	*Catalogue number*
ß III Tubulin	mouse IgG m2b	1:250	Sigma	T8660
O4	mouse IgM	1:50	Sigma	O7139
GFAP	rabbit	1:500	Agilent (Dako)	Z0334

2.9 Perfusion and brain sectioning

Mice were deeply anesthetized with an intraperitoneal injection of ketamine 100 mg/ml and 2% xylazin (0.01 ml/g body weight) and transcardially perfused with ice-cold PBS (*see Section 2.1*) followed by 4% PFA (*see Section 2.1*) for 20 min each. Stab wound-injured wildtype (WT) and $CCR2^{-/-}$ mice brains were post-fixed in 4% PFA for 2 h and incubated in sucrose 30% in PBS overnight for dehydration and cryoprotection. These brains were sectioned with the cryostat in 40 µm thick coronal slices. Brains from GLAST/Confetti mice and C57Bl6/J from transplantation experiments were post-fixed in 4% PFA overnight, embedded in 4% agarose blocks and sectioned in 60 µm thick slices in the vibratome. GLAST/confetti brains were sectioned coronally and transplanted C57Bl6/J brains were sectioned sagitally. All sections were kept in free floating for further processing. For long-term preservation, sections were kept in storage solution (*see Section 2.1*) and maintained at -20°C.

2.10 Immunohistochemistry and EdU detection

Sections were blocked and permeabilized by incubation in PBS (*see Section 2.1*) containing 0.5% TritonX-100 (Sigma) and 10% normal goat serum (Thermo Fisher) for 1 h at room temperature. EdU detection was then performed with the Click-iT Edu Alexa Fluor 647 Imaging Kit (Thermo Fisher, C10340), by incubation with the reaction mix for 45 min at room temperature. EdU detection was always performed before incubation with all other antibodies, except for when combined with GFP immunohistochemistry (GLAST/Confetti clonal analysis experiment), in which case EdU detection was

performed afterwards (following manufacturer's instructions). Immunohistochemistry was carried out using the following primary antibodies, which were incubated overnight on a tabletop shaker at 4°C for 40 µm thick sections and over two nights for 60 µm thick sections:

Table 6. Primary antibodies used for immunohistochemistry.

Antigen / clone	*Host / isotype*	*Dilution*	*Company*	*Catalogue no.*	*Pre-treatment*
ACSBG1	rabbit	1:350	Abcam	ab65154	
Aldh1L1	mouse IgG1k	1:200	Merck/Millipore	MABN495	citrate 96°C 20 min
BrdU BU1/75	rat	1:200	Biozol	BZL20630	citrate 96°C 20 min
BrdU BU-33	mouse IgG1	1:200	Sigma	B2531	HCl 2N at RT 30 min
CD31	rat	1:50	BD / Bioscience	550274	
DCX	guinea pig	1:200	Merck/Millipore	AB2253	
GFAP	rabbit	1:250	Agilent (Dako)	Z0334	
GFAP	mouse IgG1	1:500	Sigma	G3893	
GFP	chicken	1:400	Aves Labs	GFP-1020	
Iba1	rabbit	1:500	Wako	019-19741	
Ki67	rat	1:300	Agilent (Dako)	M7248	
NeuN	mouse IgG1	1:250	Merck/Millipore	MAB377	
NG2	rabbit	1:400	Merck/Millipore	AB5320	
Olig2	rabbit	1:250	Merck/Millipore	AB9610	
RFP	rabbit	1:500	Rockland	600-401-379	
S100ß	rabbit	1:250	Sigma	S2644	

Next, sections were washed in PBS and incubated with species- and subclass-specific secondary antibodies used at 1:500 and incubated on a tabletop shaker for 3 h at room temperature. Finally, all sections were incubated for 15 min with DAPI (1:1000, Sigma, D9542) for nuclear labeling and mounted on glass slides with Aqua-Poly/Mount (Polysciences).

2.10.1 DNA denaturation with hydrogen chloride

For specific BrdU immunohistochemistry (without cross-reactivity with EdU), sections were firstly immunostained with antibodies for other antigens (e.g. GFAP, Iba1, NG2), as well as stained for EdU before acid treatment for DNA denaturation. Sections were fixed with 4% PFA (*see Section 2.1*) for 10 min, washed with PBS and incubated with 2N HCl for 30 min at room temperature on a tabletop shaker. Next, sections were incubated in sodium tetraborate buffer 0.1 M (*see Section 2.1*) for 30 min, washed, and

immunohistochemistry was performed with mouse IgG1 anti-BrdU clone BU33 and secondary antibody to mouse IgG1 Alexa Fluor 555 as described above.

2.10.2 Antigen retrieval with citrate treatment

For immunohistochemistry using the mouse IgG1k anti-Aldh1L1 or rat anti-BrdU clone BU1/75 (which detects both BrdU and EdU) antibodies, sections underwent citrate treatment for antigen retrieval. For this end, immunohistochemistry was performed with other antibodies (e.g. GFP, RFP, GFAP) as described above and sections were fixed with 4% PFA for 10 min, washed and then incubated in 0.01 M sodium citrate buffer (*see Section 2.1*) for 20 min at 96 °C in a dry bath. Sections were then washed in PBS and incubated with mouse IgG1k anti-Aldh1L1 or rat anti-BrdU clone BU1/75 and respective species- and subclass-specific fluorophore-coupled secondary antibodies as described above.

2.11 Confocal microscopy

Images were acquired using a laser-scanning confocal microscope (Zeiss, LSM 710), and analyzed with ImageJ 1.49g software. Immunohistochemistry quantifications were performed with the Cell Counter plug-in for Image J 1.49g, by careful inspection across serial optical sections (spaced at 1.5 µm) of confocal Z-stacks acquired with a 25× or 40× objective.

2.12 Purification of cells using Fluorescence-Activated Cell Sorting

Cells from young (2 months-old) and old (20 months-old) injured Aldh1l1-eGFP mice were dissociated at 5 dpi from the grey matter of the somatosensory cortex using the same procedure as described above for the neurosphere culture. Following dissociation, cells were resuspended in neurosphere medium lacking growth factors (s*ee Section 2.1*) and filtered with a 40 µm strainer. Prior to sorting, cell viability of a wild type sample processed in parallel was determined via staining with propidium iodide (1:1000, Sigma). Aldh1l1-eGFP^{+} cells were isolated by fluorescence-activated cell sorting (FACSAria, BD) with a 488 nm laser and 530/30 BP filter. Gating parameters were set by side and forward scatter to eliminate debris and aggregated cells. Gating settings for GFP

fluorescence were set with a WT sample processed in parallel. Cells were sorted into RNAse-free eppendorfs containing RLT buffer with 1% ß-mercaptoethanol and further processed for qPCR analysis.

2.13 RNA extraction and quantitative RT-PCR

RNA from FACS-sorted cells was extracted with the RNeasy Plus Micro Kit (QIAGEN) according to manufacturer's instructions, and genomic DNA was removed via enzymatic reaction. The extracted RNA was then retro-transcribed with SuperScriptIII Reverse Transcriptase and Random Primers (Roche). Quantitative qPCR was performed on a LightCycler480 (Roche) with the LightCycler Probe Master kit (Roche) and Monocolor Hydrolysis Probe (Roche), and all solutions were prepared according to manufacturer's instructions. The expression of each gene was analyzed in technical triplicates per biological sample. Each biological sample consisted on a pool of cells from 3 animals per age-group. Data was processed with the ΔΔCt method (Livak and Schmittgen, 2001). Detailed information about the primers and probes used for the qPCR is listed in the table below:

Table 7. Primers and probes used for qPCR analysis.

Gene	*Access number*	*Primer Forward*	*Primer Reverse*	*UPL*
HRPT	NM_013556.2	tcctcctcagaccgctttt	cctggttcatcatcgctaatc	95
Ccdn1	NM_007631.2	gagattgtgccatccatgc	ctcctcttcgcacttctgct	67
GFAP	NM_010277.3	acagactttctccaacctccag	ccttctgacacggatttggt	64
Ptch1	NM_008957.2	ggaaggggcaaagctacagt	tccaccgtaaaggaggctta	56
Smo	NM_176996.4	gcaagctcgtgctctggt	gggcatgtagacagcacaca	3

2.14 Statistical analysis

Statistical analysis was performed using PRISM (Graphpad, v5.03). Appropriate statistical tests were chosen depending on sample size, data distribution and number of comparisons. All data consisting of two groups (e.g. WT mice, single versus repetitive injuries) were analyzed with the non-parametric Wilcoxon-Mann-Whitney test. For comparisons of more than 2 groups (WT and CCR2$^{-/-}$ on both injury conditions, as well as data from neurosphere cultures), analysis was performed with one-way ANOVA and non-parametric Dunn's post-hoc test. The minimum level of significance was defined as

$P < 0.05$ and all values in dot plots are reported as median ± interquartile range (IQR), and values in pie charts are reported as mean ± standard deviation (SD). Image processing was performed with ImageJ and Adobe Illustrator CS6 (Adobe Systems) for preparation of multipanel figures.

3 Results

3.1 Modulation of the proliferative behavior of reactive astrocytes via repetitive pathological stimuli

3.1.1 Thymidine analogue-based analysis of cell proliferation following repetitive injuries: dual-labeling with BrdU and EdU

In order to assess whether and to which extent a larger number of astrocytes *in vivo* could be stimulated to proliferate, and, in particular, whether the same astrocytes may proliferate several times or self-renew, we analyzed the acquisition of cycling activity of reactive astrocytes in response to a repetitive pathological event in the adult cerebral cortex gray matter. For this purpose, we used a dual-labeling strategy to follow cycling cells during S-phase *in vivo* by combining two thymidine analogues, 5-bromo-2'-deoxyuridine (BrdU) and 5-ethynyl-2'-deoxyuridine (EdU) at different time periods after SW injury in the somatosensory cortex gray matter.

Thymidine analogues have been long used as a tool to study cell proliferation, and were particularly valuable for early studies providing evidence for adult mammalian neurogenesis (Altman, 1962; Altman and Das, 1965). This tool works on the basis that cells incorporates thymidine analogues indiscriminately into the DNA upon synthesis and the correlation between analogue incorporation and cell cycling activity has been confirmed by co-labeling with other known mitotic markers, such as Ki-67 (Kee et al., 2002). Therefore, this tool allows one to label cells that were mitotically active on the time point during which the analogue was at the cell's disposal.

As our goal in this study was to analyze the dynamics of astrocyte proliferation following multiple injuries, we took advantage of the distinct properties of the two thymidine analogues we used in order to develop an experimental paradigm that would allow us to answer our scientific questions. Both analogues - BrdU and EdU - can be detected separately through antibody binding and a chemical reaction, respectively. In order to effectively use this dual-labeling method to define the cycling activity of reactive

astrocytes according to the time frame of BrdU and/or EdU incorporation it is essential to be able to detect each of the analogues in a precise manner.

We had to first establish this dual labeling method in our experimental setting, and therefore it was crucial to ascertain we could effectively and reliably label and detect the cells within the paradigm.

To check for specificity of BrdU and EdU detection and rule out the cross-reactivity of antibodies and chemical reaction detection methods, we performed immunohistochemical analysis and stainings in coronal sections of animals that received BrdU and/or EdU in drinking water and analyzed the labeling of cells in the SEZ, a region with abundant proliferative activity in the adult murine brain (Figure 3A). More specifically, we analyzed if EdU chemical reaction could detect BrdU-labeled DNA and if BrdU antibody could detect EdU-labeled DNA (Figure 3B).

In animals that received only one of the analogues in drinking water we could not identify any cross-reactivity on the detection of the other analogue, being it BrdU or EdU (Figure 3C,D). Furthermore, when we delivered BrdU and EdU sequentially in drinking water we could identify cells that were single labeled ($BrdU^+$ or EdU^+) and also double labeled cells ($BrdU^+/EdU^+$) (Figure 3E), indicating that our labeling and detection protocols are suitable for tracing cell proliferation to a precise temporal frame of BrdU and EdU delivery.

In order to evaluate if the incorporation affinity and detection of both thymidine analogues were comparable, we analyzed the pattern of labeled cells in the SW lesion of the cortical gray matter of an animal that received both BrdU and EdU combined in drinking water after SW injury (Figure 4A,B). Immunohistochemical quantitative analysis indicated that, regardless of cell type, the vast majority of proliferating cells in the lesion area were double labeled ($BrdU^+/EdU^+$), indicating no difference in BrdU and EdU incorporation as well as sensitivity of the detection methods used (Figure 4C).

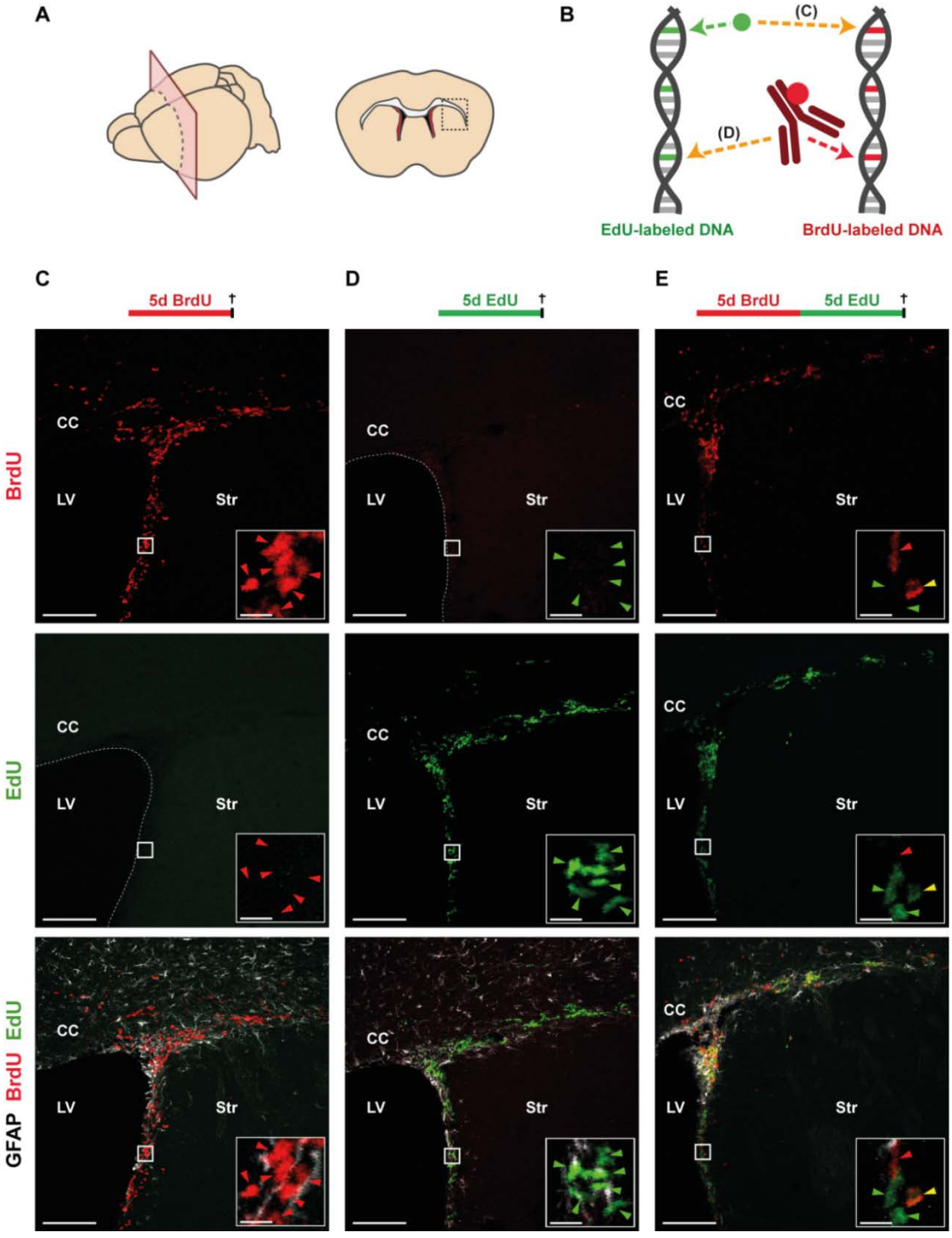

Figure 3. Specific detection of cycling cells using dual-labeling of BrdU and EdU *in vivo*. (**A**) Controls for cross-reactivity in BrdU/EdU detection were performed in coronal sections of the SEZ, a region with abundant proliferative activity. (**B**) BrdU and EdU are thymidine analogues that get incorporated into the DNA upon replication and can be detected via antibody immunohistochemistry and fluorophore labeling via chemical reaction, respectively. We investigated whether EdU detection reaction could bind to BrdU-labeled DNA (c) or vice-versa (d). (**C**) EdU detection reaction did not cross-react with BrdU in an animal that received only BrdU in drinking water, and (**D**) BrdU antibody did not bind to EdU in a mouse that received only EdU. (**E**) When BrdU and EdU were delivered sequentially, we could identify cells that were single labeled for $BrdU^+$ (red arrowheads) or EdU^+ (green arrowheads), and double labeled $BrdU^+/EdU^+$ cells

(yellow arrowheads). Scale bars represent 100 μm and 10 μm on inlays. LV: lateral ventricle, CC: corpus callosum, Str: Striatum.

To analyze whether the order of delivery of the thymidine analogues could have an effect in their incorporation into the DNA, an animal was delivered BrdU and EdU water in an inverse order (EdU water in the first, and BrdU water in the second time frame), and the number of labeled cells was similar regardless of the order of BrdU/EdU delivery (Figure 4D,E,G). Lastly, to investigate whether the interaction between both thymidine analogues could have toxic effects on astroglial cells ($GFAP^+$) that incorporate them, a group of animals received only BrdU water for both time frames, and showed similar numbers of labeled cells than the animals that received both thymidine analogues in a sequential manner (Figure 4F,G).

Altogether, we could confirm that our dual-labeling method based on BrdU and EdU thymidine analogue delivery is a good tool to investigate the dynamics of the astrocyte proliferative pool following injury, since both analogues can be identified in a precise and reliable manner, which allows us to trace the injury-induced proliferative response of cells in a temporally defined manner.

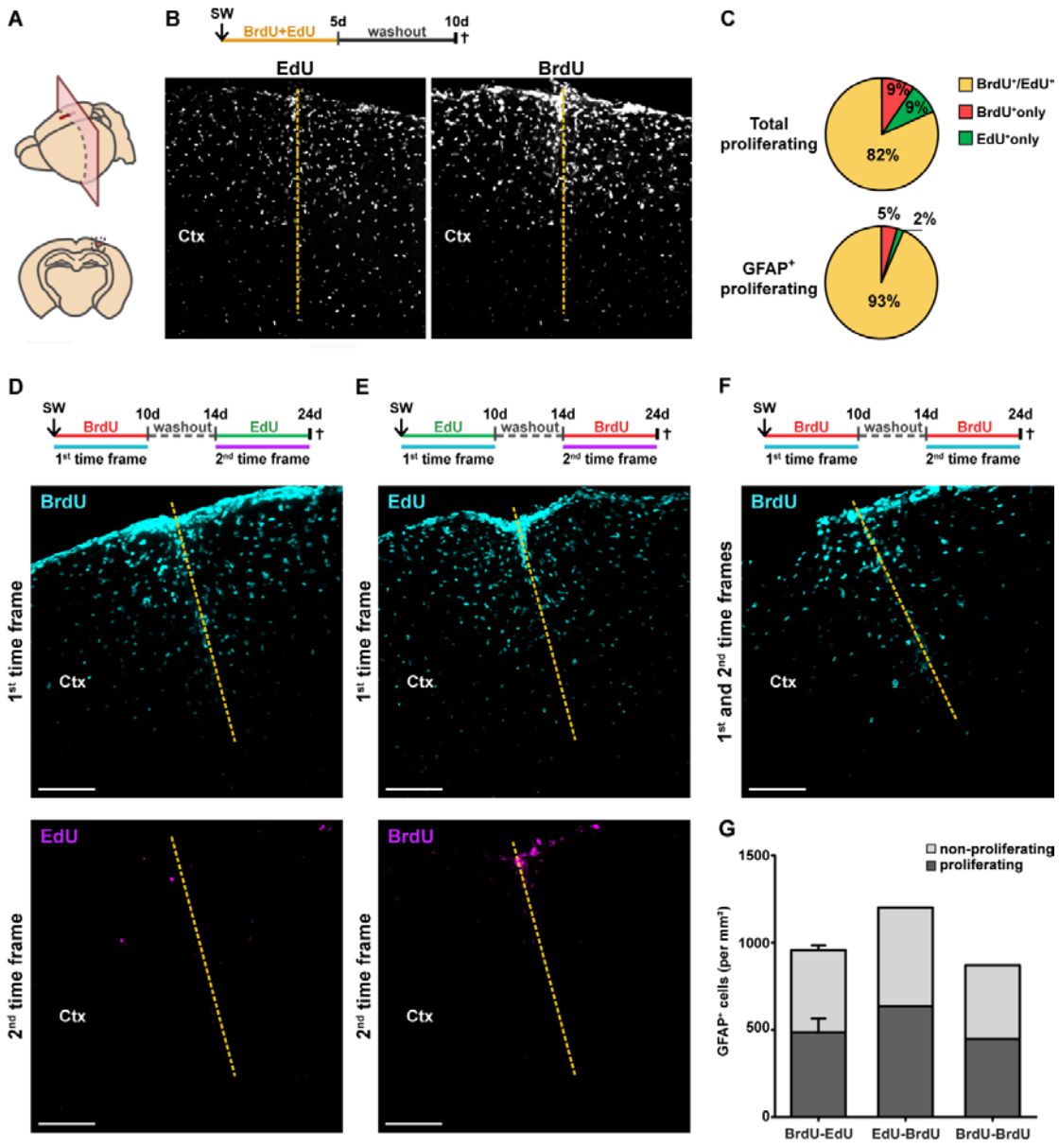

Figure 4. BrdU and EdU have similar incorporation profiles and detection sensitivity. (**A**) We analyzed BrdU and EdU incorporation in coronal sections of the injured somatosensory cortex. (**B**) When BrdU and EdU were administered together in drinking water there were no major differences in their detection sensitivity. (**C**) When both analogues were delivered together in drinking water, quantifications depict that the majority of detected proliferating cells were double-labeled ($BrdU^+/EdU^+$), both in the total and also within the astrocytic population ($GFAP^+$). (**D,E**) Administration of BrdU and EdU in different sequential orders yielded similar results in the detection of proliferating astrocytes. (**F**) Administration of BrdU in both time periods yielded a similar labeling pattern, suggesting a lack of toxicity effects that could arise from the incorporation of two different thymidine analogues by proliferating cells. (**G**) Quantifications of the three different BrdU/EdU administration paradigms show comparable numbers of labeled cycling astrocytes ($GFAP^+$ proliferating cells). Data is depicted as mean ± SD. Scale bars represent 100 μm. Yellow dashed line indicates the lesion site. SW: stab wound lesion, Ctx: cortex.

3.1.2 Repetitive injuries induce changes in the proliferative repertoire of cortical gray matter astrocytes

In order to investigate whether parenchymal astrocytes were able to self-renew *in vivo* or if we could modulate a change in the proliferative behavior of the astrocytic pool, we decided to provide stimuli that are known to trigger astrocyte proliferation, namely the SW lesion. To challenge and boost proliferative response in these cells, we delivered two SW lesions sequentially into the same location in order to stimulate a certain population of astrocytes with both lesions. We compared the results to single-lesioned animals in order to analyze changes in astrocyte proliferation in response to the second lesion.

To analyze the cycling activity of cortical gray matter astrocytes in response to single or repetitive injuries, we delivered BrdU and EdU in separate time frames following lesion and performed a pulse-chase analysis. In this way, we were able to characterize the proliferative profile of astrocytes according to their temporal proliferation pattern (Figure 5A). More specifically, we could identify different subsets of proliferative astrocytes according to the time frame in which they went through cell division ($BrdU^+$, EdU^+ or $BrdU^+/EdU^+$ labeled cells) (Figure 5A).

Quantitative analysis of reactive astrocytes ($GFAP^+$ cells) around the lesion site surprisingly showed that the total numbers of reactive astrocytes were similar after single or repetitive injuries, suggesting the existence of a mechanism for restoration and maintenance of the astrocytic population at homeostatic numbers following multiple injuries (Figure 5B).

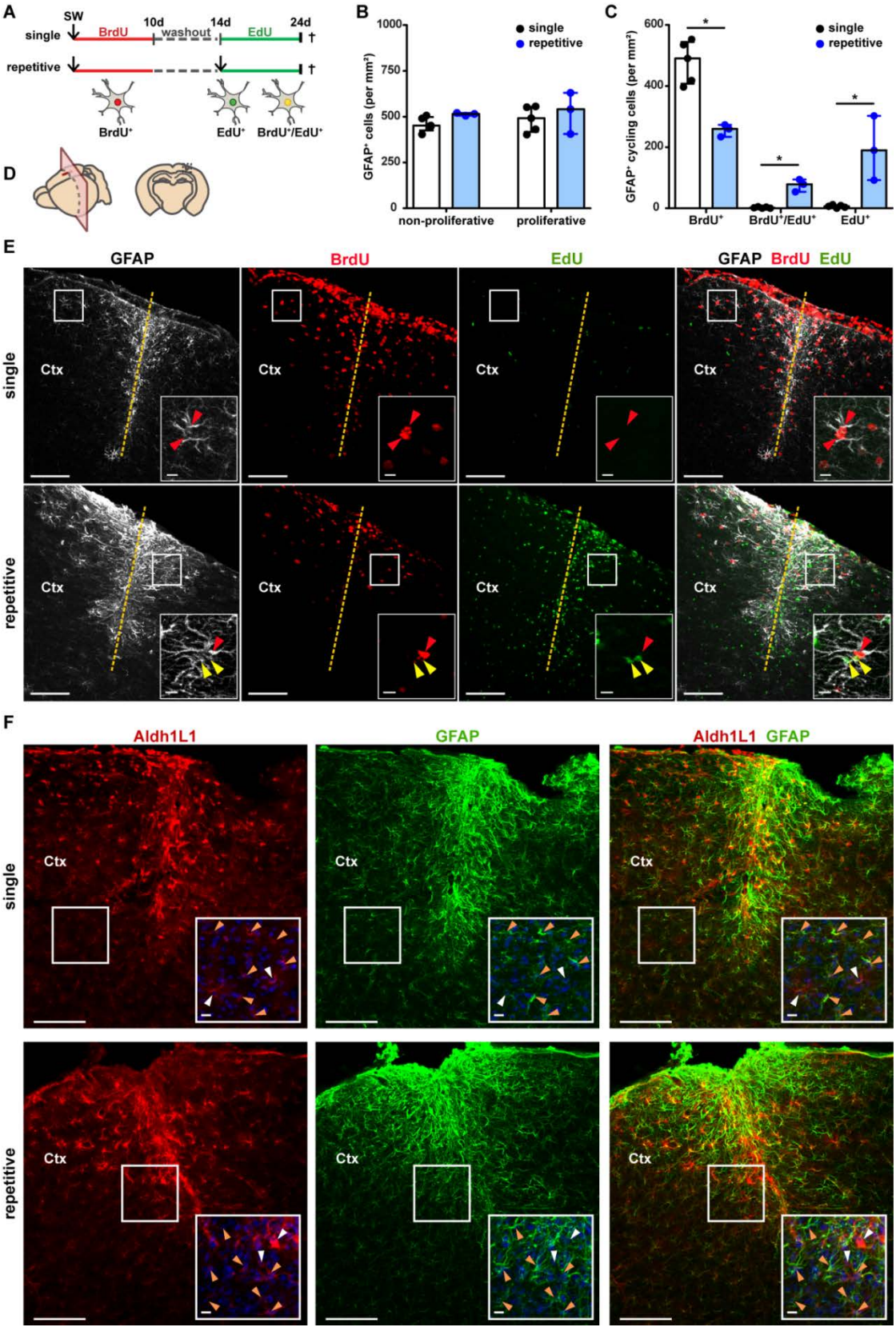

Figure 5. Repetitive injuries induce changes in astrocyte proliferative behavior. (**A**) The experimental paradigm used to analyze astrocyte proliferation in response to single and multiple pathological stimuli consisted on sequential BrdU and EdU labeling with long-term detection of cycling cells. This paradigm allowed us to detect 3 different groups of cycling cells according to the

time of proliferation ($BrdU^+$, EdU^+ and $BrdU^+/EdU^+$). (**B**) Numbers of total and proliferating reactive astrocytes ($GFAP^+$ cells) on the lesion site were similar on both injury conditions. (**C**) Repetitive injuries led to an increase in cell division rate ($GFAP^+/BrdU^+/EdU^+$) as well as recruitment of previously quiescent astrocytes into proliferation ($GFAP^+/EdU^+$), together with a decrease in the numbers of the astrocytes that proliferated only in response to the first lesion ($GFAP^+/BrdU^+$) (*P=0.0357) (**D,E**) Representative immunostainings from coronal sections within the lesion site depict the area used for cell quantifications. A second injury induced marked proliferation around the lesion site (EdU^+ cells). Arrowheads indicate single positive $BrdU^+$ cells (in red), single positive EdU^+ cells (in green) and double positive $BrdU^+/EdU^+$ cells (in yellow). Yellow dashed line indicates the lesion site. (**F**) The vast majority of astrocytes ($Aldh1L1^+$) around the lesion site were $GFAP^+$. The few $Aldh1L1^+/GFAP^-$ astrocytes are indicated by white, and $Aldh1L1^+/GFAP^+$ astrocytes by orange arrowheads. Data is depicted as median ± IQR. Scale bars represent 100 μm and 10 μm on inlays. SW: stab wound lesion, Ctx: cortex.

Although the numbers of proliferating reactive astrocytes were similar on both injury conditions, the composition of their proliferative pool showed marked changes upon a second microlesion (Figure 5C-E). Following a single lesion, virtually all cycling astrocytes showed proliferative activity within 10d after injury ($GFAP^+/BrdU^+$ cells, Figure 5C), consistent with previous observations by live *in vivo*-imaging after SW injury in the cortical gray matter (Bardehle et al., 2013). However, a second lesion induced proliferation of previously quiescent astrocytes ($GFAP^+/EdU^+$), and induced a subset of astrocytes to reenter the cell cycle ($GFAP^+/BrdU^+/EdU^+$) (Figure 5C). These results show for the first time that the proliferative capacity of astrocytes is not ultimately limited to a particular subset of parenchymal astrocytes, and that some astrocytes can proliferate more than once in response to subsequent pathological stimuli.

GFAP is not expressed in immunohistochemically detectable levels by all astrocytes in the healthy CNS and as it is upregulated upon injury or inflammation, and therefore is used as a cell marker for astrocyte reactivity. Since we observed similar numbers of $GFAP^+$ cells in both injury conditions, we evaluated if this could arise due to a change of GFAP expression in astrocytes or if the total numbers of astrocytic cells at the lesion site was indeed the same in these conditions. For that, we performed immunohistochemical analysis at the lesion site with Aldh1L1, a global astrocytic marker (Cahoy et al., 2008), and evaluated if GFAP labeling covered the whole astrocytic population in the penumbra. We observed that in the vicinity of the lesion in both injury paradigms there were only very few astrocytes identified with the global Aldh1L1 astrocytic marker that did not express GFAP ($Aldh1L1^+/GFAP^-$ cells, representing less than 2% of all Aldh1L1 cells) (Figure 5F). Therefore our analysis based on GFAP immunohistochemistry comprises the total astrocytic population in the lesion site.

Our observations thus suggest the existence of mechanisms modulating the transition of reactive astrocytes into the proliferative state to ensure the maintenance of

astrocyte population homeostasis, similar to the homeostatic regulation that has been described for NG2-glia and microglia following ablation or injury (for review, see Jäkel and Dimou, 2017).

3.1.3 Clonal analysis as a methodological approach to investigate astrocyte proliferation in vivo

DNA incorporation of thymidine analogues is not a definite indicative of cell cycling activity and division, but of DNA synthesis, and thus can be an indicative of many other events in which DNA synthesis occurs, such as DNA repair, abortive cell cycle reentry and gene duplication (Taupin, 2007). In order to verify our observations of cell cycle activity from our thymidine analogue based approach, we used a second methodological tool, namely, the clonal analysis. This method consists on labeling cells *in vivo* and following the progeny of individual cells over time. As we were interested in astrocytes, we took advantage of GLAST-CreER^{T2}-mediated recombination of cells in the multicolor R26-Confetti reporter mice (Bardehle et al., 2013; Calzolari et al., 2015). The GLAST-CreER^{T2} mouse functions based on the Cre-LoxP-system, which is a tool that allows cell and time-specific genomic DNA modifications.

The Cre enzyme is a recombinase that targets, cuts, and recombines specific sequences of DNA, denominated LoxP sites. Placing these LoxP sites through genome editing in specific locations of the DNA allows genes to be activated, repressed or exchanged for other genes (Feil et al., 2009). In the GLAST-CreER^{T2} mouse (*see Section 2.2*), the expression of Cre enzyme is driven by the GLAST gene promoter, which encodes a protein that is present in astrocytes, the glutamate aspartate transporter. Therefore, this enzyme will only be active in this specific GLAST- expressing cell type. Moreover, in these transgenic mice it is possible to control Cre activity and determine, for example the time point for it to be activated and perform the DNA modifications. This is achieved in this mouse line through the fusion of Cre to a modified estrogen receptor ligand binding domain, ER^{T2}. Through this fusion, Cre remains in the cytoplasm of the cell and can only enter the nucleus upon ligand binding to estrogen receptor. Upon application of the ligand (in this case, tamoxifen), Cre can enter the nucleus and perform the DNA modifications in the cell through LoxP site recombination. Finally, we crossed this transgenic mouse line to a reporter line, namely, the R26-Confetti mice (*see Section 2.2*), which contain the editable DNA sites that Cre can recombinate. In this mouse line, Cre activity leads to expression of different fluorescent proteins in a stochastic manner.

Altogether, by using the double transgenic GLAST/Confetti mice, one can permanently label astrocytes with different fluorescent proteins through tamoxifen application. As this label is inheritable, it allows one to follow the cells and their progeny over time.

In order to follow the progeny of an individual cell, that is to say, to be at the clonal level, it is necessary to achieve a sparse recombination. To define a recombination protocol that would allow us to address our experimental hypothesis, we first tested 5 different tamoxifen concentrations for inductions consisting of a single i.p. injection (40, 60, 80, 100 and 120 µg tamoxifen per gram of body weight). Mice underwent SW surgery 1 week after tamoxifen treatment and received BrdU in drinking water following injury to label cells proliferating at the lesion site (Figure 6A).

In the control animal that didn't receive tamoxifen there were no recombined cells, whereas tamoxifen application induced a sparse labeling of astrocytes throughout the brain of treated animals in all the different tested concentrations (Figure 6B). As expected from previous observations, in the contralateral cortex there were no labeled astrocytes that had incorporated BrdU (data not shown) (for review see Sofroniew and Vinters, 2010). However, even at the highest recombination rate achieved we could barely identify recombined astrocytes in the penumbra that were also positive for BrdU (1 cell per brain analyzed, Figure 6C).

Therefore, we increased the tamoxifen induction protocol by using a serial administration of 3 i.p. injections of 80 µg tamoxifen per gram of body weight, which is much below the level of induction that can lead to toxicity in mice (Lagace et al., 2007). With this new protocol we could detect recombined astrocytes that were also labeled with BrdU and therefore used it for the clonal analysis of proliferating astrocytes (Figures 7 and 8).

As our ultimate goal was to analyze astrocyte proliferation, we based our clone definition on the incorporation of proliferation markers. Therefore, in our analysis, clones were defined as cells that were recombined (fluorescent positive cells: GFP^+ or RFP^+) and had incorporated proliferation markers ($BrdU^+$ and/or EdU^+). By basing our clonal analysis on the combination of two independent factors – presence of fluorescent protein and labeling with proliferation marker – we could increase the tamoxifen treatment to achieve a higher number of recombined cells while still remaining at a sparse distribution of proliferative cell clones. This enabled us to use this experimental

paradigm to effectively perform clonal analysis of proliferating astrocytes and their progeny after single and repetitive injuries (Figures 7 and 8).

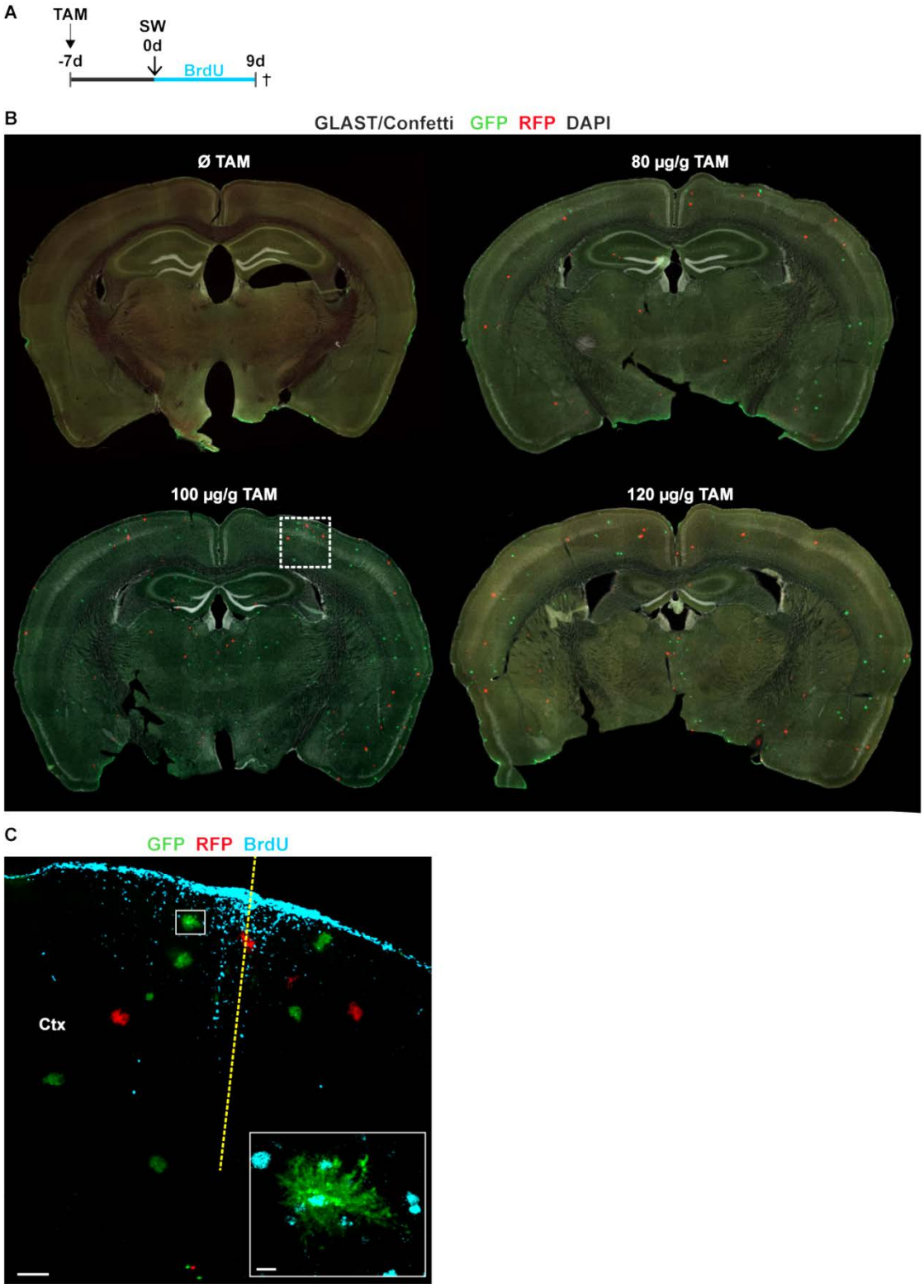

Figure 6. Establishing a tamoxifen induction protocol for clonal analysis of GLAST/Confetti mice. (**A**) The experimental paradigm used to test different induction concentrations of tamoxifen consisted on induction followed by a lesion and labeling of proliferating cells with BrdU in

drinking water. (**B**) Overview of brain sections of mice induced with different tamoxifen concentrations and of a control brain that was not induced with tamoxifen. White dashed box indicates area of inset represented in (c). (**C**) Lesion area with BrdU labeled cells of the animal that showed the highest recombination rate of cells, where we could find one $BrdU^+$ recombined astrocyte (inlay). Yellow dashed line indicates the lesion site. Scale bars represent 100 µm and 10 µm on inlay. TAM: tamoxifen, SW: stab wound lesion, Ctx: cortex.

To perform clonal analysis of proliferating reactive astrocytes in our injury paradigm, we had to first establish a multicellular clone definition based on set parameters in our analysis. For this, it was essential to establish a threshold for the maximum distance between the single cells in a given clone. To achieve a meaningful and safe threshold value, we measured in all of the sections analyzed the minimum distance between two proliferating cells ($BrdU^+$ and/or EdU^+) with different fluorescent protein expression, which could, therefore, not have been originated from the same cell, and were named here as "false positive clones" (Figure 7 A,B). In other words, we measured the minimum distance between a proliferating GFP^+ cell and a proliferating RFP^+ cell.

The minimum distance we could measure between "false positive clones" in all sections was of 20 µm (Figure 7B). In many sections we could not find false positive clones (Figure 7C), which indicates that the labeling we obtain with our recombination protocol is sparse enough to avoid the appearance of false positives that could be close enough to be interpreted as multicellular clones, but still enables us to analyze a meaningful number of clones.

Although the minimum distance observed between "false positive clones" was of 20 µm (Figure 7D), we took a conservative approach and determined the threshold for clone definition at a 5 µm maximum distance between two cell somata. Previous live *in vivo* imaging observations has shown that cortical gray matter astrocytes do not migrate following SW injury and that daughter cells do not drift apart following cell division (Bardehle et al., 2013). Thus, this threshold should be safe enough to both reliably and effectively detect multicellular astrocytic clones at the injury site.

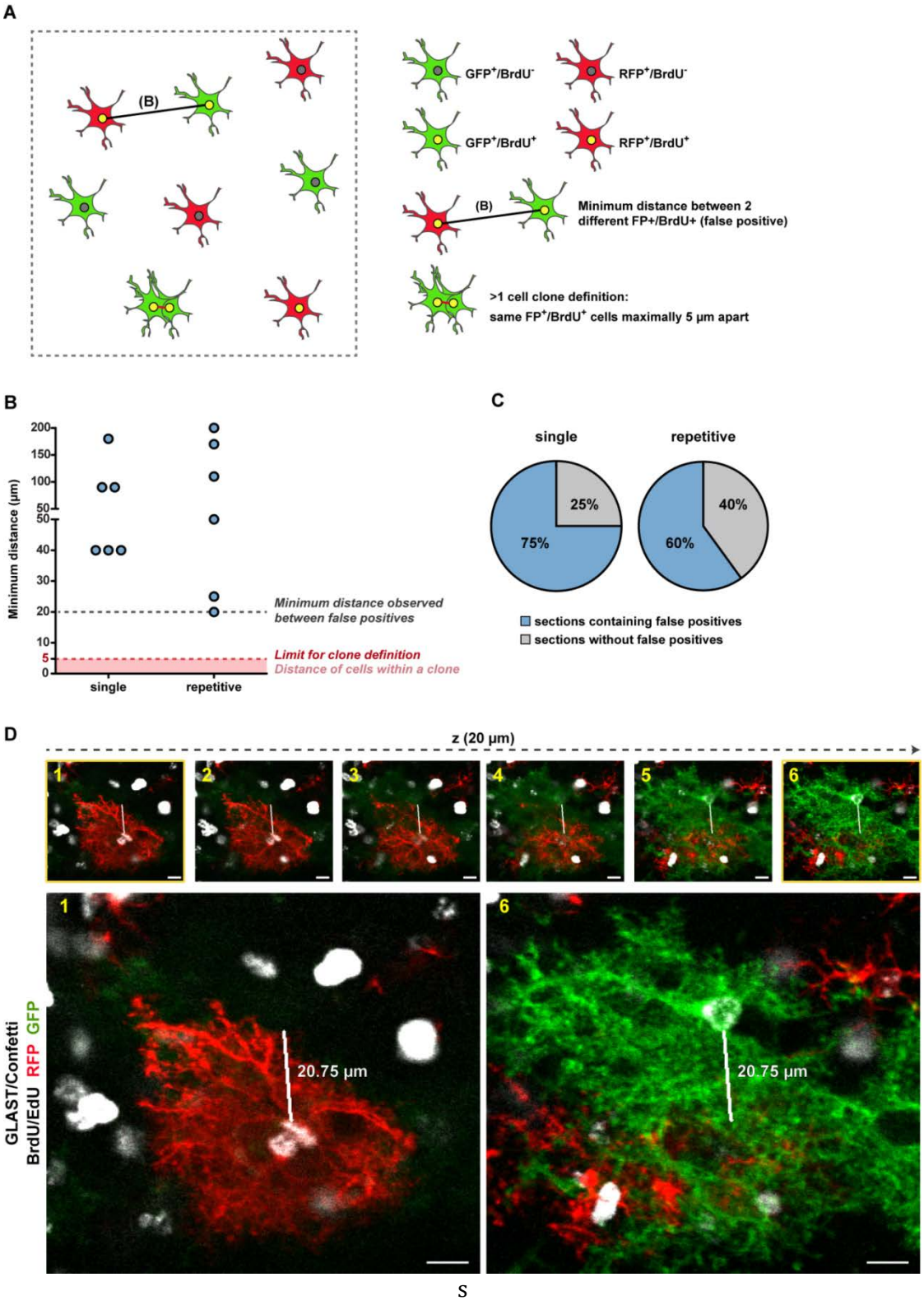

S

Figure 7. Criteria used for multicellular clone definition: establishing a distance threshold between cells within a clone. (**A**) Measurement performed for determining the minimum distance between two proliferating cells with different fluorescent protein expression ("false positive clones"), and an example of what we defined as a multicellular clone. (**B**) The minimum distance we could measure between "false positive clones" in all sections analyzed was 20 µm, and we established the threshold of a 5 µm as the distance threshold for clone definition. Each dot on

the chart represents the minimum distance in each section analyzed. (**C**) Pie chart depicting the percentage of sections where it was not possible to measure the distance between "false positive clones" (in gray), as there were no two proliferating cells expressing different fluorescent proteins in the same section. (**D**) False positive clone with the shortest measured distance. Figures 1 to 5 indicate the z-position in a 20 µm z-stack. Scale bars represent 10 µm. FP^+: fluorescent protein expressing cell (GFP^+ or RFP^+).

3.1.4 Repetitive injuries induced generation of larger astrocytic clones

Recombination in GLAST/Confetti mice left an inheritable expression of fluorescent protein in astrocytic cells, which allowed us to follow the progeny of astrocytes that underwent cell division in response to single or repetitive lesions and incorporated proliferation markers (Figure 8A-C). Unfortunately, we did not succeed in achieving an immunostaining with the concomitant use of 4 markers (GFP, RFP, BrdU and EdU). Therefore, to analyze the total proliferative pool of astrocytes, we performed immunohistochemistry with an antibody that detects both BrdU and EdU with the same efficiency (anti-BrdU clone BU1/75) (Liboska et al., 2012). Thus the analysis is based on thymidine analogue-positive proliferating cells, without making a distinction between BrdU or EdU labeling.

Interestingly, there was no difference in the number of recombined cells (GFP^+ or RFP^+) in the lesion site (ipsilateral cortex) and a corresponding area in the contralateral cortex (Figure 8D,F), indicating a reestablishment of astrocyte numbers following injury. Furthermore, there was no difference in the numbers of total and proliferating astrocytes between both injury conditions (Figure 8E,F). Altogether, these results confirm the population-based observations obtained in WT mice and suggest the existence of a mechanism for restoration of astrocyte population homeostasis following single and repetitive injuries.

An unexpected, but yet interesting finding, was that on both groups a substantial amount of labeled astrocytes that incorporated proliferative markers (33-38%) constituted single cell clones (Figure 8G,H), indicating that many of the astrocytes that incorporate thymidine analogues do not generate long lasting progeny, which could be either due to a faulty or incomplete cell cycle or to the death of a daughter cell.

However, most of the clones that incorporated proliferation markers did generate progeny, and after a single lesion we could find no clones with more than 2 cells (Figure 8G,H), confirming previous live imaging data showing that astrocytes divide once and generate only 2 daughter cells after SW injury (Bardehle et al., 2013). After repetitive

injuries, however, we could observe the generation of clones consisting of 3 daughter cells (Figure 8G,H), indicating that a subset of reactive astrocytes can be activated by multiple pathological stimuli to undergo more than one round of cell division, consistent with our results obtained with BrdU and EdU sequential labeling in WT animals.

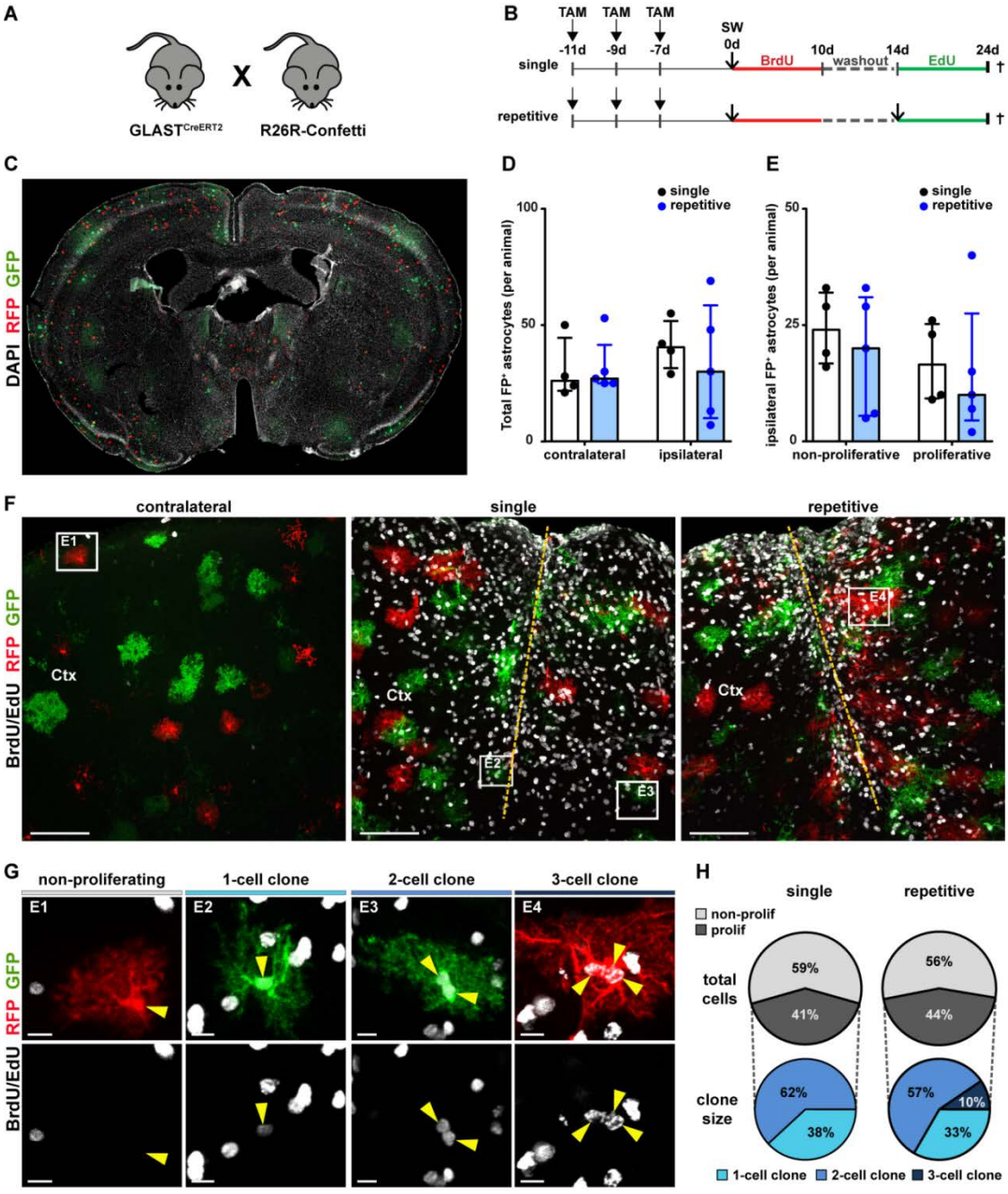

Figure 8. Repetitive injuries induced an increase in astrocyte clone size. (**A**) Clonal analysis was performed in GLAST/Confetti mice, a double-transgenic mouse line resulting from the crossing between GLAST^{CreERT2} and R26R-Confetti lines. (**B**) The experimental paradigm used for this analysis consisted on the same injury and BrdU/EdU delivery conditions applied to WT animals, and only differed in the administration of tamoxifen prior to the first injury for recombination of astrocytes. (**C**) Induction with tamoxifen led to recombination and expression of different fluorescent proteins in astrocytes throughout the entire brain (**D**) The number of

recombined astrocytes (FP^+) was similar in both intact (contralateral) and injured (ipsilateral) hemispheres, suggesting a repopulation of astrocytes to the same initial levels after single and repetitive injuries. (**E**) The number of non-proliferating and proliferating astrocytes in the lesion area (ipsilateral) was similar on both injury conditions. (**F**) Representative immunostainings depict recombined cells in the contralateral cortex and on the lesion site on both injury conditions (single and repetitive). Yellow dashed line indicates the lesion site. (**G**) Examples of clones analyzed and (**H**) quantifications of total recombined cells (upper pie charts) and clone size (lower pie charts) in each injury condition. Repetitive injuries induced an increase in astrocyte clone size, confirming our results obtained previously in WT animals with a population-based analysis. Yellow arrowheads indicate cell somata. Data is depicted as median ± IQR for dot plots and total percentage for pie charts. Scale bars represent 100 μm in (f) and 10 μm in (g). TAM: tamoxifen induction, SW: stab wound lesion, Ctx: cortex.

3.1.5 Reactive astrocyte stem cell potential in vitro was not changed following repetitive injuries

It has been demonstrated that different types of lesion trigger distinct levels of plasticity in reactive astrocytes, and that there is a positive correlation between astrocyte proliferation *in vivo* and stem cell potential *in vitro* (Sirko et al., 2013). As we observed that repetitive pathological stimuli could induce a change in the proliferative behavior of reactive astrocytes *in vivo*, we investigated whether this injury condition could also modulate the stem cell potential of reactive astrocytes *in vitro* through the neurosphere assay, in which one can characterize the capacity of a cell to self-renew and its multipotency (Figure 9A) (Reynolds and Weiss, 1992).

Contrary to what we expected, reactive astrocytes derived from the penumbra after repetitive pathological events showed no difference in plasticity *in vitro* when compared to those obtained from single lesioned tissue. Based on quantitative and qualitative analysis there were no changes in their potential to generate neurospheres (Figure 9B), as well as their ability to self-renew (Figure 9C) or in their differentiation potential (Figure 9D,E). This data indicates that a second lesion did not elicit a change in astrocyte stem cell potential; however this result could also be due to changes within the repetitive injured parenchyma at intrinsic and/or extracellular levels in the multiply injured parenchyma that could affect astrocyte plasticity.

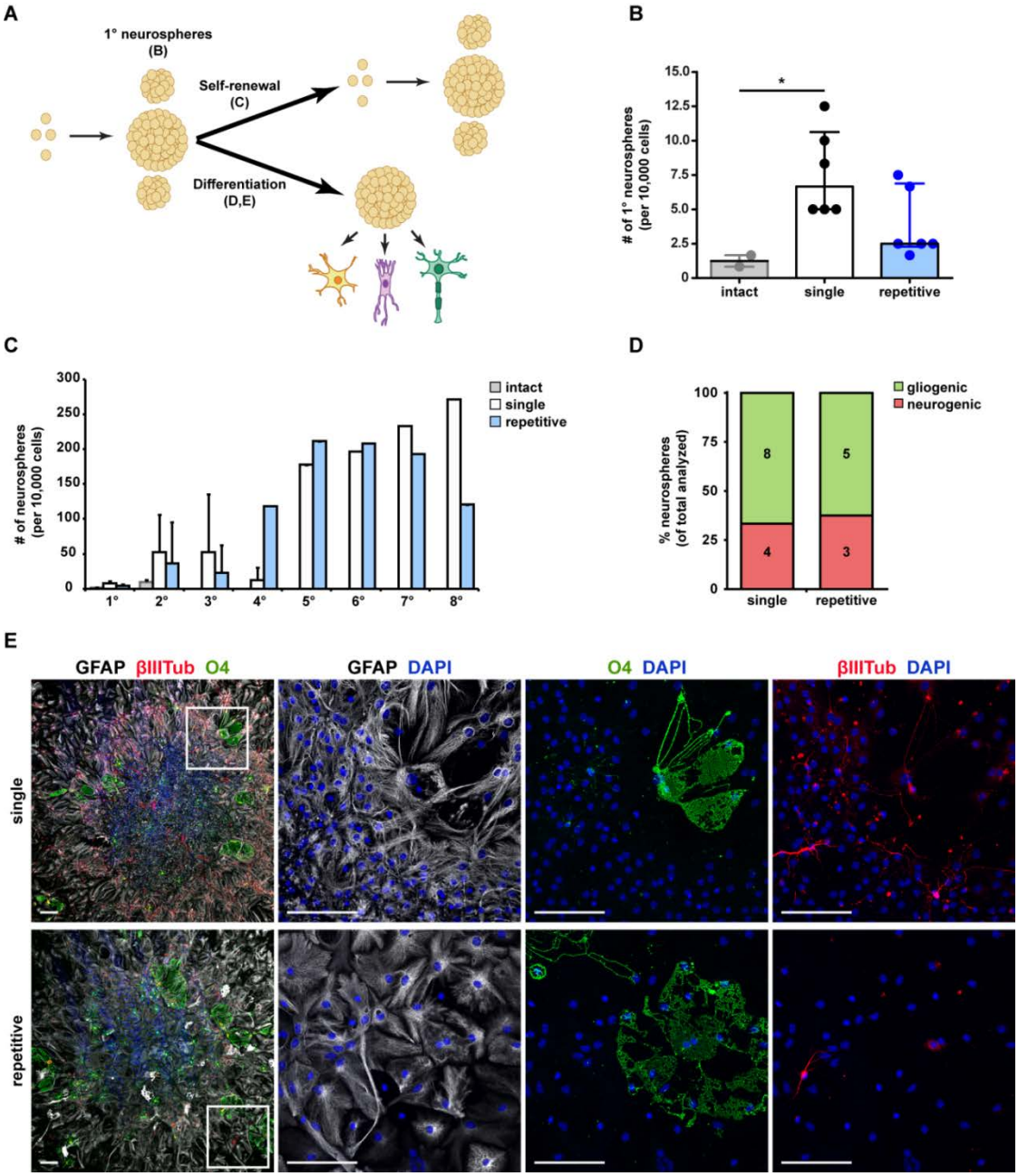

Figure 9. Repetitive injuries did not induce a change in astrocyte stem cell potential *in vitro*. (**A**) The neurosphere assay is the gold standard method for analysis of stem cell potential, in which two hallmarks of stem cells – self-renewal and differentiation – are investigated. (**B,C**) The number of neurospheres formed in the first (**B**) and on subsequent passages (**C**) was increased in the lesioned versus intact cortex, but there was no difference between the two injury paradigms (n=2 animals in intact, and 6 in single and repetitive lesions group). *P= 0.0246 in Kruskal-Wallis Test and P<0.05 in Dunn's Multiple Comparison post hoc test. (**D**) Differentiation assay analysis showed no difference in the differentiation potential of neurospheres obtained from both injury paradigms. (**E**) Examples of neurospheres analyzed, in which the presence of 3 different neural cell types (astrocytic: GFAP, oligodendrocytic: O4, and neuronal: βIII-tubulin) was analyzed in each neurosphere to determine its differentiation potential (gliogenic or neurogenic). Data is depicted as median ± IQR in (c) and percentage and total number of neurospheres analyzed in (d). Scale bars represent 100 μm.

3.1.6 *Repetitive injuries induced changes in the lesion environment, evidenced by an exacerbated proliferation of microglia/macrophages*

It is known that other types of glial cells, such as NG2-glia and microglia show a pronounced proliferative response to different types of brain injury (Dimou and Götz, 2014; Simon et al., 2011). Following repetitive pathological stimuli, we observed a marked increase in the proliferative activity of non-astrocytic GFAP$^-$ cells, so we set out to determine the proliferative response of NG2-glia and microglia upon repetitive pathological events. Immunohistochemical analysis revealed that NG2-glia (NG2$^+$) and microglia/macrophages (Iba1$^+$) also proliferate after repetitive lesions (Figure 10A). Interestingly, similar to astroglial cells, NG2$^+$ cells also showed a comparable number of proliferating cells following single and repetitive injuries and maintained homeostatic cell numbers across the different injury paradigms (Figure 10B,C). However, microglia/macrophages (Iba1$^+$ cells) react to the secondary injury with an increased proliferation, resulting in an also increased population size in the penumbra after repetitive lesions (Figure 10B,C), which is a known phenomenon termed microglia priming (Witcher et al., 2015).

Cycling cells quantified with the use of 3 distinct markers (GFAP, NG2 and Iba1) amounted to almost 100% of the total proliferative cells, and although it is known that also other cell types in the brain proliferate in response to invasive injury (e.g. endothelial cells, our analysis suggests they do not represent a substantial amount of cells within the total proliferative population.

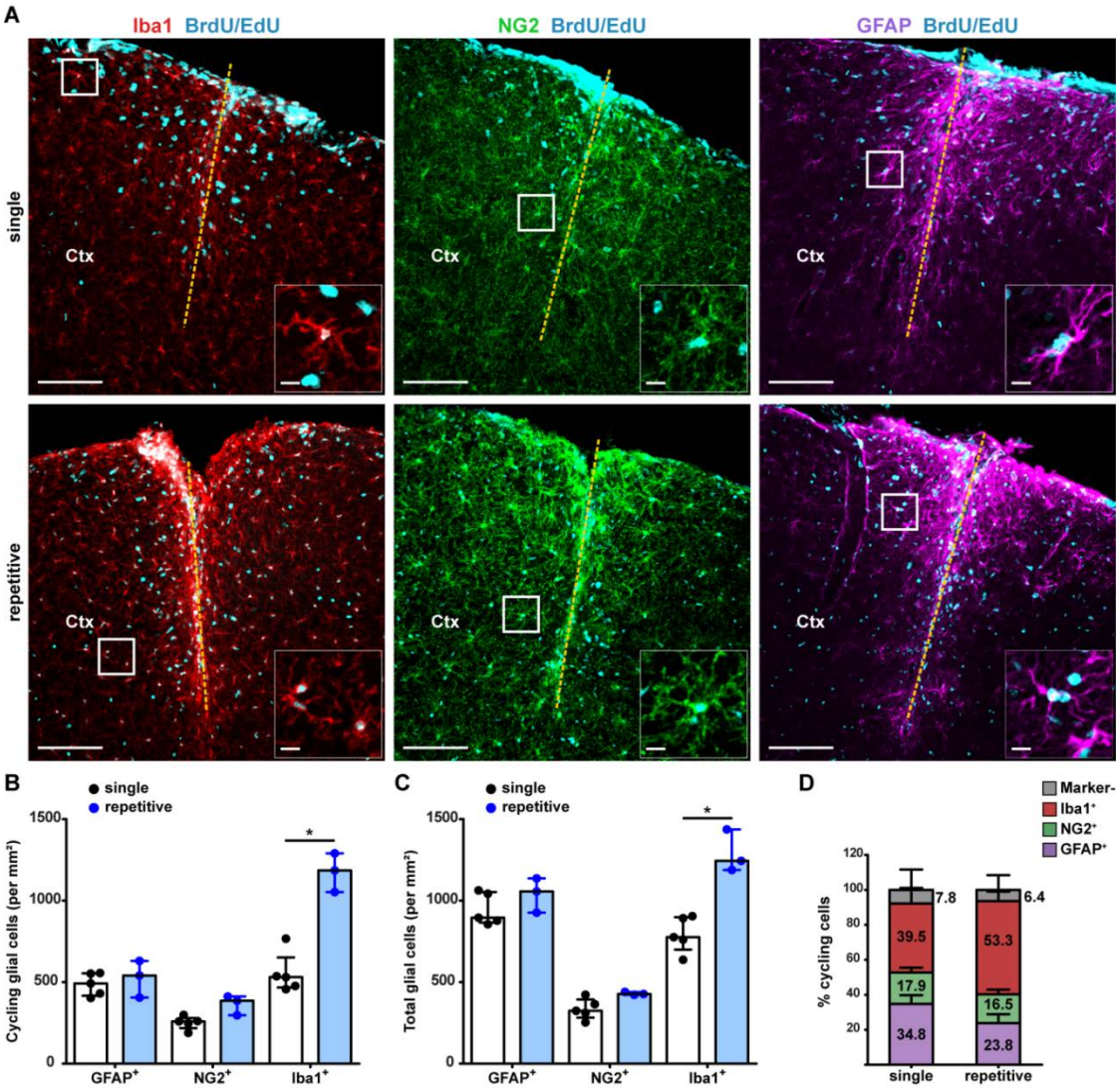

Figure 10. Macro- and microglial cells show different proliferative response to repetitive injuries. (**A**) Representative immunostainings depict the area used for quantifications of different glial cells on the injury site based on the markers Iba1 (microglia/macrophages), NG2 (NG2-glia) and GFAP (astrocytes). Examples of proliferating cells (BrdU⁺ and/or EdU⁺) are depicted in inlays. Yellow dashed line indicates the lesion site. (**B**) While the number of proliferating macroglia (GFAP⁺ and NG2⁺) was not changed in repetitive injuries compared to a single injury, microglia/macrophages (Iba1⁺) showed an exacerbated proliferative response after a second lesion (P=0.0357). (**C**) The total number of macroglial cells (GFAP⁺ and NG2⁺) remained the same after single or repetitive injuries; however, microglia/macrophages (Iba1⁺) showed an increase in the total population number following repetitive injuries (P=0.0357). (**D**) Quantifications of GFAP⁺, NG2⁺ and Iba1⁺ proliferating cells amounted to nearly 100% of all proliferating cells in the injury site. Data is depicted as median ± IQR for dot plots and mean ± SD for graph with percentage data in (d). Scale bars represent 100 µm and 10 µm on inlays. Ctx: cortex.

3.1.7 *Absence of infiltrating monocytes induced a change in the mode of recruitment of astrocytes into proliferation following repetitive lesions*

The observation that the microglia/macrophage Iba1$^+$ cell population was largely increased upon a second lesion, while macroglia cell population numbers remained unchanged, led us to question whether the inflammatory environment could have an effect on modulating the proliferation of astrocytes.

As one of the outcomes of traumatic brain injury is the upregulation of chemokines (e.g. CCL2) by astrocytes and microglia, leading to the recruitment of monocytes into the brain parenchyma (Gyoneva and Ransohoff, 2015), we questioned whether an impairment of monocyte infiltration could have an influence in astrocyte proliferative behavior upon repetitive lesions, for example on the regulation of the relative contribution of self-renewing astrocytes versus new recruitment of astrocytes into proliferation.

In order to address this question, we performed the same lesion and labeling paradigm in CCR2$^{-/-}$ mice (Saederup et al., 2010), in which monocyte infiltration from the blood vessels into the brain parenchyma after injury is impaired and has been shown to strongly increase astrocyte proliferation (Frik et al., 2018).

Quantitative analysis of cycling activity of cells within the penumbra indicated significant changes in the lesion environment in CCR2$^{-/-}$ mice compared to WT mice after single and repetitive lesions, with a visible increase of BrdU-labeled cells in the absence of monocyte infiltration in both conditions (Figure 11A).

In CCR2$^{-/-}$ mice there was a significant increase of non-astrocytic proliferating cells (GFAP$^-$) compared to WT mice following a single lesion, but this difference was not observed between both genotypes after repetitive injuries (Figure 11 B). Further analysis of the different subsets of non-astrocytic cycling cells according to their temporal profile of proliferation showed that, after a single lesion, only the population of GFAP$^-$/BrdU$^+$ cells was changed, showing an increased number in CCR2$^{-/-}$ compared to WT mice (Figure 11C). However, following repetitive lesions, there was an increased number of all subsets of proliferating cells, with an increase in both BrdU-labeled populations (GFAP$^-$/BrdU$^+$ and GFAP$^-$/BrdU$^+$/EdU$^+$) and a decrease in the GFAP$^-$/EdU$^+$ population in CCR2$^{-/-}$ compared to WT mice (Figure 11D).

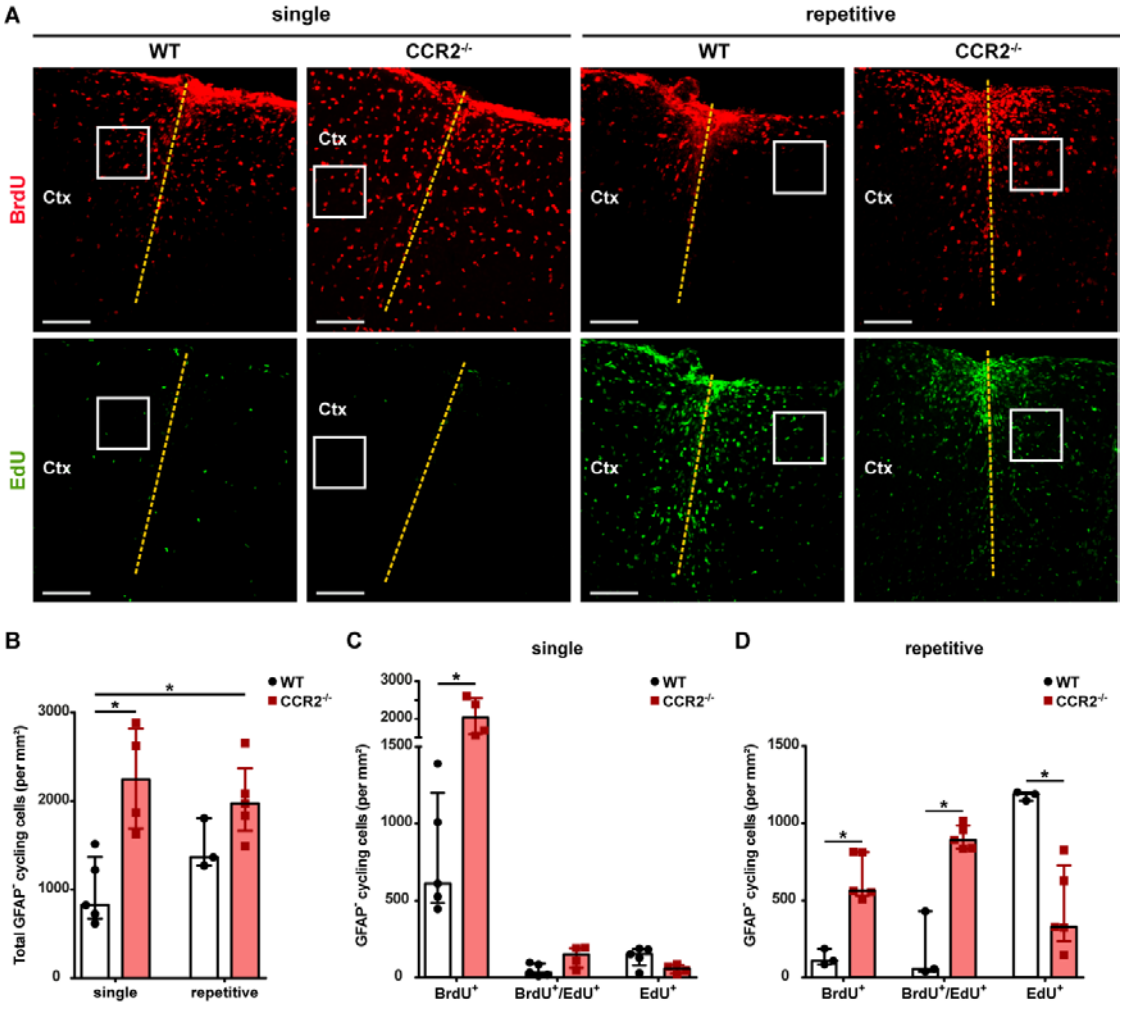

Figure 11. Proliferation of cells in the lesion area is modulated by monocyte infiltration. (**A**) Representative immunostainings show marked changes in the lesion environment depending on the presence (WT) or absence (CCR2$^{-/-}$) of infiltrating monocytes, with increased number of BrdU^{+} cells in CCR2$^{-/-}$ mice compared to WT mice after single and repetitive injuries. Yellow dashed line indicates the lesion site. (**B**) The number of non-astrocytic (GFAP^{-}) proliferating cells was increased in CCR2$^{-/-}$ mice after single and repetitive injuries compared to single injured WT animals (*P=0.0159). (**C**) In the absence of infiltrating macrophages (CCR2$^{-/-}$) following a single lesion there was an increase of non-astrocytic BrdU^{+} cells compared to WT animals (*P=0.0159). (**D**) Upon repetitive lesions, there was an increase of non-astrocytic BrdU^{+} and BrdU^{+}/EdU^{+} cells and decrease of EdU^{+} cells in the absence of invading monocytes (CCR2$^{-/-}$) (*P=0.0357). Data is depicted as median ± IQR. Scale bars represent 100 µm and 10 µm on inlays. Ctx: cortex.

Our experimental paradigm using double labeling with BrdU and EdU is, unfortunately, not optimal for the characterization of subsets of highly proliferative cells, since the thymidine analogue that is delivered first (BrdU) can get diluted out of the cell's DNA in case of multiple cell divisions. As a matter of fact, this BrdU dilution can be observed both visually in immunostainings of WT animals after repetitive lesions compared to single lesion (Figure 11A), and in the quantifications of GFAP^{-} proliferating cells, in which there is a substantial decrease in the number of GFAP^{-}/BrdU^{+} cells and concomitant increase of GFAP^{-}/EdU^{+} cells after a second lesion in WT animals. This could

arise from either the death of GFAP$^-$/BrdU$^+$ cells upon a second injury, or due to a high proliferative response of these cells to the second lesion, the latter being suggested in our results by the huge increase in the number of GFAP$^-$/EdU$^+$ cells that we observe upon a second injury in WT mice.

Therefore, although this thymidine labeling paradigm is not optimal to analyze highly proliferative cells, one can speculate about the overall higher number of GFAP$^-$/BrdU$^+$ cells and lower number of GFAP$^-$/EdU$^+$ cells in CCR2$^{-/-}$ mice. One hypothetical explanation for this could be that, in these mice, microglia (which are the main GFAP$^-$ proliferative population in WT mice) achieve a state of exhaustion after exacerbated proliferation following a single lesion and don't show a further increased proliferation following a second insult (Figure 11B). It would, therefore, be interesting to further analyze the microglia response capacity or microglia priming in the context of multiple injuries in CCR2$^{-/-}$ mice, in order to evaluate the importance of monocyte infiltration in the modulation of local microglia proliferation.

Altogether, our results show that the proliferative cellular milieu of non-astrocytic cells is drastically changed at the lesion site of mice in which monocyte invasion is impaired both after single and repetitive injuries.

Analysis of the effects of the absence of monocyte infiltration on astrocyte proliferation surprisingly showed that, also in CCR2$^{-/-}$ mice, astrocyte numbers were perfectly maintained after single and repetitive injuries (Figure 12A-C). However, the proliferative repertoire of astrocytes was changed in CCR2$^{-/-}$ mice compared to WT after repetitive lesions (Figure 12D). After a single SW injury, we observed no increase of astrocyte proliferation over the first 24 days after injury in CCR2$^{-/-}$ mice (Figure 12E). Upon repetitive injuries, however, the absence of invading monocytes enhanced cell-cycle reentry of reactive astrocytes, resulting in a 2-fold increase in the proportion of GFAP$^+$/BrdU$^+$/EdU$^+$ cells within the penumbra of CCR2$^{-/-}$ mice compared to WT animals (Figure 12F). This switch to self-renewing proliferation was accompanied by significantly reduced recruitment of quiescent astrocytes into the cell cycle, with much reduced EdU$^+$ astrocytes after repetitive injury in CCR2$^{-/-}$ mice (Figure 12F). Thus, our analysis strongly suggests that invading monocytes play a key role in recruiting previously quiescent astrocytes into proliferation.

Altogether, these observations imply that signals coming from invading monocytes in the lesioned environment regulate the proliferative behavior of reactive astrocytes, especially upon multiple injuries.

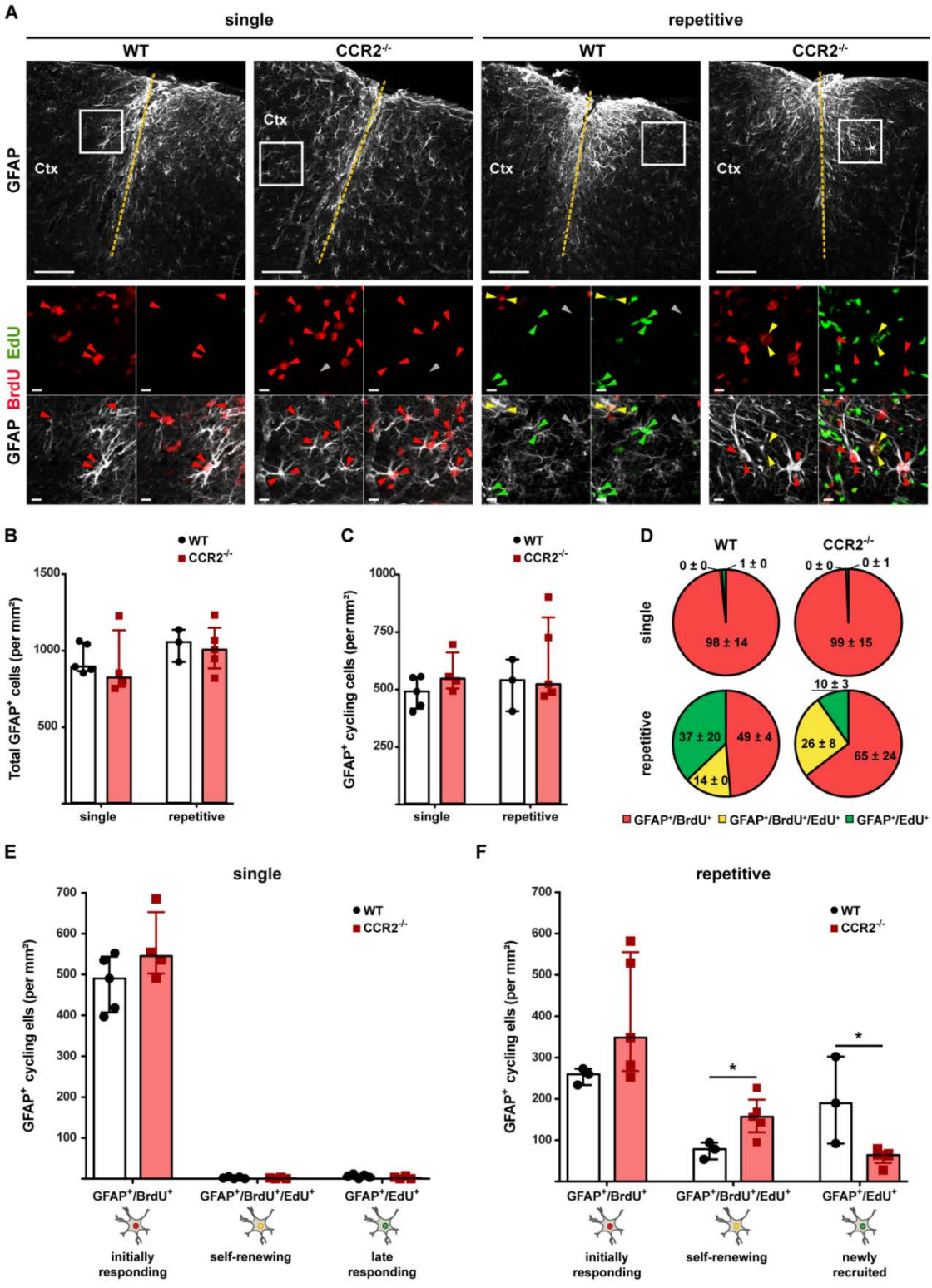

Figure 12. Astrocyte proliferative behavior is modulated by the infiltration of monocytes in the lesion area. (**A**) Representative immunostainings show GFAP expression in different genetic

backgrounds and injury conditions. Inlays represented in the lower panels contain examples of the different subsets of proliferative astrocytes: GFAP+/BrdU+ (red arrowheads), GFAP+/BrdU+/EdU+ (yellow arrowheads) and GFAP+/EdU+ (green arrowheads). Yellow dashed line indicates the lesion site. While the numbers of total (B) and proliferating (C) astrocytes were comparable across genotypes and injury paradigm, the proliferative repertoire (D) of astrocytes was modulated by the presence (WT) or absence (CCR2-/-) of monocyte infiltration following repetitive lesions. (E) Quantitative analysis of the proliferative populations of astrocytes yielded similar results in both genetic backgrounds following a single lesion. (F) Upon repetitive injuries, the absence of infiltrating macrophages (CCR2-/-) resulted in an increase in the number of self-renewing astrocytes (GFAP+/BrdU+/EdU+) and decrease of newly recruited astrocytes into proliferation (GFAP+/EdU+) (*P=0.0357). Data is depicted as median ± IQR for dot plots and mean ± SD for pie charts. Scale bars represent 100 μm and 10 μm on inlays. Ctx: cortex.

3.1.8 Age-related changes in reactive astrocyte transcriptional regulation

As demonstrated in the previous section of this thesis, reactive astrocytes show different responses to injury depending on environmental cues. The effect of the lesion environment on modulating reactive astrocyte properties has been previously described in many different pathological contexts (Anderson et al., 2014; Ferrer, 2017; Frik et al., 2018; Liddelow et al., 2017; Sirko et al., 2013).

Although much progress has been done to understand astrocytic responses in different pathological environments, until recently, little was known about the properties of reactive astrocytes in the injured aged brain.

Natural aging is associated with a plethora of changes in microglia and immune system function (von Bernhardi et al., 2015; Hefendehl et al., 2014), and recovery outcomes from damage are worse in the aged compared to young brains (Fonarow et al., 2010; Zhang et al., 2005). Therefore, our work group addressed the question of whether astrocyte response to lesion was changed in the aged brain where there seem to be different environmental cues. We found that astrocytes in the post-traumatic aged cortex have an impaired proliferation, and this leads to a reduction of their population cell numbers in the penumbra (Heimann et al., 2017). Interestingly, these proliferation deficits seem to be intrinsic, as astrocytes become refractory to signaling factors that promote proliferation, such as SHH (Heimann et al., 2017; Sirko et al., 2013).

In order to get more insight on possible mechanisms for this impaired proliferative response, we performed transcriptional analysis of genes known for regulation of proliferation or astrocyte reactivity. For this purpose, I isolated reactive astrocytes from the post-traumatic cortical parenchyma of Aldh1L1-eGFP mice through FACS-sorting and processed the material for qPCR analysis (Figure 13A,B).

Gene expression analysis showed a trend towards downregulation of mRNA levels of SHH transducer Smoothened (Smo), SHH receptor Patched (Ptch1) and their effector cyclin D1 (Ccnd1) in GFP⁺ astrocytes from the aged brain (Figure 13C). These transcriptional changes in different players of the SHH pathway imply an interference with this pathway in astrocytes from the aged brain, which could explain why they are refractory to SHH signaling and suggest an intrinsic proliferation deficit of these cells. Interestingly, mRNA levels of GFAP showed a trend towards downregulation in astrocytes isolated from aged animals (Figure 13C), which could have implications in the overall poor outcome of tissue restoration and recovery from lesion.

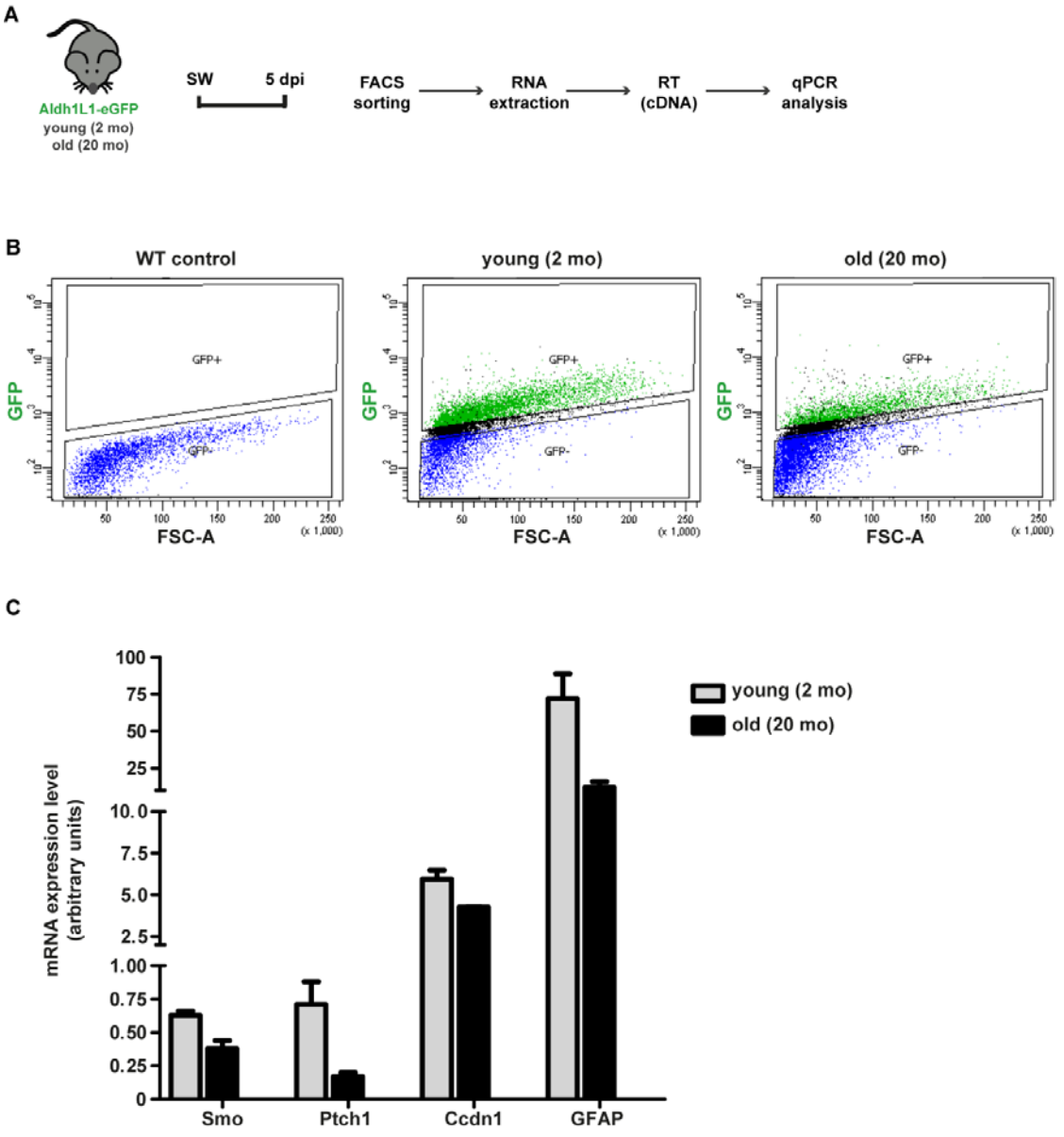

Figure 13. Gene expression analysis of astrocytes from the post-traumatic young and aged cerebral cortex. (A) Experimental paradigm used for isolation of reactive astrocytes via FACS-sorting and steps involved in material processing for gene expression analysis with RT-qPCR. (B)

FACS plots show the final sorting gate used for isolation of GFP+ astrocytes, based on cell size (forward scatter area, FSC-A) and GFP expression. A WT sample processed in parallel was used to set the gate for GFP fluorescence (shown in the left). GFP+ cells (upper part of graph) were positively sorted from cell suspensions of young and aged injured brains. (C) Bar graphs depict levels of mRNA from different genes determined by qRT-PCR (data is plotted as mean ± SEM of technical triplicates, n=3 animals/group, pooled in 1 sample per group).

3.2 Environment-dependent plasticity of cerebral cortex reactive astrocytes

3.2.1 Transplantation as a tool to evaluate differentiation potential of cortical reactive astrocytes and aNSCs in vivo

In order to assess whether cortical reactive astrocytes can give rise to different cell types *in vivo* when relocated to a more plastic environment, and to evaluate to which extent the local environment can influence their differentiation potential, we isolated and transplanted these cells into neurogenic environments and characterized them after a few weeks to assess their cell fate.

For this purpose, we isolated tissue from the injured cortical gray matter of actin-GFP mice at 5 days after cortical SW injury and also from the SEZ, which contains a bona fide NSC population, which we used for comparison in our analysis. We cultured both populations of cells for 2 weeks *in vitro* through the neurosphere culture for expansion and transplanted these as single cell suspensions into the hippocampal DG in the adult mouse brain, and into the lateral ventricles of the developing brain of E13 embryos of WT animals, in which there is a high level of ongoing neurogenesis (Figure 14A). As an additional control to validate our transplantation experiments, we transplanted the SEZ-derived cells homotypically into the SEZ of WT animals. We analyzed the fate of transplanted cells at 2 and 4 weeks post transplantation (wpt) in all different host environments through immunohistochemistry using well-established cell markers for different types of cells: GFAP (astroglia), Olig2 (oligodendroglia), DCX (immature neurons) and NeuN (mature neurons) (Figure 14A).

SEZ-derived cells transplanted homotypically into the SEZ could migrate from the transplantation site through the rostral migratory stream (RMS) into the olfactory bulb (OB) at 2 and 4 wpt (Figure 14B). As there were no differences in the distribution and differentiation of the transplanted cells analyzed at both time points, only the data from 4 wpt is shown here (Figure 14C,D).

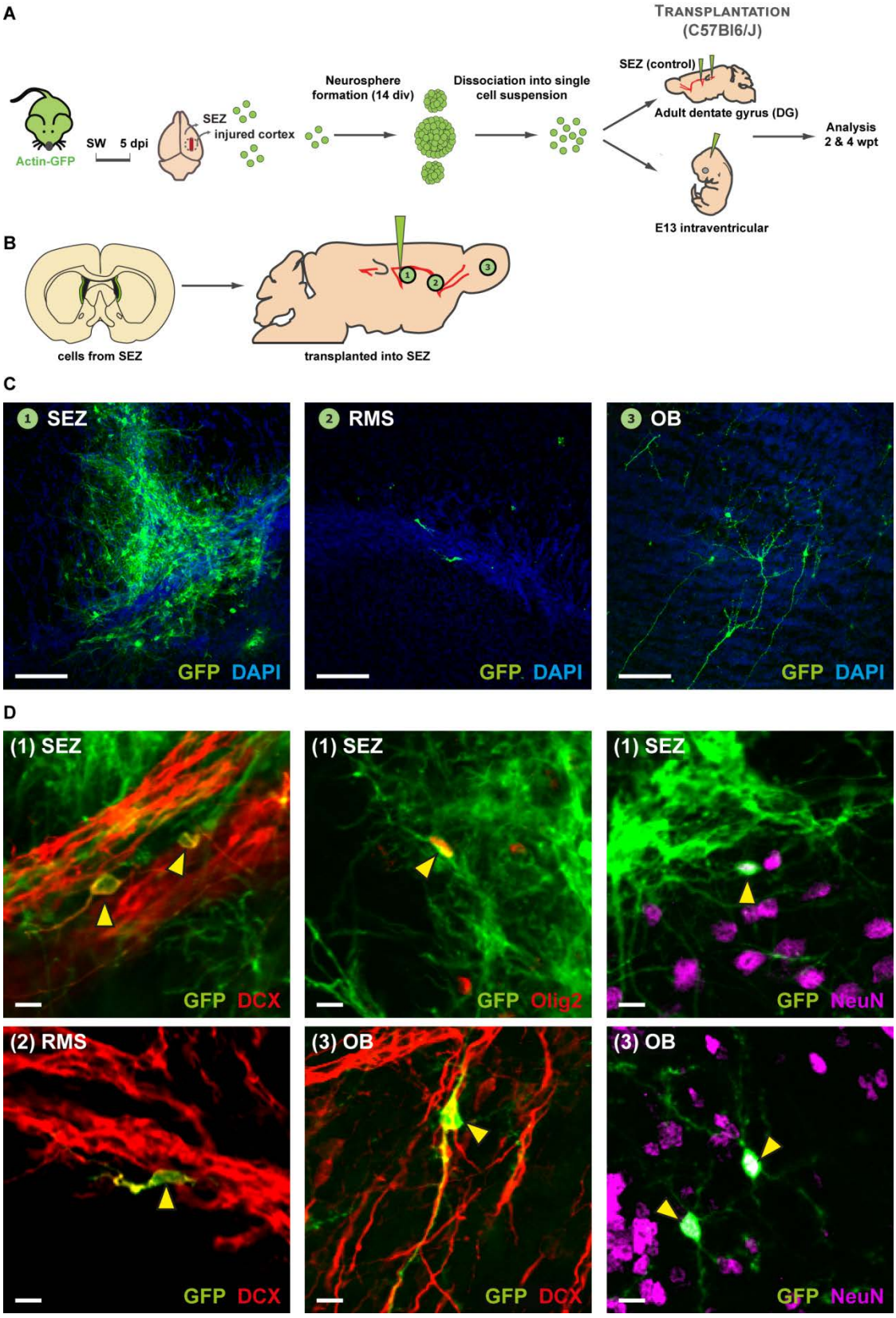

Figure 14. Transplantation of actin-GFP neurosphere-derived cells from the injured cortical gray matter and SEZ into neurogenesis-permissive environments. (**A**) Experimental paradigm used to assess the differentiation potential of cortical reactive astrocytes compared to bona fide aNSCs in different neurogenic environments. (**B**) As a positive control to validate our

transplantation experimental procedure, we performed homotypic transplantations of SEZ-derived aNSCs into the SEZ. (**C**) At 4 weeks post transplantation, the majority of transplanted cells could still be found within the transplantation site (SEZ), few cells were located within the RMS with a migratory morphology and many cells could be found within the OB and showed a distinct mature neuronal morphology. (**D**) Examples of distinct cell types that SEZ-derived cells could differentiate into within the SEZ (few DCX^+, $Olig2^+$ and $NeuN^+$), RMS (mainly DCX^+) and in the OB (mostly $NeuN^+$, with few DCX^+ cells). Yellow arrowheads indicate double-positive cells. Scale bars represent 100 µm in (c) and 10 µm in (d). SW: stab wound lesion, SEZ: subependymal zone of the lateral ventricle, DG: dentate gyrus of the hippocampus, dpi: days post injury, OB: olfactory bulb, RMS: rostral migratory stream, wpt: weeks post transplantation.

The majority of cells could be found in the transplantation site and remained in the astrocytic lineage ($GFAP^+$), but there were also a few GFP^+ transplanted cells in the SEZ that differentiated into other cell types, evidenced by their expression of DCX, Olig2 and NeuN markers (Figure 14D). The few transplanted cells found within the RMS were mostly DCX^+ and had a distinct migratory morphology. On the other hand, the vast majority of the cells present in the OB were $NeuN^+$ with a mature neuronal morphology, with a few DCX^+ cells exhibiting also a neuronal morphology (Figure 14D).

These results indicate that our methodological approach as a whole – from the isolation, neurosphere culture and transplantation of cells – is suitable for analyzing cell differentiation potential *in vivo*, since we were able to confirm the expected phenotype of SEZ cells when we transplanted these homotypically into their region of origin in host WT animals.

3.2.2 Differentiation potential of SEZ aNSCs and cortical reactive astrocytes in the adult hippocampal DG

Analysis of differentiation potential after at 2 and 4 weeks of heterotypical transplantation of cells into the adult DG indicated a higher plasticity of SEZ-derived cells compared to cells derived from the injured cortex, as they gave rise to cells of three different lineages - astrocytic ($GFAP^+$), oligodendrocytic ($Olig2^+$) and immature neurons (DCX^+) (Figure 15). Cells derived from the SEZ remained mostly in the astrocytic lineage ($GFAP^+$) at both time points analyzed, but also gave rise to a substantial amount of oligodendrocytic cells ($Olig2^+$) and immature neurons (DCX^+). Surprisingly, despite the presence of many immature neurons in both time points analyzed, SEZ-derived cells largely did not differentiate into mature neurons ($NeuN^+$), even at 4 wpt (Figure 15A,B).

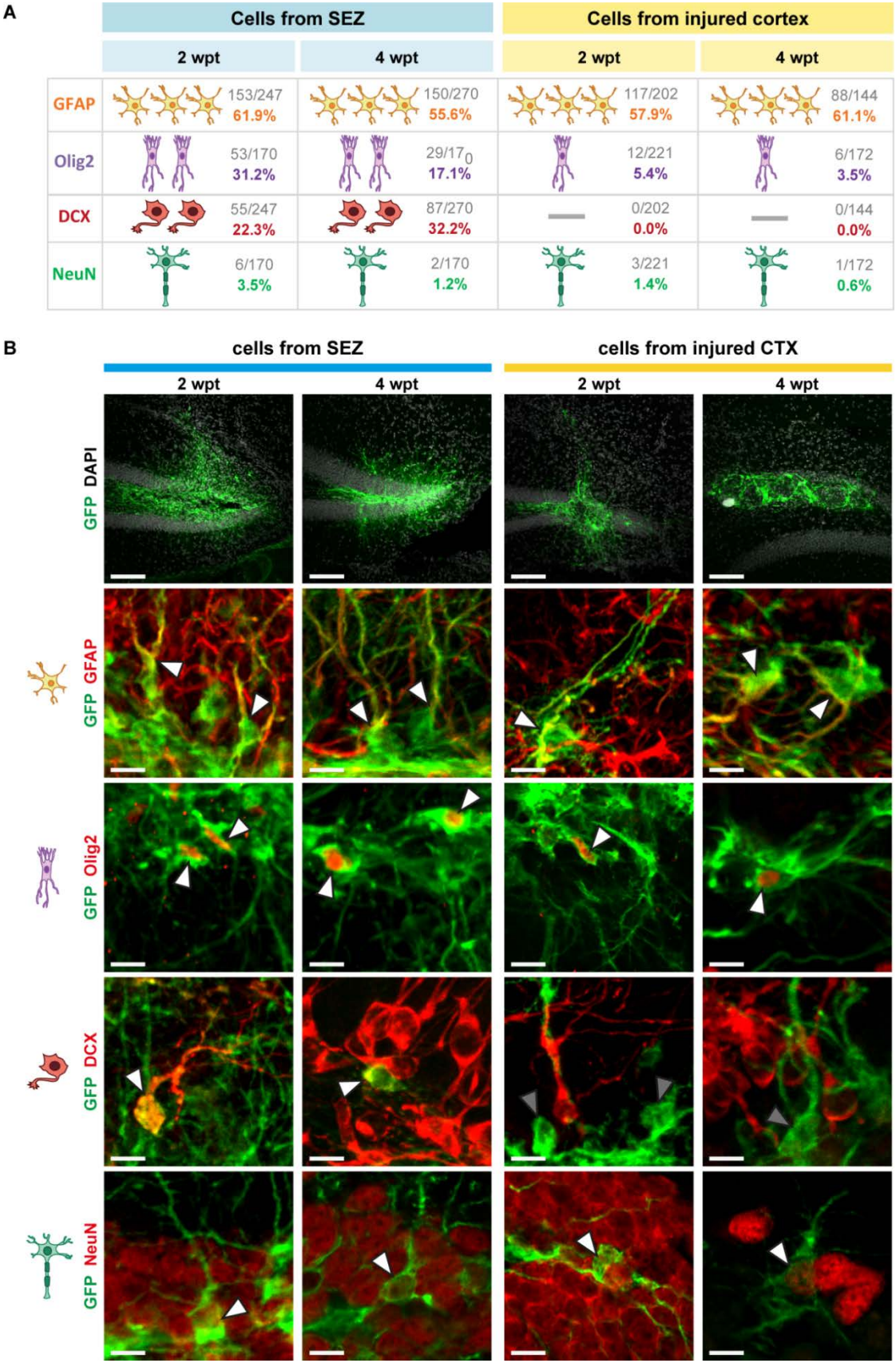

Figure 15. Transplantation of actin-GFP neurosphere-derived cells from the SEZ and injured cortical gray matter into the adult DG. (**A**) Summary table of results obtained from differentiation analysis of transplanted cells from both sources into the DG. SEZ-derived cells

showed a greater differentiation potential than cortical reactive astrocytes (higher proportion of Olig2$^+$ and DCX$^+$ cells), but still failed to give rise to mature neurons (NeuN$^+$) in this environment. Reactive astrocytes derived from the injured cortex remained in the glial lineage and largely did not give rise to neurons (immature or DCX$^+$ and mature or NeuN$^+$). Data represented in total cell numbers analyzed and relative proportions for each combined immunostaining (n=1-2 animals per condition). (**B**) Examples of transplants from both sources at different analysis time points in overview (upper row), and of different cell fates identified based on well-defined cell markers. White arrowheads indicate double-positive cells, and gray arrowheads indicate GFP$^+$ transplanted cells that are negative for the cell marker analyzed. Scale bars represent 100 µm on upper row and 10 µm on the subsequent rows. SEZ: subependymal zone, DG: dentate gyrus, wpt: weeks post transplantation.

Since we have shown that upon homotypic transplantation SEZ cells could migrate into the OB and differentiate into mature neurons within 2 weeks, these results indicate that the DG environment, although being neurogenic, may lack key signals to support the maturation of SEZ-derived neuroblasts.

Cells derived from the injured cortex remained in the glial lineage after 2 and 4 wpt, with the vast majority of the cells keeping their astrocytic fate (GFAP$^+$) and very few differentiating into oligodendrocytic cells (Olig2$^+$). We could find virtually no immature neurons within the transplants from injured cortex derived cells, which also raises concerns for interpreting the few mature neurons (NeuN$^+$) that we could find in these transplants, as well as the ones derived from SEZ cells, since they are very low in number (Figure 15A,B). Therefore, we can conclude that both cell sources largely failed to give rise to mature neurons (NeuN$^+$) in this adult neurogenic niche.

Since even the cells derived from the SEZ, which is a neurogenic niche containing bona fide aNSCs, failed to generate mature neurons in the adult DG, we decided to analyze the differentiation potential of both cell types in yet another highly pro-neurogenic environment with a more robust generation of neurons: the developing brain of the E13 embryo.

3.2.3 Differentiation potential of aNSCs and cortical reactive astrocytes in the embryonic brain

In order to further assess the differentiation potential of cortical reactive astrocytes and SEZ aNSCs *in vivo,* we transplanted these cells in a different neurogenesis supportive environment, namely the E13 developing brain.

As we performed intraventricular transplantations, we characterized the distribution of transplanted cells obtained from the different sources throughout the brains at the time points of our analysis (Figure 16A,B).

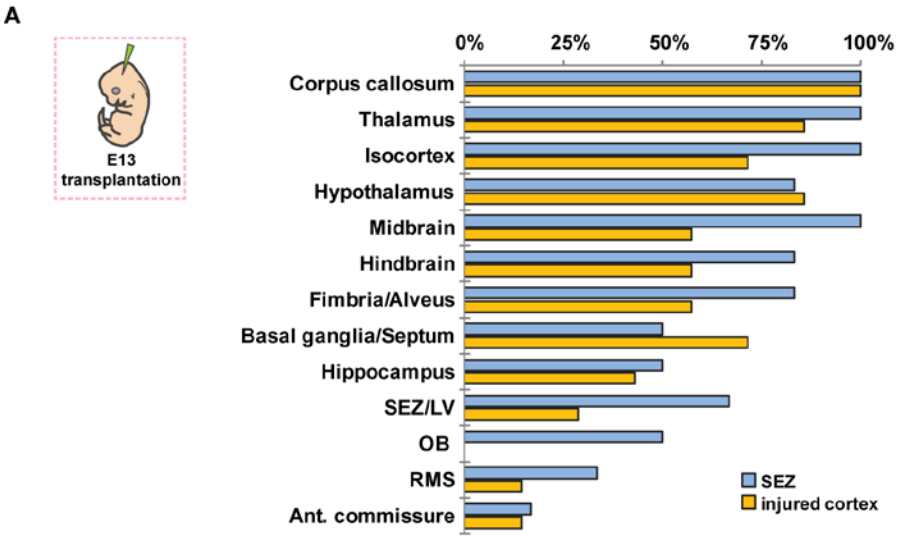

B

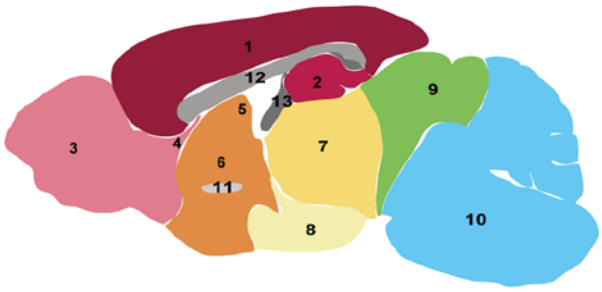

	SEZ						injured cortex						
	2 wpt				4 wpt		2 wpt				4 wpt		
	# 1		# 2		# 2		# 2				# 1		# 2
Isocortex (1)	103	305	24	171	106	40		10	2	1	12		2
Hippocampus (2)	246	9		1306				1		5	1		
OB (3)	44	47				47							
RMS (4)	1	7									5		
SEZ/LV (5)	39	26		33		5					1		4
Basal ganglia/Septum (6)	7	456		4				1		4	24	59	56
Thalamus (7)	15	42	77	13	5	72	1	29	1	5	30		14
Hypothalamus (8)	44	109	16	19	27		12	1		18	54	5	8
Midbrain (9)	84	890	3	682	77	5	1	63		43		7	
Hindbrain (10)		17	13	8	15	23	1	1	8			10	
Anterior commissure (11)		40										121	
Corpus callosum (12)	420	148	18	110	140	137	8	41	2	8	24	12	12
Fimbria/Alveus (13)	12		45	1100	3	1	24			7	11	6	

1-10
11-50
51-100
101-200
> 200

Figure 16. Homing of adult SEZ and injured cortex derived cells in the developing brain. (A) Frequency of integration of transplanted cells in the different brain regions over both time points analyzed. Data represented in percentages (number of brains in which transplanted cells were detected in a given region over all brains containing transplanted cells). (B) Heat map displays number of transplanted cells quantified in each brain region in a serial analysis of brain sections. Each column contains data from a single brain. Cell source, time point of analysis and the experiment number are indicated on the top rows. Data was collected in two independent experiments, n=2-4 embryos per condition. Wpt: weeks post transplantation, OB: olfactory bulb, SEZ: subependymal zone, LV: lateral ventricle.

We were able to find transplanted cells derived from both SEZ and injured cortex in different regions throughout the neuraxis, with a widespread antero-posterior and dorso-ventral distribution. Furthermore, we observed a preferential distribution of transplanted cells in certain brain regions (corpus callosum, thalamus, hypothalamus) that was similar on cells originated from both sources (Figure 16A,B).

However, some differences in distribution on the transplanted cells depending on the cell source were evident in our analysis. We found transplanted cells derived from the SEZ in regions related to the endogenous migration pathway of these cells (SEZ, RMS and OB) with a higher frequency than cells derived from the injured cortex. As a matter of fact, we did not find transplanted cells in the OB in any of the brains transplanted with cortically derived cells. On the other hand, it was interesting to note that cells derived from the SEZ displayed homing at the isocortex at a much higher frequency than cortically derived cells (Figure 16A,B).

Cells derived from SEZ neurospheres that were transplanted into the E13 brain gave rise to neurons (NeuN) both at 2 and 4 wpt. Interestingly, the generation of neurons in the OB (which is expected from these cells) could be observed in half of the transplanted embryos at 2 and 4 wpt, whereas the generation of neurons in ectopic regions (hypothalamus and midbrain) was only observed at 2 wpt (Figure 17A,B). It is interesting to note that in all of the brains transplanted with SEZ-derived cells in which there were transplanted cells in the OB, we were able to find neurons among these cells. However, even though we found transplanted cells in the hypothalamus and midbrain of almost all of the transplanted embryos, neurons within these regions were found in few brains. This suggests that SEZ-derived cells are highly responsive to local environmental cues present in the OB for neuronal differentiation, whereas the cues present in other brain regions, such as the hypothalamus and midbrain, although eliciting neuronal differentiation in some cases, do not show the same success in this process as the ones present in the OB, which is the endogenous terminal differentiation region of these cells.

Outside of the aforementioned regions, the SEZ-derived cells gave rise to cells that did not have neuronal morphology or express the neuronal markers that we used in our analysis (NeuN and DCX) and mainly displayed the morphology and expression markers of glial cells ($GFAP^+$ and $Olig2^+$) (Figure 17A,B).

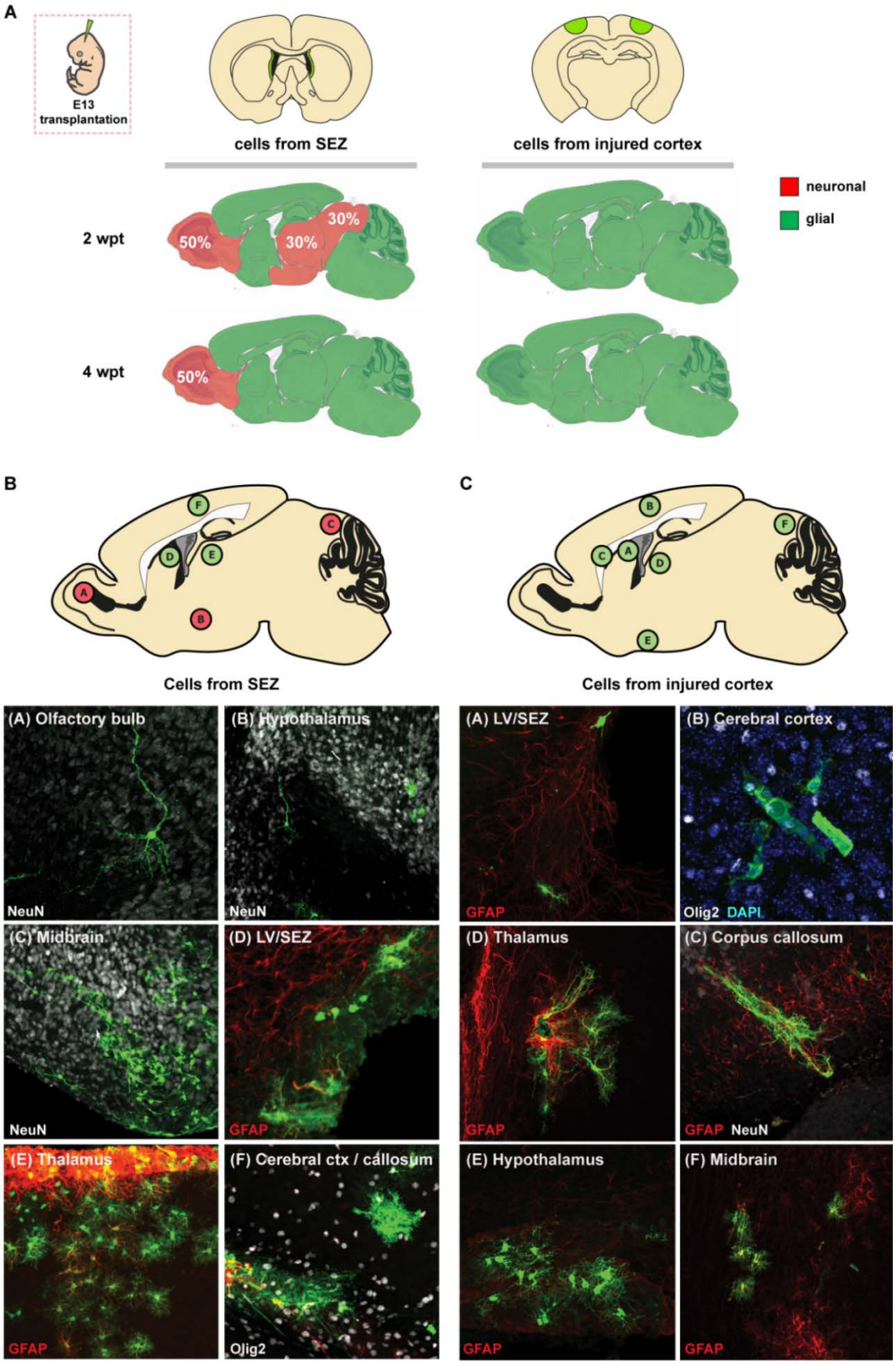

Figure 17. Differentiation of adult SEZ- and injured cortex-derived cells in the developing embryonic brain. (**A**) Summary of results of differentiation potential analysis of both cell sources

upon transplantation in the E13 embryonic brain at 2 and 4 wpt. Cells derived from the SEZ gave rise to neurons (NeuN) in the OB of 50% of the transplanted brains at both time points. Neuronal differentiation in SEZ non-related regions (hypothalamus and midbrain) was observed only at 2 wpt. All of the transplanted cells found in the regions indicated in green did not express neuronal markers and were largely glial (GFAP or Olig2). Transplanted cells derived from the injured cortex did not give rise to neurons in the developing brain in any brain region at 2 or 4 wpt. Data was collected in 2 independent experiments, n=2-4 embryos per condition. (**B**) Examples of different cell phenotypes derived from transplanted cells and their integration site in different brain regions at 2 and 4 wpt. Wpt: weeks post transplantation, SEZ: subependymal zone, LV: lateral ventricle, ctx: cortex.

In all of the brains that were transplanted with cells derived from injured cortex neurospheres, we weren't able to find any cells that had either a neuronal morphology or expressed neuronal cell markers. We could identify many glial cells in different regions of the brain expressing astrocytic (GFAP) or oligodendrocytic (Olig2) cell markers (Figure 17A,B).

In summary, analysis of SEZ and injured cortex-derived cells transplanted into the embryonic brain indicates once more that cortical reactive astrocytes largely do not give rise to neuronal cells *in vivo*, despite showing a widespread migration along the neuraxis and being found in many different brain regions. Bona fide aNSCs derived from the SEZ, on the other hand, can differentiate into neuronal cells in the developing brain and preferentially do so in their intrinsic neurogenic niche, generating mature neurons mainly in the OB.

Altogether our results from transplantations in neurogenesis-supportive environments in both the adult and embryonic brain show that, despite having the potential to generate neurons *in vitro*, reactive astrocytes are largely incapable of giving rise to neurons *in vivo*.

3.3 Origin of neurosphere-forming cells in the injured cerebral cortex gray matter

3.3.1 Analysis of origin of neurosphere-forming cells in Emx1-GFP mice

In order to investigate whether the neurosphere forming cells present in the injured cortical tissue are locally derived from resident parenchymal astrocytes that acquire plasticity following lesion, or if they consist of SEZ cells that migrate into the cortical lesion site, we used transgenic mouse line tools to label and follow cells according to their region of origin.

More specifically, we used double transgenic Emx1-GFP mice obtained from crossings between the $Emx1^{Cre}$ (Iwasato et al., 2000) and CAG-CAT-eGFP reporter lines (Nakamura et al., 2006). Emx1 is a gene expressed exclusively in the dorsal telencephalon from embryonic stages of development to adulthood, and the $Emx1^{Cre}$ transgenic line shows a pattern of Cre expression specific to this brain region (Iwasato et al., 2000). Therefore, in our double transgenic Emx1-GFP mouse line we expected to obtain permanent GFP labeling in cells located in the cortex and hippocampus, but not in the SEZ.

Immunohistochemical analysis of intact brains largely confirmed the expression pattern we expected to find, with a broad labeling of cells in the dorsal telencephalon, but not in other brain regions (Figure 18A). We identified many GFP-labeled cells in the cortex that were also expressing astrocytic markers (GFAP/S100β), and these were distributed through all cortical layers (Figure 18B). The SEZ was mainly devoid of GFP-labeled cells, but we could find one GFP^+ cell at the ventricular zone that was also $GFAP/S100\beta^+$ upon analysis of serial sections of two intact mouse brains. There were many GFP^+ astrocytic cells in the neighboring striatal area (Figure 18B).

Altogether, through immunohistochemical analysis of intact Emx1-GFP brains we were able to detect robust GFP labeling of cortical cells, while only very few GFP-labeled cells were found in the SEZ, confirming that this double transgenic mouse line could be used to investigate if the neurospheres derived from injured cortical tissue were originated from resident cortical cells.

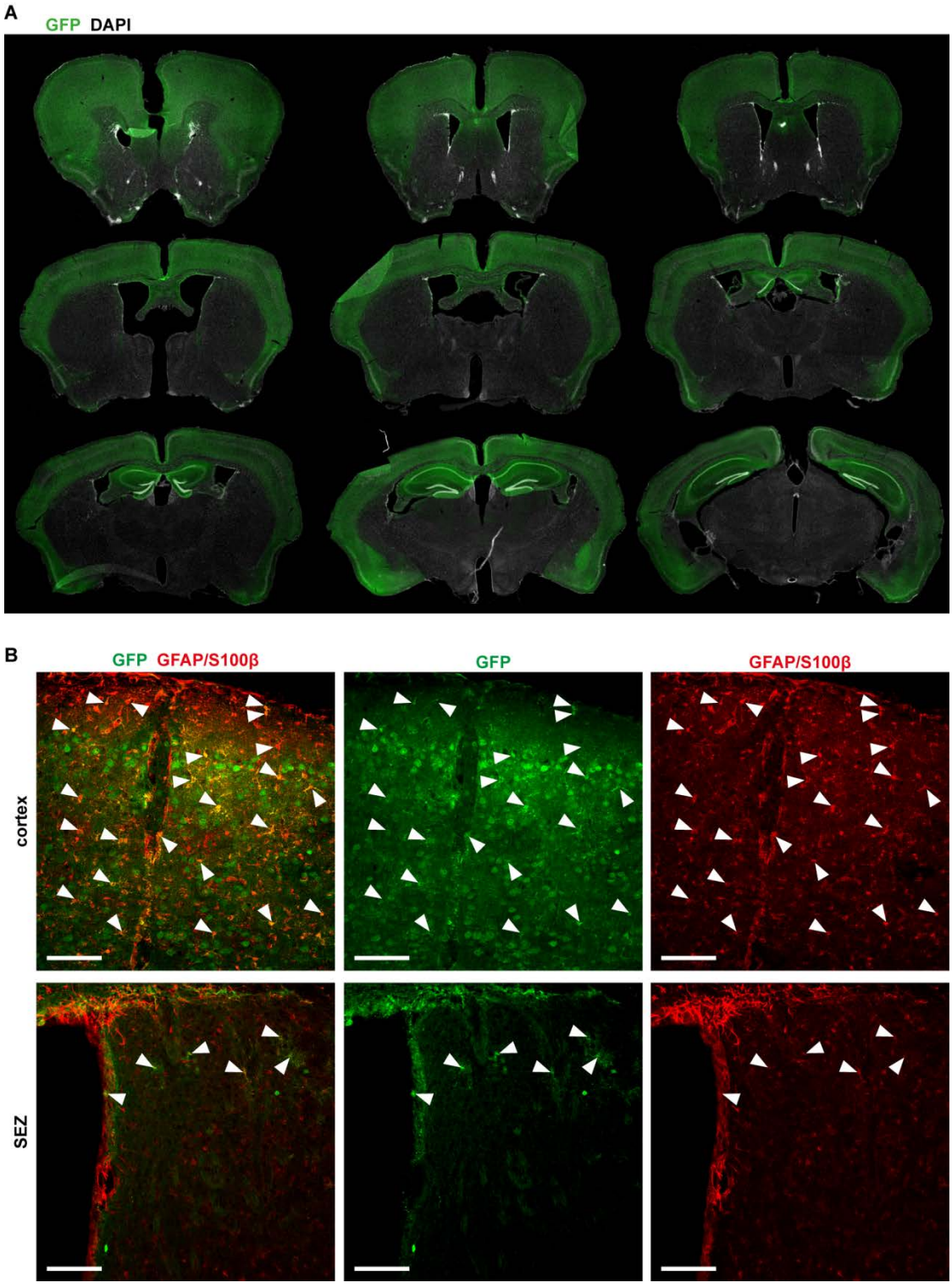

Figure 18. Emx-GFP brain sections show expression of GFP reporter largely localized to the dorsal telencephalon. (**A**) Overview of serial coronal sections presented in an anterior to posterior sequence shows a broad GFP labeling of cells in the dorsal telencephalic areas (isocortex and hippocampus), while ventral telencephalic areas and midbrain are mainly devoid of GFP expression. (**B**) Immunohistochemical analysis showed a broad labeling of GFP cells in the cortex (upper row), with many GFP-labeled cells also expressing astrocytic markers (GFAP/S100β). The SEZ (lower row) was mainly devoid of GFP-labeled cells, but we could find a GFP$^+$ cell at the ventricular zone that was also GFAP/S100β$^+$. Many GFP-labeled astrocytic cells were found in the

adjacent striatal area. Arrowheads indicate double positive cells (GFP^+ and $GFAP/S100\beta^+$). Scale bars represent 100 µm.

We performed the neurosphere assay with SEZ and cortical tissue that we extracted from intact or stab wound-lesioned mouse brains at 5 dpi (n=3 animals per condition). Cells were cultured for 14 div and at this time point we quantified the number of neurospheres as well as their GFP expression for each condition (Figure 19A).

Neurospheres obtained from SEZ tissue in all conditions were largely GFP^- (Figure 19B) but we could find few neurospheres that were either GFP^+ or were a mix of GFP^+ and GFP^- cells, which were termed $GFP^{+/-}$ mosaic neurospheres. On the other hand, in the neurospheres obtained from cortical tissue there was overall a higher proportion of GFP^+ neurospheres, albeit at a very lower number compared to the total amount of neurospheres we obtained from the SEZ (Figure 19C).

This substantial difference in the proportion of GFP^+ neurospheres that we found between SEZ tissue (1.3-2.6%) and cortical tissue (30-50%) strongly suggests that the neurosphere-forming cells present in the injured cortical tissue are indeed originated from resident parenchymal astrocytes, and not from SEZ-derived cells that migrate into the cortical lesion site. However, due to the presence of few GFP^+ cells in the SEZ detected via immunohistochemistry in intact brains of Emx1-GFP mice, as well as the few GFP^+ neurospheres we could identify in the different SEZ-derived cultures, we cannot formally exclude that these few GFP^+ cells present in the SEZ under physiological conditions could migrate to the cortex following an injury and thus contribute to neurosphere formation.

We proceeded by developing another experimental paradigm, where our goal was to achieve a more specific labeling of cortical cells, with no labeling of cells in the SEZ region. For this purpose, we tested a labeling approach with an AAV vector injection in the intact somatosensory cortex (Figure 20).

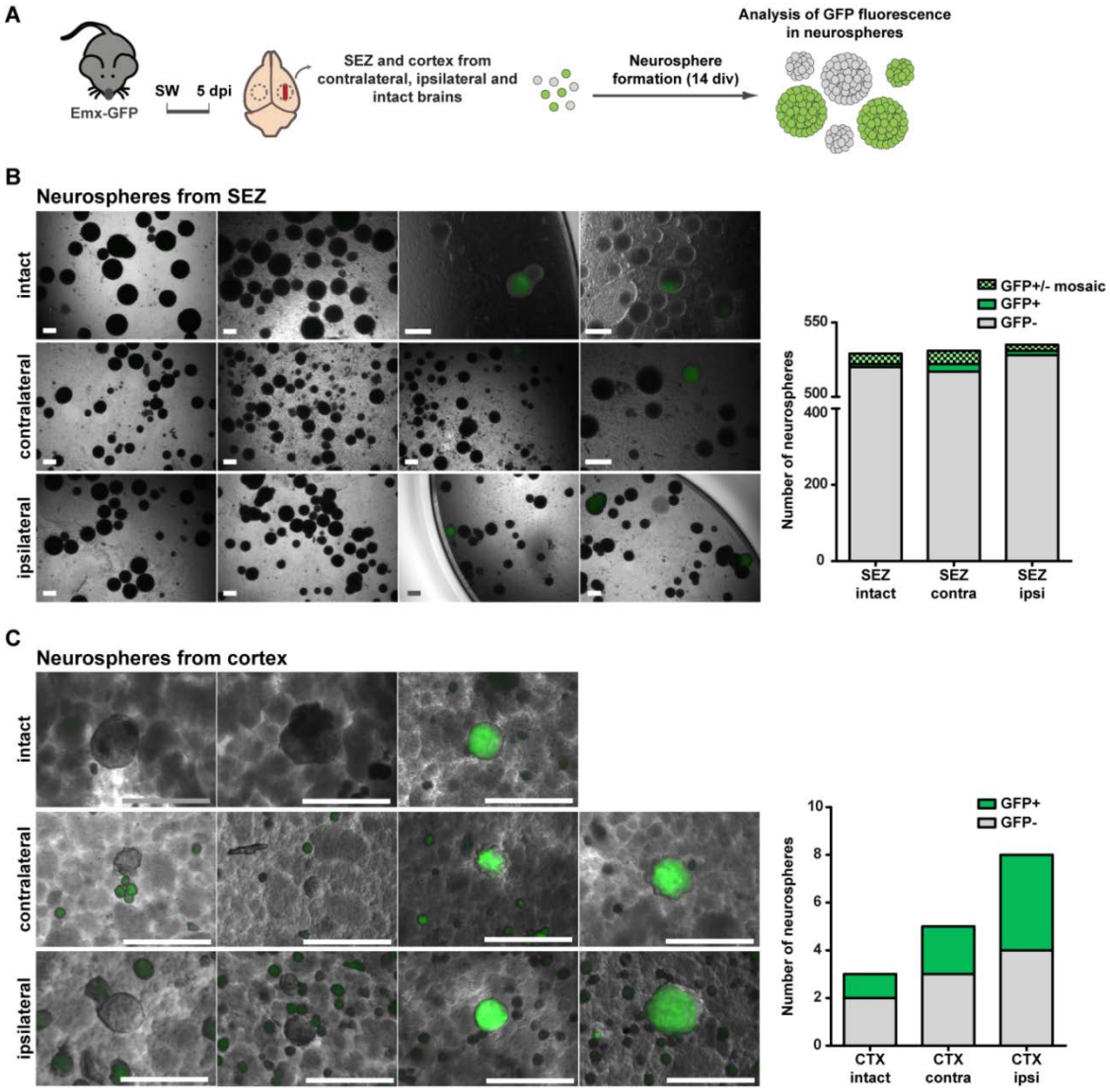

Figure 19. Neurospheres from intact and injured brains of Emx1-GFP mice show evidence for local origin of neurosphere-forming cells in the cortex. (**A**) Experimental paradigm used to investigate the origin of neurosphere-forming cells present in the injured cortical tissue. We extracted both intact or SW injured brains at 5 dpi from Emx1-GFP mice and performed the neurosphere assay with tissue obtained from the SEZ or cortex. The cells were cultured for 14 div, after which the neurospheres were quantified and characterized according to the presence or absence of GFP expression. (**B**) Almost all of the neurospheres generated from SEZ tissue in all different conditions were GFP^-. Examples of neurospheres quantified from SEZ cultures are shown in the pictures to the left, and the total numbers of neurospheres quantified per condition, as well as their GFP expression pattern, are indicated on the bar graphs to the right. (**C**) Between 30-50% of the neurospheres generated from cortical tissue in all of the conditions were GFP^+. Examples of neurospheres quantified from cortical tissue cultures are shown in the pictures to the left, and the total numbers of neurospheres and their GFP expression are indicated on the bar graphs to the right. Data is represented in absolute numbers, n=3 animals per condition. Scale bars represent 200 μm.

3.3.2 Labeling of cerebral cortex astrocytes with an AAV reporter vector

In order to achieve an experimental paradigm where we can rule out the existence of any fluorescent protein labeled cells in the SEZ, we investigated if we could achieve cortex-specific labeling via injection of viral vectors in the cortex.

For this purpose, we injected AAV-TdTomato viral vectors with reporter expression driven by a GFAP promoter (*see Section 2.5.4*) (Shigetomi et al., 2013) into the intact somatosensory cortex gray matter of WT mice. Through this approach, we expected to achieve a region- and cell-specific labeling of cortical astrocytes.

Immunohistochemical analysis showed a widespread labeling of cortical astrocytes around the injection site, but labeling was specific to this region and no labeled cells were detected in the SEZ and surrounding areas (Figure 20A,B). This indicates that our approach is optimal to achieve specific labeling of cortical cells (or in this case, of cortical astrocytes), and can be employed to further investigate the origin of neurosphere-forming cells present in injured cortical tissue. As AAV vectors don't integrate into the genome, this labeling approach with the AAV-TdTomato reporter would not be an optimal tool to evaluate reporter expression in the neurospheres, as highly proliferative cells would dilute the viral DNA and loose reporter expression.

In order to circumvent this problem, we carried on to set up a new experimental paradigm using injections of AAV-iCre (*see Section 2.5.4*) (Druckmann et al., 2014) in floxed GFP-Reporter mice (Nakamura et al., 2006) to achieve a permanent labeling of cortical astrocytes.

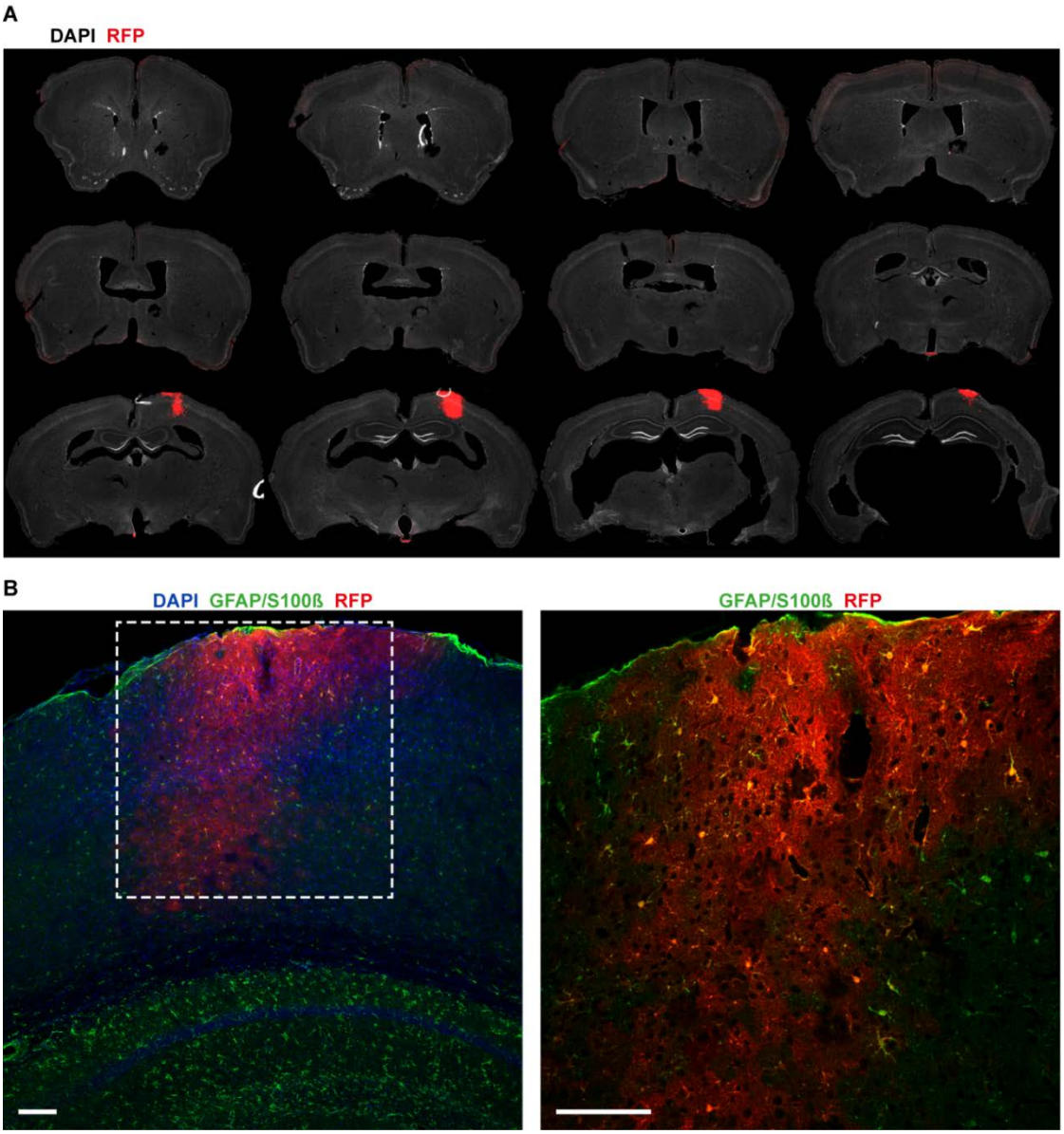

Figure 20. Specific labeling of cortical astrocytes through AAV-tdTomato virus injection in the intact cortex. (**A**) Immunohistochemistry of serial coronal brain sections shows the viral spread through the antero-posterior axis, with reporter expression localized mainly to the somatosensory cortex. SEZ and surrounding regions were completely devoid of TdTomato reporter labeling (n=3 animals). (**B**) Immunohistochemistry of injection site depicts reporter expression pattern, with many labeled astrocytes (RFP^+ and $GFAP/S100\beta^+$). Scale bars represent 100 μm.

3.3.3 Analysis of origin of neurosphere-forming cells in GFP-Reporter mice injected with AAV-iCre viral vector to label cortical cells

In order to assess whether cortical astrocytes could acquire neurosphere-forming potential following injury, we injected floxed GFP-Reporter mice with the AAV-iCre viral vector driven by GFAP expression (*see Section 2.5.4*) in the intact cortical gray matter to

label resident astrocytes. SW lesions were inflicted in the injected area 2 weeks after injection, and animals were sacrificed 5 days later for immunohistochemical analysis or neurosphere assay (Figure 21A).

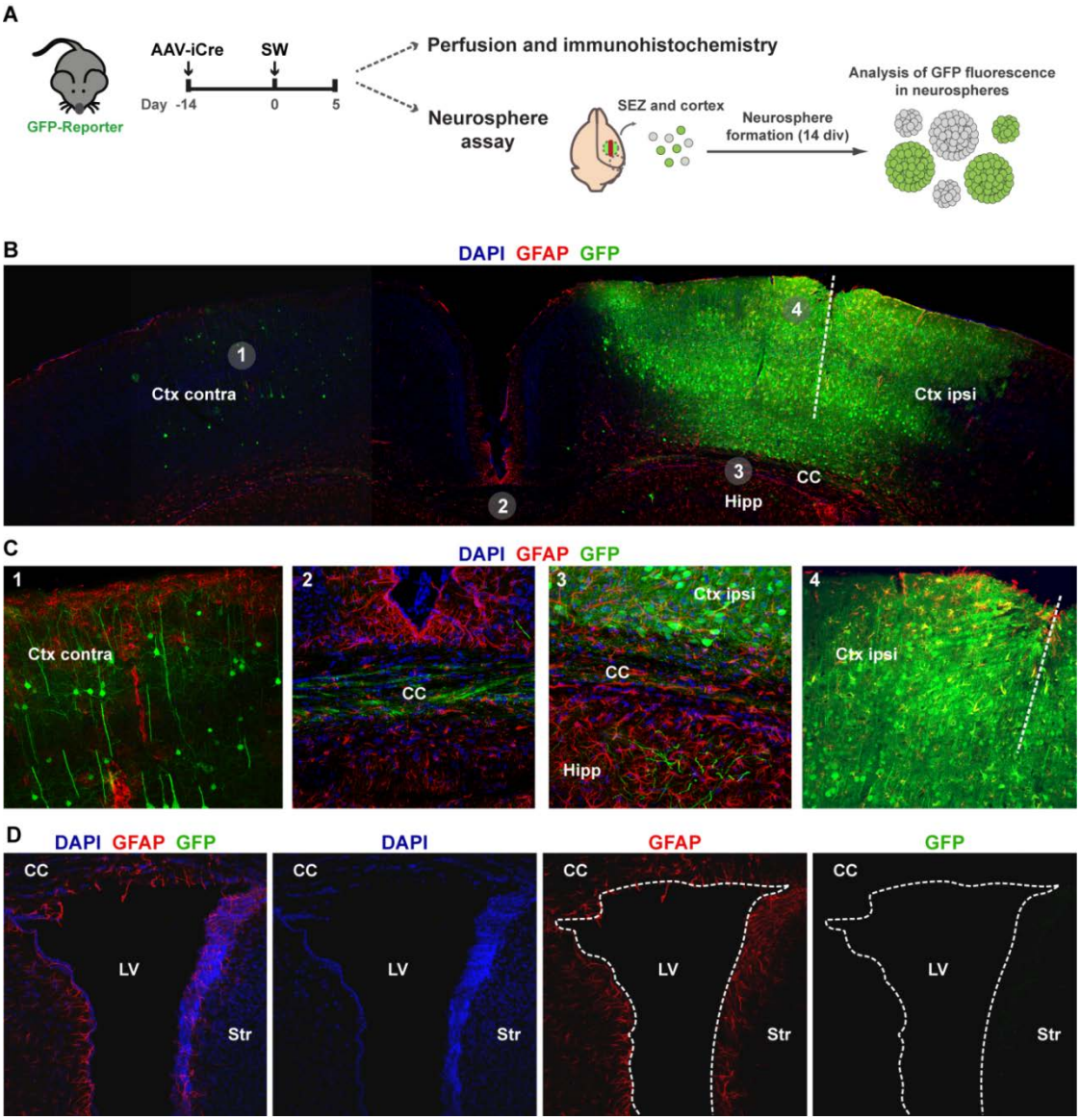

Figure 21. Permanent labeling of cortical cells through injection of AAV-iCre in floxed GFP-Reporter mice. (**A**) Experimental paradigm used for specific and permanent labeling of cortical cells. Mice injected in the same experimental batch were either perfused for immunohistochemical analysis or taken for neurosphere assay. (**B**) Overview of injection site in the ipsilateral cortex with widespread GFP expression throughout the cortical gray matter. GFP$^+$ cells could also be found in contralateral cortex, as well as GFP$^+$ fibers in the corpus callosum. (**C**) Higher magnifications of areas containing GFP-labeled cells and processes, with corresponding locations depicted in (b). (**D**) In the SEZ there were virtually no GFP-labeled cells, confirming this experimental setting to be suitable for the following neurosphere assay analysis.

Immunohistochemical analysis of injected brains showed a widespread labeling of cells throughout all layers of the ipsilateral cortex, detected through GFP expression (Figure 21B). Labeling was present in, but not restricted to astrocytes, as it could be

clearly seen in layer 5 cortical neurons (Figure 21B). Moreover, there were labeled axonal fibers in the corpus callosum and in many cells (including neurons) in the contralateral hemisphere, indicating axonal transport of viral particles (Figure 21B,C). Furthermore, a few GFP-labeled fibers were identified in the hippocampus (Figure 21B,C).

Importantly, virtually no GFP-labeled cells were present in the SEZ (Figure 21D) in the animals analyzed. Therefore, with this experimental paradigm we were able to successfully label cortical cells in a permanent and region-specific manner.

Animals that were injected in parallel to the ones analzyed via immunohistochemistry were taken for preparation of cell cultures and neurosphere assay analysis. By using a fluorescent lamp we could identify the injection site (Figure 22A) and used this to restrict the cortical dissection to GFP-expressing tissue (Figure 22B).

Consistent with our results from immunohistochemical analysis, virtually all of the neurospheres originated from SEZ tissue were negative for GFP (Figure 22C). On the other hand, in cultures prepared from injured cortical tissue there were GFP^+ neurospheres, indicating that cells of cortical origin can give rise to neurospheres following an invasive injury, such as the SW lesion (Figure 22D). Of note, many of the cortical neurospheres were GFP^-, which could have two possible explanations. Either they are originated from cortical cells that were not infected or did not turn on the expression of GFP, or they are formed by cells of non-cortical origin that migrate to the lesion site.

Altogether, these results cannot rule out the possibility that cells of non-cortical origins contribute to the pool of neurosphere-forming cells at the lesion site. However, this evidence demonstrates that cells within the cortical parenchyma are able to dedifferentiate and give rise to neurospheres following injury.

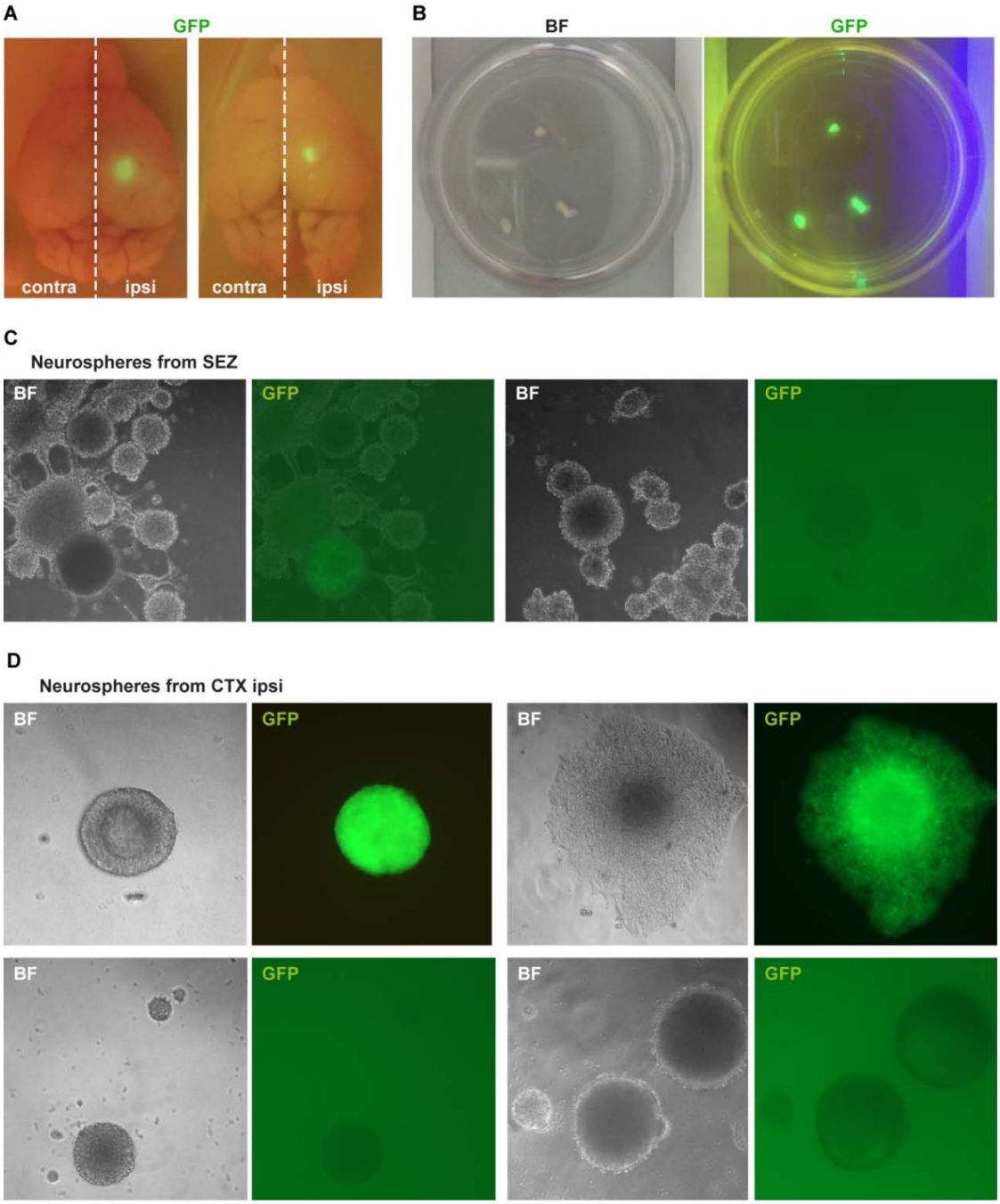

Figure 22. Cortical cells give rise to neurospheres following injury, as observed through AAV-iCre injection in floxed GFP-reporter mice. (**A**) Overview of injected brains prior to dissection in which strong GFP fluorescence area can be seen at the site of injection and lesion. (**B**) Cortical tissue samples after dissection are labeled with GFP (n=4). (**C**) Virtually no neurospheres originated from the SEZ were GFP^+. (**D**) Cortical cells gave rise to GFP^+ and GFP^- neurospheres following injury.

4 Discussion

Although it has been shown that cerebral cortical reactive astrocytes exhibit stem cell potential *in vitro*, it remains largely unknown if these cells can enact this potential *in vivo* when exposed to different environmental cues. Through this study we achieved a better understanding of "if" and "how" reactive astrocytes can be modulated in different conditions *in vivo*.

4.1 Reactive astrocytes can re-enter the cell cycle upon repetitive lesions

By employing two independent experimental approaches – proliferative population analysis through a dual-labeling strategy with BrdU and EdU (Figure 5), and clonal analysis with GLAST/Confetti mice (Figure 8) - we have shown that astrocytes can undergo more than one round of cell division upon repetitive injuries. Even though the proportion of astrocytes that can be activated re-enter the cell cycle in this condition is significant (10-14% of proliferating astrocytes, Figures 8H,12D), their progeny is rather limited compared to other glial cell populations (Schneider et al., 2016; Tay et al., 2017), as we could not observe any clones that were bigger than 3 cells in our clonal analysis (Figure 8H). This limitation also reflects the results we obtained in the neurosphere assay, as a second lesion did not induce any observable changes in the self-renewal and differentiation potential of reactive astrocytes *in vitro* (Figure 9).

Although our data show that astrocyte self-renewal as one hallmark of stem cell identity is limited *in vivo*, this property can be modulated by injury conditions and the presence of monocytes in the lesion site. Upon the absence of infiltrating monocytes there was a 2-fold increase in the proportion of self-renewing $GFAP^+/BrdU^+/EdU^+$ astrocytes in the penumbra of $CCR2^{-/-}$ mice compared to WT animals following repetitive lesions (Figure 12D,F). Monocytes evidently play an important role in regulating astrocyte recruitment into proliferation, and it would be interesting to investigate which mechanisms or factors are involved in this process. In a previous study it was shown through proteome analysis in $CCR2^{-/-}$ compared to WT mice that at 5 days after SW injury there is an increase in GSK3a, a protein involved in many signaling pathways that are

important for proliferation (such as Wnt, EGF, retionoic acid and PDGF), as well as regulation of many proteins that interact with EGFR, which is an important receptor for activation of aNSC and reactive astrocyte proliferation (Frik et al., 2018). Furthermore, in this study it was shown that there is a decreased permeability of the BBB in CCR2$^{-/-}$ mice in the acute phase after injury (3 dpi), which could have an effect on the signals that are entering the penumbra and modulating astrocyte proliferation (Frik et al., 2018).

Another intriguing question would be to assess whether the new astrocytes that are generated after single or repetitive injuries perform the same functions as the astrocytes that were lost through damage. In a study with NG2-glia ablation, for example, even though the NG2 cell population was fully restored in a short time after depletion, mice suffered from motor dysfunctions due to differentiation deficits in the newly generated NG2-glia (Schneider et al., 2016). Therefore, in the context of single and repetitive traumatic brain injuries, it would be interesting to evaluate whether the different groups of subsets of reactive astrocytes are functionally equivalent or if newly generated astrocytes in these injury conditions show functional deficits.

Moreover, it has been recently shown that there is a big degree of astrocyte heterogeneity within the cortex, evidenced by differences in morphology and gene expression profiles of astrocytes in distinct cortical layers (Lanjakornsiripan et al., 2018). There seems to be layer-specific interactions between astrocytes and neurons, and astrocytes could have layer-specific functions. It would be interesting to evaluate whether these specific profiles and functions are maintained in such a layer-specific organization following damage.

4.2 Astrocyte proliferative pool is adaptable and driven towards homeostatic maintenance of astrocyte population

Another key finding of this study is that the proliferative capacity of astrocytes is not strictly restricted to a fixed subset of cells, but can actually be activated in different sets of astrocytes by repetitive lesions. Our data show that upon a second lesion there is substantial recruitment of previously quiescent astrocytes into proliferation (GFAP^{+}/EdU^{+} cells, Figure 5C). Therefore, even though a greater pool of parenchymal astrocytes located at the lesion site is potentially able to proliferate, only a restricted number of them actually enter cell division following a single injury (around 50% of astrocytes 250 µm away from the lesion core, Figure 5B).

Surprisingly, the number of total parenchymal astrocytes was consistently maintained (Figures 5B, 8D, 12B) after single and repetitive lesions across all genotypes we analyzed (WT, GLAST/Confetti and CCR2$^{-/-}$ mice). Astrocyte loss after traumatic brain injury has been previously described (Frik et al., 2018; Zhao et al., 2003), and it has been shown that astrocyte loss is restored through cell proliferation in young adult mice (Frik et al., 2018; Heimann et al., 2017). Nevertheless, it is interesting to note that, even after double lesions, the astrocytic population numbers were reestablished over the time course of a few days. Altogether, this astrocyte population recovery that we observed is a strong indicative of the existence of a mechanism for maintenance of the astrocytic population at homeostatic cell numbers, as it has been described for other glial cells (NG2-glia and microglia) (Elmore et al., 2014; Hughes et al., 2013; Jäkel and Dimou, 2017).

Interestingly, we observed that this recovery can be achieved through different strategies, in other words, through the activation of different subsets of astrocytes into proliferation. In WT animals we observed a preferential recruitment of previously quiescent astrocytes into proliferation upon a second injury (Figure 12D,F). However, in the absence of invading monocytes we observed a clear shift towards an increase of astrocyte cell-cycle reentry, and this was accompanied by a reduced recruitment of quiescent astrocytes into proliferation (Figure 12D,F). Although different subsets of astrocytes are recruited into proliferation in the absence or presence of invading monocytes, in both scenarios the same end result of reestablishment of parenchymal astrocyte numbers was achieved (Figure 12B).

It has been shown that in the aged brain there is an impaired recovery of astrocytic loss following traumatic brain injury, and that this failure is mainly due to deficits in astrocytic cell division and their lowered response to proliferative stimuli (Heimann et al., 2017). We showed evidence that suggests this deficit is intrinsically regulated by changes in the expression levels of important key regulators of cell proliferation (Figure 13) (Heimann et al., 2017). It would be interesting to investigate the mechanisms involved in shutting down the proliferative machinery that we observe in young astrocytes that occurs during aging and turns them refractory to proliferative signals, leading to a disruption in the homeostatic maintenance of their population numbers following injury.

Altogether, our findings provide insights into a unique adaptation capacity of the proliferative repertoire of astrocytes that leads to the prevention of astroglia depletion in distinct lesion microenvironments.

4.3 Impairment of monocyte infiltration leads to changes in the overall cellular environment at the penumbra

We have shown through immunohistochemical analysis of sections with single and double lesioned brains that the non-astrocytic ($GFAP^{-}$) proliferative population is mostly comprised of microglia/macrophages (Figure 10B,D). After a single injury in WT animals, we observed an exacerbated increase in the number of proliferating $Iba1^{+}$ microglia/macrophages, which ultimately led to an increase of the total $Iba1^{+}$ population (Figure 10B,C). This phenomenon of exacerbated response of macrophages in the CNS to a second pathological insult has been described in different types of injury and is known as microglia priming (Witcher et al., 2015).

It was surprising to see, however, that in the absence of invading monocytes the numbers of proliferative non-astrocytic cells was comparable following single and repetitive injuries. Since most of the $GFAP^{-}$ proliferating cells in WT animals were $Iba1^{+}$ microglia/macrophages, one can speculate that in $CCR2^{-/-}$ animals these cells suffer an exhaustion due to their exacerbated proliferation following a first insult (possibly due to an overload caused by the lack of infiltrated monocytes) and are less responsive to a second insult. In order to confirm this speculative hypothesis it is necessary to further investigate how the monocyte-free environment affects the proliferation of microglia in response to repetitive injuries in the $CCR2^{-/-}$ mice.

4.4 Neurosphere-derived cortical reactive astrocytes are largely unable to give rise to neurons *in vivo*

Parenchymal cortical astrocytes have been shown to acquire stem cell potential following invasive brain injury and can give rise to different cell types *in vitro*, including neurons (Buffo et al., 2008; Shimada et al., 2012; Sirko et al., 2013). It has also been shown that striatal astrocytes have a latent neurogenic program and can generate immature neurons *in vivo* upon stroke (Magnusson et al., 2014). Since the cerebral cortex is a gliogenic environment and does not support neurogenesis (Seidenfaden et al., 2006), we questioned whether cortical reactive astrocytes would be able to give rise to neurons

in vivo if relocated to environments with robust neurogenesis – the adult hippocampal DG and the developing forebrain of the E13 embryo.

Although reactive astrocytes derived from cortical neurospheres could survive in the host brain following transplantation, they largely failed to give rise to immature and mature neurons (DCX^+ and $NeuN^+$ cells) at 2 and 4 wpt and remained within the glial cell lineage ($GFAP^+$ or $Olig2^+$ cells) both in the adult hippocampal neurogenic niche (Figure 15), and in the developing embryonic brain (Figure 17). These results are consistent with a previous report in which reactive astrocytes derived from the cortical peri-infarct area after stroke did not give rise to neuronal cells when transplanted into adult neurogenic niches (SEZ , RMS and DG) or the neonatal brain (Shimada et al., 2012).

Therefore, although cortical reactive astrocytes can be instructed to give rise to neurons through forced reprogramming *in vitro* (Heinrich et al., 2010) and *in vivo* (Buffo et al., 2005; Gascón et al., 2016, 2017), the signals present in the DG neurogenic niche or in the E13 developing brain are not successful in locally supporting neuronal differentiation in these cells.

Surprisingly, also neurosphere-derived cells from the SEZ, which contain bona fide aNSCs, were not successful in giving rise to mature neurons in the adult DG within 4 weeks after transplantation, even though they could generate a substantial amount of neuroblasts in this neurogenic niche (Figure 15). These results are contrary to another study, in which rat SEZ neurospheres were transplanted into the DG, and 2 weeks after transplantation 35% of the transplanted cells exhibited immunohistochemical and morphological features of hippocampal granule cell neurons (Richardson et al., 2005). This inconsistency could be due to species-specific differences in the neurogenic niches and therefore it would be interesting to confirm this on further studies.

Furthermore, although these aNSCs could give rise to a few mature NeuN-expressing neurons in different brain regions of the developing brain, their neurogenic potential was mostly confined to their own OB neurogenic niche, as at 4 wpt only the neurons generated in this region could survive (Figure 17).

Altogether, although both the adult DG and the E13 embryonic brain are pro-neurogenic environments that can support and orient some levels of neuronal differentiation for non-endogenous SEZ aNSCs, it seems that these cells are very much restricted and unresponsive to neuronal differentiation cues from neurogenic niches other than their own.

4.5 Neurosphere-derived cells from the SEZ and injured cortex show very distinct differentiation profiles upon transplantation in neurogenic environments

Although cells derived from reactive cortical neurospheres did not give rise to neurons *in vivo* in both neurogenic environments we evaluated, it is important to note that these cells showed a clearly distinct differentiation profile compared to cells from SEZ-derived neurospheres.

In the adult DG, cells derived from SEZ neurospheres gave rise to a substantial amount of oligodendrocytic cells (Olig2$^+$, 17-30%) and immature neurons (DCX$^+$, 22-32%) at 2 and 4 wpt, whereas cells derived from injured cortex neurospheres gave rise to few oligodendrocytic cells (Olig2$^+$, 3-5%) and to virtually no immature neurons (DCX$^+$, 0%) over the same time points analyzed (Figure 15).

Moreover, when transplanted intraventricularly into the E13 brain, SEZ neurosphere-derived cells could migrate into the OB and generate mature NeuN-expressing neurons. Additionally, these cells could also give rise, albeit at a lower frequency and only at 2 wpt, to mature neurons in the hypothalamus and midbrain (Figure 17). On the other hand, injured cortex neurosphere-derived cells could neither migrate into the OB, nor give rise to neurons in any brain region, even in the hypothalamus and midbrain, where they were commonly found to integrate (Figures 16 and 17).

Taken together, in light of recent debate regarding the origin and identity of neurosphere-forming cells in the injured cortex, our results from transplantation experiments with SEZ- and injured cortex-derived neurospheres bring clear evidence that the neurosphere-forming cells in these two regions are distinct from each other, both in their differentiation and migration profiles *in vivo*. This new evidence highlights the importance of performing additional experiments to further investigate and evaluate this question, which is the last topic of this thesis.

4.6 Cortical cells give rise to neurospheres after injury

10 years ago it was shown that cortical reactive astrocytes de-differentiate after injury and acquire stem cell potential, evidenced by the formation of self-renewing, multipotent neurospheres *in vitro* (Buffo et al., 2008). When this phenomenon was first

described, evidence was provided to classify the neurosphere-forming cells as resident cortical parenchymal astrocytes that de-differentiate and acquire stem cell properties upon traumatic brain injury. However, recently new evidence has been shown for an alternative hypothesis, namely, that the neurosphere-forming cells present at the cortical lesion site are actually SEZ aNSCs that are generated at the lateral ventricle and migrate to the cortex upon an ischemic injury (Faiz et al., 2015).

Both studies have some shortcomings in the experimental paradigms used to analyze the origin of the cortical neurospheres and possible contributions from cells of other brain regions. In Buffo et al. 2008, this was analyzed through injection of VSVG-pseudotyped lentiviral vector containing GFP reporter into the SEZ ipsilateral to the site of SW injury to label the cells, and could not identify any cell migration from SEZ cells into the cortex through immunohistochemistry or FACS analysis. The limitation of this paradigm is that the labeling obtained in SEZ cells through lentiviral vector injections was very low, more precisely, 2.6% of SEZ cells were GFP^+. Therefore, the absence of evidence for migration of SEZ cells to the cortex does not necessarily mean that this would not be the case if a greater number of cells could be labeled and followed.

On the other hand in the Faiz. et al 2015 study, although they can follow a substantial number of SEZ cells through fate-mapping in the Nestin-$CreER^{T2}$ mouse model, they do not provide convincing controls to show that they have specific labeling of SEZ cells, but not of cortical cells.

Therefore, we thought it was important, to revisit this fundamental question and assess if the discrepancy of the data between the studies is due to the different injury models used (traumatic lesion or ischemic injury), or if indeed one of the two hypothesis would not be sustained in light of new results gathered from further experiments that could address possible methodological shortcomings in the studies performed so far.

Data gathered on *in vitro* and *in vivo* properties of neurospheres derived from SEZ aNSCs and cortical reactive astrocytes show an obvious difference in the self-renewal and differentiation properties of these cells. Consistent across different cortical regions and also injury types, cells derived from the injured cortex show a lower number of neurosphere-formation in primary and also subsequent passages, and also decreased size and multipotency compared to SEZ-derived neurospheres (Shimada et al., 2012; Sirko et al., 2009, 2013). Furthermore, when transplanted into the brains of neonatal mice, neurospheres derived from the SEZ could give rise to neurons, whereas

neurospheres derived from the lesioned cortex could not (Shimada et al., 2012). Our transplantation study discussed in the previous section also shows the same results: cells derived from SEZ neurospheres could give rise to immature neurons in the adult DG and to mature neurons in the developing embryonic brain, whereas cells derived from injured cortex neurospheres could not (*see Section 3.2*).

Taken together, comparative data from SEZ and injured cortex neurospheres indicate that either these two neurospheres are generated from different cell types, or if the aNSCs do migrate from the SEZ to the lesioned cortex and are the cells that generate the cortical neurospheres, they undergo drastic changes in this migration that ultimately lead to alterations in their intrinsic program, resulting in differences that can be still seen when cells from these two different sources are placed into a new environment.

We set out to evaluate whether cortical cells could give rise to neurospheres upon injury and designed simple experimental paradigms to answer this question, which consisted on labeling cortical cells before injury and evaluating if they could give rise to neurospheres thereafter. We achieved permanent labeling of cortical cells through the double transgenic Emx1-GFP mice, and AAV-iCre injection into the cortex of floxed GFP-Reporter mice. While in the Emx1-GFP mice there were a few GFP-labeled cells in the SEZ (Figure 18) and a few GFP^+ neurospheres from the SEZ (Figure 19), in the GFP-Reporter mice injected with AAV-iCre there were literally no GFP-labeled cells in the SEZ (Figure 21) or GFP^+ neurospheres from SEZ tissue (Figure 22). Our data from both experimental paradigms (but most convincingly from AAV-iCre injected mice) show that cortical cells can give rise to neurospheres *in vitro* after SW lesion. However, with this experimental design we cannot exclude that SEZ aNSCs could contribute to neurosphere formation in cortical tissue. In order to answer this question, one possibility would be to label SEZ cells using the same viral vector and mouse line and performing the neurosphere assay.

Nonetheless, the positive evidence for neurosphere formation from local cortical cells that we have shown is in contradiction with the results from Faiz et al. (2015), which means that either these differences are due to lesion-specific differences (between SW lesion and ischemic stroke), or due to false conclusions drawn on the aforementioned dubious experimental paradigm. It could still well be that part of the neurospheres isolated from injured cortical tissue are formed by cells of non-cortical origin, but now we can ascertain that cortical cells can give rise to at least part of these neurospheres upon SW lesion.

4.7 General conclusions

Our results show that cortical gray matter reactive astrocytes exhibit an overall limited stem cell potential (self-renewal and differentiation) *in vivo* when stimulated in different environments and injury conditions. However, our data indicate that astrocyte proliferation in the post-traumatic brain is an adaptable process. Our results show that astrocyte cycling activity is not restricted to a subset of astrocytes and the activation of proliferation of different groups of astrocytes is dynamically regulated by environmental cues. Intriguingly, astrocyte proliferation seems to be a tightly regulated process, with a strong drive towards population homeostasis. The functional implications of the different astrocyte proliferative behaviors and population homeostasis in CNS function remain to be seen, and a better comprehension of these processes could forward the advancement of approaches to repair the damaged CNS in the future.

Altogether, the novel findings of this thesis advance the understanding of the biology of reactive astrocytes and open many new exciting questions for future investigation in this field.

REFERENCES

Allaman, I., Bélanger, M., and Magistretti, P.J. (2011). Astrocyte-neuron metabolic relationships: For better and for worse. Trends Neurosci. *34*, 76–87.

Altman, J. (1962). Are new neurons formed in the brains of adult mammals? Science *135*, 1127–1128.

Altman, J. (1963). Autoradiographic Investigation of Cell Proliferation in the Brains of Rats and Cats. Anat. Rec. *145*, 573–591.

Altman, J., and Das, G.D. (1965). Autoradiographic and histologicalevidence of postnatal hippocampal neurogenesis in rats. J. Comp. Neurol. *124*, 319–335.

Altman, J., and Das, G.D. (1966). Autoradiographic and Histological Studies o Postnatal Neurogenesis. J. Comp. Neurol. *126*, 337–389.

Amankulor, N.M., Hambardzumyan, D., Pyonteck, S.M., Becher, O.J., Joyce, J.A., and Holland, E.C. (2009). Sonic Hedgehog Pathway Activation Is Induced by Acute Brain Injury and Regulated by Injury-Related Inflammation. J. Neurosci. *29*, 10299–10308.

Anderson, M.A., Ao, Y., and Sofroniew, M. V. (2014). Heterogeneity of reactive astrocytes. Neurosci. Lett. *565*, 23–29.

Anderson, M.A., Burda, J.E., Ren, Y., Ao, Y., O'Shea, T.M., Kawaguchi, R., Coppola, G., Khakh, B.S., Deming, T.J., and Sofroniew, M. V. (2016). Astrocyte scar formation aids central nervous system axon regeneration. Nature *532*, 195–200.

Araque, A., Carmignoto, G., Haydon, P.G., Oliet, S.H.R., Robitaille, R., and Volterra, A. (2014). Gliotransmitters travel in time and space. Neuron *81*, 728–739.

Attwell, D., Buchan, A.M., Charpak, S., Lauritzen, M., MacVicar, B.A., and Newman, E.A. (2010). Glial and neuronal control of brain blood flow. Nature *468*, 232–243.

Barbosa, J.S., Sanchez-gonzalez, R., Giaimo, R. Di, Baumgart, E.V., Theis, F.J., Ninkovic, J., Di Giaimo, R., Baumgart, E.V., Theis, F.J., Götz, M., et al. (2015). Live imaging of adult neural stem cell behavior in the intact and injured zebrafish brain. Science *348*, 789–793.

Bardehle, S., Krüger, M., Buggenthin, F., Schwausch, J., Ninkovic, J., Clevers, H., Snippert, H.J., Theis, F.J., Meyer-Luehmann, M., Bechmann, I., et al. (2013). Live imaging of astrocyte responses to acute injury reveals selective juxtavascular proliferation. Nat. Neurosci. *16*, 580–586.

Barker, R.A., Barrett, J., Mason, S.L., and Björklund, A. (2013). Fetal dopaminergic transplantation trials and the future of neural grafting in Parkinson's disease. Lancet Neurol. *12*, 85–91.

Barker, R.A., Götz, M., and Parmar, M. (2018). New approaches for brain repair—from rescue to reprogramming. Nature *557*, 329–334.

Beckervordersandforth, R., Tripathi, P., Ninkovic, J., Bayam, E., Lepier, A., Stempfhuber, B., Kirchhoff, F., Hirrlinger, J., Haslinger, A., Lie, D.C., et al. (2010). In vivo fate mapping and expression analysis reveals molecular hallmarks of prospectively isolated adult neural stem cells. Cell Stem Cell *7*, 744–758.

von Bernhardi, R., Eugenín-von Bernhardi, L., and Eugenín, J. (2015). Microglial cell dysregulation in brain aging and neurodegeneration. Front. Aging Neurosci. *7*, 1–21.

Bonaguidi, M.A., Wheeler, M.A., Shapiro, J.S., Stadel, R.P., Sun, G.J., Ming, G.L., and Song, H. (2011). In vivo clonal analysis reveals self-renewing and multipotent adult neural stem cell characteristics. Cell *145*, 1142–1155.

Buffo, A., Vosko, M.R., Erturk, D., Hamann, G.F., Jucker, M., Rowitch, D., and Gotz, M. (2005). Expression pattern of the transcription factor Olig2 in response to brain injuries: Implications for neuronal repair. Proc. Natl. Acad. Sci. *102*, 18183–18188.

Buffo, A., Rite, I., Tripathi, P., Lepier, A., Colak, D., Horn, A.-P., Mori, T., and Gotz, M. (2008). Origin and progeny of reactive gliosis: A source of multipotent cells in the injured brain. Proc. Natl. Acad. Sci. *105*, 3581–3586.

Bush, T.G., Puvanachandra, N., Horner, C.H., Polito, A., Ostenfeld, T., Svendsen, C.N., Mucke, L., Johnson, M.H., Sofroniew, M. V., Site, F., et al. (1999). Leukocyte Infiltration , Neuronal Degeneration , and Neurite Outgrowth after Ablation of Scar-Forming , Reactive Astrocytes in Adult Transgenic Mice. Neuron *23*, 297–308.

Cahoy, J.D., Emery, B., Kaushal, A., Foo, L.C., Zamanian, J.L., Christopherson, K.S., Xing, Y., Lubischer, J.L., Krieg, P. a, Krupenko, S. a, et al. (2008). A transcriptome database for astrocytes, neurons, and oligodendrocytes: a new resource for understanding brain

development and function. J. Neurosci. *28*, 264–278.

Calzolari, F., Michel, J., Baumgart, E.V., Theis, F., Götz, M., and Ninkovic, J. (2015). Fast clonal expansion and limited neural stem cell self-renewal in the adult subependymal zone. Nat. Neurosci. *18*, 490–492.

Chapouly, C., Argaw, A.T., Horng, S., Castro, K., Zhang, J., Asp, L., Loo, H., Laitman, B.M., Mariani, J.N., Farber, R.S., et al. (2015). Astrocytic TYMP and VEGFA drive blood-brain barrier opening in inflammatory central nervous system lesions. Brain *138*, 1548–1567.

Clarke, L.E., and Barres, B. (2013). Emerging roles of astrocytes in neural circuit development. Nat. Rev. Neurosci. *14*, 311–321.

Codeluppi, S., Svensson, C.I., Hefferan, M.P., Valencia, F., Silldorff, M.D., Oshiro, M., Marsala, M., and Pasquale, E.B. (2009). The Rheb-mTOR Pathway Is Upregulated in Reactive Astrocytes of the Injured Spinal Cord. J. Neurosci. *29*, 1093–1104.

Dimou, L., and Götz, M. (2014). Glial Cells as Progenitors and Stem Cells: New Roles in the Healthy and Diseased Brain. Physiol. Rev. *94*, 709–737.

Doetsch, F., Caillé, I., Lim, D.A., García-Verdugo, J.M., and Alvarez-Buylla, A. (1999). Subventricular zone astrocytes are neural stem cells in the adult mammalian brain. Cell *97*, 703–716.

Druckmann, S., Feng, L., Lee, B., Yook, C., Zhao, T., Magee, J.C., and Kim, J. (2014). Structured Synaptic Connectivity between Hippocampal Regions. Neuron *81*, 629–640.

Elmore, M.R.P., Najafi, A.R., Koike, M.A., Dagher, N.N., Spangenberg, E.E., Rice, R.A., Kitazawa, M., Matusow, B., Nguyen, H., West, B.L., et al. (2014). Colony-Stimulating Factor 1 Receptor Signaling Is Necessary for Microglia Viability, Unmasking a Microglia Progenitor Cell in the Adult Brain. Neuron *82*, 380–397.

Encinas, J.M., Michurina, T. V., Peunova, N., Park, J.H., Tordo, J., Peterson, D.A., Fishell, G., Koulakov, A., and Enikolopov, G. (2011). Division-coupled astrocytic differentiation and age-related depletion of neural stem cells in the adult hippocampus. Cell Stem Cell *8*, 566–579.

Faiz, M., Sachewsky, N., Gascon, S., Bang, K.W.A., Morshead, C.M., Nagy, A., Bang, K.W.A., Morshead, C.M., and Nagy, A. (2015). Adult Neural Stem Cells from the Subventricular Zone Give Rise to Reactive Astrocytes in the Cortex after Stroke. Cell Stem Cell *17*, 1–11.

Falkner, S., Grade, S., Dimou, L., Conzelmann, K.-K., Bonhoeffer, T., Götz, M., and Hübener, M. (2016). Transplanted embryonic neurons integrate into adult neocortical circuits. Nature *539*, 248–253.

Feil, S., Valtcheva, N., and Feil, R. (2009). Inducible Cre Mice. In Gene Knockout Protocols: 2nd Edition, pp. 343–363.

Ferrer, I. (2017). Diversity of astroglial responses across human neurodegenerative disorders and brain aging. Brain Pathol. *27*, 645–674.

Fonarow, G.C., Reeves, M.J., Zhao, X., Olson, D.M., Smith, E.E., Saver, J.L., and Schwamm, L.H. (2010). Age-related differences in characteristics, performance measures, treatment trends, and outcomes in patients with ischemic stroke. Circulation *121*, 879–891.

Frik, J., Merl-Pham, J., Plesnila, N., Mattugini, N., Kjell, J., Kraska, J., Gómez, R.M., Hauck, S.M., Sirko, S., and Götz, M. (2018). Cross-talk between monocyte invasion and astrocyte proliferation regulates scarring in brain injury. EMBO Rep. *19*.

Furutachi, S., Miya, H., Watanabe, T., Kawai, H., Yamasaki, N., Harada, Y., Imayoshi, I., Nelson, M., Nakayama, K.I., Hirabayashi, Y., et al. (2015). Slowly dividing neural progenitors are an embryonic origin of adult neural stem cells. Nat. Neurosci. *18*, 657–665.

Gao, P., Postiglione, M.P., Krieger, T.G., Hernandez, L., Wang, C., Han, Z., Streicher, C., Papusheva, E., Insolera, R., Chugh, K., et al. (2014). Deterministic Progenitor Behavior and Unitary Production of Neurons in the Neocortex. Cell *159*, 775–788.

Gascón, S., Murenu, E., Masserdotti, G., Ortega, F., Russo, G.L., Petrik, D., Deshpande, A., Heinrich, C., Karow, M., Robertson, S.P., et al. (2016). Identification and Successful Negotiation of a Metabolic Checkpoint in Direct Neuronal Reprogramming. Cell Stem Cell *18*, 396–409.

Gascón, S., Masserdotti, G., Russo, G.L., and Götz, M. (2017). Direct Neuronal Reprogramming: Achievements, Hurdles, and New Roads to Success. Cell Stem Cell *21*, 18–34.

Goldman, S.A., and Nottebohm, F. (1983). Neuronal production, migration, and differentiation in a vocal control nucleus of the adult female canary brain. Proc. Natl. Acad. Sci. *80*, 2390–2394.

Gong, S., Zheng, C., Doughty, M.L., Losos, K., Didkovsky, N., Schambra, U.B., Nowak, N.J., Joyner, A., Leblanc, G., Hatten, M.E., et al. (2003). A gene expression atlas of the central nervous system based on bacterial artificial chromosomes. Nature *425*, 917–925.

Götz, M., and Huttner, W.B. (2005). The cell biology of neurogenesis. Nat Rev Mol Cell Biol *6*, 777–788.

Götz, M., Sirko, S., Beckers, J., and Irmler, M. (2015). Reactive astrocytes as neural stem or progenitor cells: In vivo lineage, In vitro potential, and Genome-wide expression analysis. Glia *63*, 1452–1468.

Grade, S., and Götz, M. (2017). Neuronal replacement therapy: previous achievements and challenges ahead. Npj Regen. Med. *2*, 29.

Grealish, S., Heuer, A., Cardoso, T., Kirkeby, A., Jönsson, M., Johansson, J., Björklund, A., Jakobsson, J., and Parmar, M. (2015). Monosynaptic Tracing using Modified Rabies Virus Reveals Early and Extensive Circuit Integration of Human Embryonic Stem Cell-Derived Neurons. Stem Cell Reports *4*, 975–983.

Gross, C.G. (2000). Neurogenesis in the adult brain: death of a dogma. Nat. Rev. Neurosci. *1*, 67–73.

Gyoneva, S., and Ransohoff, R.M. (2015). Inflammatory reaction after traumatic brain injury: therapeutic potential of targeting cell–cell communication by chemokines. Trends Pharmacol. Sci. *36*, 471–480.

Haydon, P.G. (2001). Glia: Listening and talking to the synapse. Nat. Rev. Neurosci. *2*, 185–193.

Hefendehl, J.K., Neher, J.J., Sühs, R.B., Kohsaka, S., Skodras, A., and Jucker, M. (2014). Homeostatic and injury-induced microglia behavior in the aging brain. Aging Cell *13*, 60–69.

Heimann, G., Canhos, L.L., Frik, J., Jäger, G., Lepko, T., Ninkovic, J., Götz, M., and Sirko, S. (2017). Changes in the Proliferative Program Limit Astrocyte Homeostasis in the Aged Post-Traumatic Murine Cerebral Cortex. Cereb. Cortex *27*, 4213–4228.

Heinrich, C., Blum, R., Gascón, S., Masserdotti, G., Tripathi, P., Sánchez, R., Tiedt, S., Schroeder, T., Götz, M., and Berninger, B. (2010). Directing astroglia from the cerebral cortex into subtype specific functional neurons. PLoS Biol. *8*.

Heinrich, C., Bergami, M., Gascón, S., Lepier, A., Viganò, F., Dimou, L., Sutor, B., Berninger, B., and Götz, M. (2014). Sox2-mediated conversion of NG2 glia into induced neurons in the injured adult cerebral cortex. Stem Cell Reports *3*, 1000–1014.

Hol, E.M., and Pekny, M. (2015). Glial fibrillary acidic protein (GFAP) and the astrocyte intermediate filament system in diseases of the central nervous system. Curr. Opin. Cell Biol. *32*, 121–130.

Hughes, E.G., Kang, S.H., Fukaya, M., and Bergles, D.E. (2013). Oligodendrocyte progenitors balance growth with self-repulsion to achieve homeostasis in the adult brain. Nat. Neurosci. *16*, 668–676.

Iwasato, T., Datwani, a, Wolf, a M., Nishiyama, H., Taguchi, Y., Tonegawa, S., Knöpfel, T., Erzurumlu, R.S., and Itohara, S. (2000). Cortex-restricted disruption of NMDAR1 impairs neuronal patterns in the barrel cortex. Nature *406*, 726–731.

Jäkel, S., and Dimou, L. (2017). Glial Cells and Their Function in the Adult Brain: A Journey through the History of Their Ablation. Front. Cell. Neurosci. *11*, 1–17.

Jessen, N.A., Finmann Munk, A.S., Lundgaard, I., and Nedergaard, M. (2015). The Glymphatic System – A Beginner's Guide. Neurochem. Res. *40*, 2583–2599.

Kaplan, M., and Hinds, J. (1977). Neurogenesis in the adult rat: electron microscopic analysis of light radioautographs. Science *197*, 1092–1094.

Kee, N., Sivalingam, S., Boonstra, R., and Wojtowicz, J.M. (2002). The utility of Ki-67 and BrdU as proliferative markers of adult neurogenesis. J. Neurosci. Methods *115*, 97–105.

Kimelberg, H.K., and Nedergaard, M. (2010). Functions of astrocytes and their potential as therapeutic targets. Neurotherapeutics *7*, 338–353.

Lagace, D.C., Whitman, M.C., Noonan, M.A., Ables, J.L., DeCarolis, N.A., Arguello, A.A., Donovan, M.H., Fischer, S.J., Farnbauch, L.A., Beech, R.D., et al. (2007). Dynamic Contribution of Nestin-Expressing Stem Cells to Adult Neurogenesis. J. Neurosci. *27*, 12623–12629.

Lanjakornsiripan, D., Pior, B.J., Kawaguchi, D., Furutachi, S., Tahara, T., Katsuyama, Y., Suzuki, Y., Fukazawa, Y., and Gotoh, Y. (2018). Layer-specific morphological and molecular differences in neocortical astrocytes and their dependence on neuronal layers. Nat. Commun. *9*.

Liboska, R., Ligasová, A., Strunin, D., Rosenberg, I., and Koberna, K. (2012). Most Anti-BrdU Antibodies React with 2′-Deoxy-5-Ethynyluridine - The Method for the Effective Suppression of This Cross-Reactivity. PLoS One *7*, 1–10.

Liddelow, S.A., and Barres, B.A. (2017). Reactive Astrocytes: Production, Function, and Therapeutic Potential. Immunity *46*, 957–967.

Liddelow, S.A., Guttenplan, K.A., Clarke, L.E., Bennett, F.C., Bohlen, C.J., Schirmer, L., Bennett, M.L., Münch, A.E., Chung, W.-S., Peterson, T.C., et al. (2017). Neurotoxic reactive astrocytes are induced by activated microglia. Nature *541*, 481–487.

Lim, D.A., Fishell, G.J., and Alvarez-Buylla, A. (1997). Postnatal mouse subventricular zone neuronal precursors can migrate and differentiate within multiple levels of the developing neuraxis. Proc. Natl. Acad. Sci. U. S. A. *94*, 14832–14836.

Livak, K.J., and Schmittgen, T.D. (2001). Analysis of relative gene expression data using real-time quantitative PCR and. Methods *25*, 402–408.

Llorens-bobadilla, E., Zhao, S., Baser, A., Saiz-castro, G., Martin-villalba, A., Llorens-bobadilla, E., Zhao, S., Baser, A., Saiz-castro, G., Zwadlo, K., et al. (2015). Single-Cell Transcriptomics Reveals a Population of Dormant Neural Stem Cells that Become Activated upon Brain Injury Article Single-Cell Transcriptomics Reveals a Population of Dormant Neural Stem Cells that Become Activated upon Brain Injury. Stem Cell *17*, 329–340.

MacVicar, B.A., and Newman, E.A. (2015). Astrocyte Regulation of Blood Flow in the Brain. Cold Spring Harb. Perspect. Biol *7*, 1–15.

Magnusson, J.P., Goritz, C., Tatarishvili, J., Dias, D.O., Smith, E.M.K., Lindvall, O., Kokaia, Z., and Frisen, J. (2014). A latent neurogenic program in astrocytes regulated by Notch signaling in the mouse. Science *346*, 237–241.

Malatesta, P., Hartfuss, E., and Götz, M. (2000). Isolation of radial glial cells by fluorescent-activated cell sorting reveals a neuronal lineage. Development *127*, 5253–5263.

Merkle, F.T., Tramontin, A.D., García-Verdugo, J.M., and Alvarez-Buylla, A. (2004). Radial glia give rise to adult neural stem cells in the subventricular zone. Proc. Natl. Acad. Sci. U. S. A. *101*, 17528–17532.

Michelsen, K.A., Acosta-Verdugo, S., Benoit-Marand, M., Espuny-Camacho, I., Gaspard, N., Saha, B., Gaillard, A., and Vanderhaeghen, P. (2015). Area-specific reestablishment of damaged circuits in the adult cerebral cortex by cortical neurons derived from mouse embryonic stem cells. Neuron *85*, 982–997.

Middeldorp, J., and Hol, E.M. (2011). GFAP in health and disease. Prog. Neurobiol. *93*, 421–443.

Mori, T., Tanaka, K., Buffo, A., Wurst, W., Kühn, R., and Götz, M. (2006). Inducible gene deletion in astroglia and radial glia - A valuable tool for functional and lineage analysis. Glia *54*, 21–34.

Nakamura, T., Colbert, M.C., and Robbins, J. (2006). Neural crest cells retain multipotential characteristics in the developing valves and label the cardiac conduction system. Circ. Res. *98*, 1547–1554.

Nedergaard, M., Ransom, B., and Goldman, S. a. (2003). New roles for astrocytes: Redefining the functional architecture of the brain. Trends Neurosci. *26*, 523–530.

Neumeister, B., Grabosch, A., Basak, O., Kemler, R., and Taylor, V. (2009). Neural progenitors of the postnatal and adult mouse forebrain retain the ability to self-replicate, form neurospheres, and undergo multipotent differentiation in vivo. Stem Cells *27*, 714–723.

Nieto-Sampedro, M. (1988). Astrocyte mitogen inhibitor related to epidermal growth factor receptor. Science *240*, 1784–1786.

Oberheim, N.A., Goldman, S.A., and Nedergaard, M. (2012). Heterogeneity of Astrocytic Form and Function. *814*, 23–45.

Okabe, M., Ikawa, M., Kominami, K., Nakanishi, T., and Nishimune, Y. (1997). "Green mice" as a source of ubiquitous green cells. FEBS Lett. *407*, 313–319.

Pekny, M., and Pekna, M. (2004). Astrocyte intermediate filaments in CNS pathologies and regeneration. J. Pathol. *204*, 428–437.

Pekny, M., and Pekna, M. (2014). Astrocyte Reactivity and Reactive Astrogliosis: Costs and Benefits. Physiol. Rev. *94*, 1077–1098.

Pekny, M., Wilhelmsson, U., and Pekna, M. (2014). The dual role of astrocyte activation and reactive gliosis. Neurosci. Lett. *565*, 30–38.

Pekny, M., Pekna, M., Messing, A., Steinhäuser, C., Lee, J.M., Parpura, V., Hol, E.M., Sofroniew, M. V., and Verkhratsky, A. (2015). Astrocytes: a central element in neurological diseases. Acta Neuropathol. *131*, 1–23.

Pilz, G.-A., Bottes, S., Betizeau, M., Jörg, D.J., Carta, S., Simons, B.D., Helmchen, F., and Jessberger, S. (2018). Live imaging of neurogenesis in the adult mouse hippocampus. Science *359*, 658–662.

Pitter, K.L., Tamagno, I., Feng, X., Ghosal, K., Amankulor, N., Holland, E.C., and Hambardzumyan, D. (2014). The SHH/Gli pathway is reactivated in reactive glia and drives proliferation in response to neurodegeneration-induced lesions. Glia 1595–1607.

Rabchevsky, a G., Weinitz, J.M., Coulpier, M., Fages, C., Tinel, M., and Junier, M.P. (1998). A role for transforming growth factor alpha as an inducer of astrogliosis. J. Neurosci. *18*, 10541–10552.

Reinchisi, G., Parada, M., Lois, P., Oyanadel, C., Shaughnessy, R., Gonzalez, A., and Palma, V. (2013). Sonic Hedgehog modulates EGFR dependent proliferation of neural stem cells during late mouse embryogenesis through EGFR transactivation. Front. Cell. Neurosci. *7*, 166.

Reynolds, B. a., and Weiss, S. (1992). Generation of neurons and astrocytes from isolated cells of the adult mammalian central nervous system. Science *255*, 1707–1710.

Reynolds, B.A., and Rietze, R.L. (2005). Neural stem cells and neurospheres: re-evaluating the relationship. Nat. Methods *2*, 333–336.

Richardson, R.M., Broaddus, W.C., Holloway, K.L., Sun, D., Bullock, M.R., and Fillmore, H.L. (2005). Heterotypic neuronal differentiation of adult subependymal zone neuronal progenitor cells transplanted to the adult hippocampus. Mol. Cell. Neurosci. *28*, 674–682.

Riquelme, P.A., Drapeau, E., and Doetsch, F. (2008). Brain micro-ecologies: neural stem cell niches in the adult mammalian brain. Philos. Trans. R. Soc. Lond. B. Biol. Sci. *363*, 123–137.

Robel, S., Berninger, B., and Götz, M. (2011). The stem cell potential of glia: lessons from reactive gliosis. Nat. Rev. Neurosci. *12*, 88–104.

Rothstein, J.D., Dykes-Hoberg, M., Pardo, C.A., Bristol, L.A., Jin, L., Kuncl, R.W., Kanai, Y., Hediger, M.A., Wang, Y., Schielke, J.P., et al. (1996). Knockout of glutamate transporters

reveals a major role for astroglial transport in excitotoxicity and clearance of glutamate. Neuron *16*, 675–686.

Saederup, N., Cardona, A.E., Croft, K., Mizutani, M., Cotleur, A.C., Tsou, C.L., Ransohoff, R.M., and Charo, I.F. (2010). Selective chemokine receptor usage by central nervous system myeloid cells in CCR2-red fluorescent protein knock-in mice. PLoS One *5*.

Schneider, S., Gruart, A., Grade, S., Zhang, Y., Kröger, S., Kirchhoff, F., Eichele, G., Delgado García, J.M., and Dimou, L. (2016). Decrease in newly generated oligodendrocytes leads to motor dysfunctions and changed myelin structures that can be rescued by transplanted cells. Glia *64*, 2201–2218.

Seidenfaden, R., Desoeuvre, A., Bosio, A., Virard, I., and Cremer, H. (2006). Glial conversion of SVZ-derived committed neuronal precursors after ectopic grafting into the adult brain. Mol. Cell. Neurosci. *32*, 187–198.

Seri, B., García-Verdugo, J.M., McEwen, B.S., and Alvarez-Buylla, A. (2001). Astrocytes give rise to new neurons in the adult mammalian hippocampus. J. Neurosci. *21*, 7153–7160.

Shigetomi, E., Bushong, E.A., Haustein, M.D., Tong, X., Jackson-Weaver, O., Kracun, S., Xu, J., Sofroniew, M. V., Ellisman, M.H., and Khakh, B.S. (2013). Imaging calcium microdomains within entire astrocyte territories and endfeet with GCaMPs expressed using adeno-associated viruses. J. Gen. Physiol. *141*, 633–647.

Shimada, I.S., LeComte, M.D., Granger, J.C., Quinlan, N.J., and Spees, J.L. (2012). Self-Renewal and Differentiation of Reactive Astrocyte-Derived Neural Stem/Progenitor Cells Isolated from the Cortical Peri-Infarct Area after Stroke. J. Neurosci. *32*, 7926–7940.

Simon, C., Götz, M., and Dimou, L. (2011). Progenitors in the adult cerebral cortex: Cell cycle properties and regulation by physiological stimuli and injury. Glia *59*, 869–881.

Sirko, S., Neitz, A., Mittmann, T., Horvat-Brcker, A., Holst, A. Von, Eysel, U.T., and Faissner, A. (2009). Focal laser-lesions activate an endogenous population of neural stem/progenitor cells in the adult visual cortex. Brain *132*, 2252–2264.

Sirko, S., Behrendt, G., Johansson, P.A., Tripathi, P., Costa, M., Bek, S., Heinrich, C., Tiedt, S., Colak, D., Dichgans, M., et al. (2013). Reactive Glia in the Injured Brain Acquire Stem Cell Properties in Response to Sonic Hedgehog. Cell Stem Cell *12*, 426–439.

Sirko, S., Irmler, M., Gascón, S., Bek, S., Schneider, S., Dimou, L., Obermann, J., De Souza

Paiva, D., Poirier, F., Beckers, J., et al. (2015). Astrocyte reactivity after brain injury: The role of galectins 1 and 3. Glia *63*, 2340–2361.

Snippert, H.J., van der Flier, L.G., Sato, T., van Es, J.H., van den Born, M., Kroon-Veenboer, C., Barker, N., Klein, A.M., van Rheenen, J., Simons, B.D., et al. (2010). Intestinal crypt homeostasis results from neutral competition between symmetrically dividing Lgr5 stem cells. Cell *143*, 134–144.

Sofroniew, M. V. (2009). Molecular dissection of reactive astrogliosis and glial scar formation. Trends Neurosci. *32*, 638–647.

Sofroniew, M. V (2005). Reactive astrocytes in neural repair and protection. Neuroscientist *11*, 400–407.

Sofroniew, M. V., and Vinters, H. V. (2010). Astrocytes: Biology and pathology. Acta Neuropathol. *119*, 7–35.

Suhonen, J.O., Peterson, D. a, Ray, J., and Gage, F.H. (1996). Differentiation of adult hippocampus-derived progenitors into olfactory neurons in vivo. Nature *383*, 624–627.

Taupin, P. (2007). BrdU immunohistochemistry for studying adult neurogenesis: Paradigms, pitfalls, limitations, and validation. Brain Res. Rev. *53*, 198–214.

Taverna, E., Götz, M., and Huttner, W.B. (2014). The Cell Biology of Neurogenesis: Toward an Understanding of the Development and Evolution of the Neocortex.

Tay, T.L., Mai, D., Dautzenberg, J., Fernández-Klett, F., Lin, G., Sagar, S., Datta, M., Drougard, A., Stempfl, T., Ardura-Fabregat, A., et al. (2017). A new fate mapping system reveals context-dependent random or clonal expansion of microglia. Nat. Neurosci. *20*, 793–803.

Verkhratsky, A., Nedergaard, M., and Hertz, L. (2014). Why are Astrocytes Important? Neurochem. Res. 389–401.

Weissman, I.L. (2000). Stem cells: units of development, units of regeneration, and units in evolution. Cell *100*, 157–168.

Witcher, K.G., Eiferman, D.S., and Godbout, J.P. (2015). Priming the Inflammatory Pump of the CNS after Traumatic Brain Injury. Trends Neurosci. *38*, 609–620.

You, T., Bi, Y., Li, J., Zhang, M., Chen, X., Zhang, K., and Li, J. (2017). IL-17 induces reactive

astrocytes and up-regulation of vascular endothelial growth factor (VEGF) through JAK/STAT signaling. Sci. Rep. *7*, 1–15.

Zhang, Y., and Barres, B. a. (2010). Astrocyte heterogeneity: An underappreciated topic in neurobiology. Curr. Opin. Neurobiol. *20*, 588–594.

Zhang, L., Zhang, R.L., Wang, Y., Zhang, C., Zhang, Z.G., Meng, H., and Chopp, M. (2005). Functional recovery in aged and young rats after embolic stroke: Treatment with a phosphodiesterase type 5 inhibitor. Stroke *36*, 847–852.

Zhao, X., Ahram, A., Berman, R.F., Muizelaar, J.P., and Lyeth, B.G. (2003). Early Loss of Astrocytes After Experimental Traumatic Brain Injury. Glia *44*, 140–152.

LIST OF FIGURES

LIST OF TABLES

LIST OF ABBREVIATIONS

Abbreviation	Stands for
AAV	adeno-associated virus
Aldh1L1	aldehyde dehydrogenase 1
aNSCs	adult neural stem cells
BrdU	5-bromo-2'-deoxyuridine
BSA	bovine serum albumin
CC	corpus callosum
CCL2	C-C chemokine ligand type 2
CCR2	C-C chemokine receptor type 2
CNS	central nervous system
CTX	cerebral cortex
DAPI	4',6-diamidino-2-phenylindole
DCX	doublecortin
DG	dentate gyrus of the hippocampus
div	days *in vitro*
DMEM	dulbecco's modified eagle medium
dNTPs	deoxynucleotide triphosphates
dpi	days post injury
EdU	5-ethynyl-2'-deoxyuridine
EGF	epidermal growth factor
Emx1	empty spiracles homeobox 1
FBS	fetal bovine serum
FGF	fibroblast growth factor
FP	fluorescent protein
GFAP	glial fibrillary acidic protein
GFP	green fluorescent protein
GLAST	glutamate aspartate transporter
HCl	hydrogen chloride
HEPES	4-(2-hydroxyethyl)-1-piperazineethanesulfonic acid
Iba1	ionized calcium binding adaptor molecule 1

i.p.	intraperitoneal
IQR	interquartile range
NeuN	neuronal nuclei
NG2	neuron glia antigen-2
NGS	normal goat serum
O4	oligodendrocyte marker O4
OB	olfactory bulb
Olig2	oligodendrocyte transcription factor 2
PBS	phosphate-buffered saline
PCR	polymerase chain reaction
PFA	paraformaldehyde
RFP	red fluorescent protein
RGC	radial glia cell
RMS	rostral migratory stream
S100β	S100 calcium-binding protein β
SD	standard deviation
SEZ	subependymal zone of the lateral ventricle
SHH	sonic hedgehog
SW	stab wound injury
TAM	tamoxifen
wpt	weeks post transplantation
WT	wildtype

ACKNOWLEDGMENTS

First and foremost, I would like to thank Magdalena for making the accomplishment of this PhD project possible, and for giving me excellent guidance throughout these years. I learnt a lot from you, and I very much appreciate your great enthusiasm for science and your liveliness in all our discussions. Along the same line I would like to thank Lana for the great supervision and for always being there to offer support on challenging occasions. It was very enjoyable to work with both of you and I cannot thank you enough for how much I have learnt from your guidance. I also would like to thank Sven, who was a great collaborator and performed all experiments with impeccable efficiency and care.

One of the best things about my PhD experience was definitely the people who I met along the way and I cannot thank enough all of my wonderful colleagues for the great scientific and personal exchange throughout these years. It was a great experience to be part of this team! Special thanks to Sofia (my twin sister), Radhika (the always good-humored and cheerful friend), Daisy (the one to count on any occasion) and to Gianluca (my adventure and travel buddy). You have become my Munich family and I am very grateful to have you to share all the good, but also bad moments of my life!

I would also like to specially thank Elisa, Manja, Sergio, Nico, Judith, Amel, Gia, Anita, Tjasa for always being so kind and making the work in the lab even more fun. We are a big group and it is difficult to thank everyone individually, but I am very grateful for the exchanges that I had with each and every one of you.

Many thanks also to the technical staff, who took care that everything in the lab ran smoothly, which helped me immensely to focus on my project. Special thanks to Manja, Tatjana, Detlef, Sabine, Chulan, Andrea, Franz Rucker, Carmen, Ines and Gabi for always being so attentive and supportive. I would also like to thank all the supporting staff of the Biomedical Center and Helmholtz Center, particularly the animal caretakers, for the great work they do in the background.

Also in these lines, I would like to thank both Lana Polero and Elsa for their incredible efficiency and kindness in supporting me with all the paperwork throughout

these years, and for being always so friendly. And a very big “thank you” to Suada, who always received me with a smile and made my days in the lab so much more enjoyable.

From my first day onwards, my experience in Munich has been wonderful. Much of this is directly connected to have been taken care of by this amazing graduate program, which I am very glad to be part of, the GSN. Special thanks to Benedikt Grothe and Alexander Kaiser for making this graduate school such an enriching experience both in professional and personal aspects. I would also like to thank Lena Bittl, Stefanie Bosse, Maj-Catherine Botheroyd-Hobohm, Birgit Reinbold, Renate Herzog and Raluca Deac for excellent support in all aspects of this program. I cannot thank you enough for your help and assistance throughout these years!

I would also like to thank my TAC members, Dr. Florence Bareyre and Dr. Christian Haass for the great input and positive exchange in our meetings, which was essential to further improve and develop this project.

Many other people who were not directly involved with this PhD project were fundamental for this accomplishment. I would like to thank Xu, Kô, Murilo, Nori and Rê for bringing Brazil so much closer to Germany. In these lines I also thank my Göttingen family: Tati, Lucas, Thaís, Eduardo, Everlyn, Florian, Lucas, Cuca, Caio, Luisa, Olga and Vinícius for always being so supportive and for all the fun moments we spent together.

I would also like to thank my roommates Eva and Peter for always being there for me, for pampering me with tasty Plätzchen and for fixing my bike every once in a while. Also a big „thank you“ to Huong and Hannah for welcoming me so well in Germany and for remaining such good friends over all this time.

Although far away, I would like to thank my amazing Panela sisters and brothers for being simply the best! Piolha, Moita, Poka, Pamonha, Cocota, Mestre and Dio: there is no distance that can bring us appart. I love you all and am most thankful for your friendship!

A big „thank you“ also to all of my Campinas friends, specially to Lia, Pri, Flavinha, Belinha, Manu, Gui, Kiko and Soba. It is always a great feeling to be around friends who have always been part of my life, some of you even before I can remember.

All of this would definitely not be possible without the support of my amazing family! Mom and Dad, you always showed me that life is full of fun adventures and interesting places, and you always stood by all my decisions and rooted for me in

whatever goal I set in my mind. Thank you for being such incredible parents. Paula and Deco, you are my heroes and I am very lucky to have had you as examples throughout my life to look up to. You are amazing! Pedro and Dani, although you have entered my life only a few years (or months) ago, you have brought a lot of good moments and joy to our family and I look forward to all that we are still going to live together. Bob, Irene, Vic, Vera and Tom: thank you for always being so kind and loving. Each and everyone of you has taught me so much and I love you all.

Last but not least, I would like to thank my sweet and lovely boyfriend, Ricardo, who was a major contributor for the background work of this thesis. I cannot thank you enough for your support and companionship, for sharing the good and bad moments, and for helping me day by day become a better person. And also a big „thank you“ to my family in Ribeirão and Franca for always being so kind and for always throwing great parties.

There is, indeed, a lot to be thankful for in this incredible 5-year chapter of my life. I am deeply grateful for being around so many great colleagues, friends, and family who have taught me so much in this time. And for all of those who also contributed to this work, but whose names I didn't explicitly mention, I thank you as well and leave here my sincere apologies.

DECLARATION OF AUTHOR CONTRIBUTIONS

Experiments involving embryonic transplantations were performed in collaboration with Dr. Sven Falk and presented upon his consent. The results of these experiments are presented in this thesis in Figures 16 and 17.

EIDESSTATTLICHE VERSICHERUNG / AFFIDAVIT

Hiermit versichere ich an Eides statt, dass ich die vorliegende Dissertation „Regenerative capacity of reactive astrocytes *in vitro* and *in vivo*“ selbstständig angefertigt habe, mich außer der angegebenen keiner weiteren Hilfsmittel bedient und alle Erkenntnisse, die aus dem Schrifttum ganz oder annähernd übernommen sind, als solche kenntlich gemacht und nach ihrer Herkunft unter Bezeichnung der Fundstelle einzeln nachgewiesen habe.

I hereby confirm that the dissertation „Regenerative capacity of reactive astrocytes *in vitro* and *in vivo*“ is the result of my own work and that I have only used sources or materials listed and specified in the dissertation.

München, den 28.06.2018 Luisa Lange Canhos

Unterschrift (signature)